Influence of Temperature, Concentration, Anion and Alkyl Chain Length in the Imidazolium Cation on the Thermophysical Properties of Imidazolium Based Ionic Liquids with Acetophenone

By

Kgomotso Masilo

BSc; BSc (Hons) (NWU)

Submitted in partial fulfillment of the
Requirements for the degree of Masters of Science, (Chemistry) in the
Department of Chemistry
Faculty of Agriculture, Science and Technology
North-West University (Mafikeng Campus)

Supervisors : Dr Indra Bahadur
: Prof Eno. E. Ebenso

May 2016

DECLARATION

I hereby declare that the dissertation entitled "Influence of temperature, concentration, anion and alkyl chain length in the imidazolium cation on the thermophysical properties of imidazolium based ionic liquids with acetophenone" submitted to the Department of Chemistry, North-West University, Mafikeng Campus for the fulfillment of the degree of Master of Science in Chemistry is a faithful record of original research work carried out by me under the guidance and supervision of Dr Indra Bahadur and Prof Eno. E. Ebenso. No part of this work has been submitted by any other researcher or students. Sources of my information have been properly acknowledged in the reference pages.

Signature..... Date...30/09/2016.....

Kgomotso Masilo

Signature..... Date...30-09-2016.....

Dr Indra Bahadur

Signature..... Date...30th Sept 2016.....

Prof Eno. E. Ebenso

ACKNOWLEDGEMENTS

I would like to thank the almighty God for all that I have accomplished and for giving me the strength to complete my studies. I am very thankful and appreciative to my supervisors, **Dr Indra Bahadur** and **Prof Eno. E. Ebenso** for their continuous support, guidance, for believing in me and for their patience throughout my research. I am also thankful to all the academic and support staff members in the Chemistry department, all the chemistry laboratory technicians, colleagues and members of the Material Science Innovation & Modelling (MaSIM) research group.

I am sincerely thankful to the Department of Chemistry, Durban University of Technology, Durban, South Africa, for providing the facilities to carry out some of the present work. Furthermore, I wish to express my sincere gratitude to my sponsors, NWU Postgraduate Bursary, Sasol Inzalo Foundation and NRF, South Africa for funding. Lastly I would like to thank my family and friends for the encouragement and support during my studies.

ABSTRACT

The present study, reports thermophysical properties namely: densities (ρ), sound velocities (u), viscosities (η), and refractive index (n_D) of a series of alkyl imidazolium-based ionic liquids (ILs) with same cation and different anion and vice versa: 1-butyl-3-methylimidazolium tetrafluoroborate $[BMIM]^+[BF_4]^-$, 1-butyl-3-methylimidazolium hexafluorophosphate $[BMIM]^+[PF_6]^-$, 1-ethyl-3-methylimidazolium ethyl sulphate $[EMIM]^+[EtSO_4]^-$ and 1-ethyl-3-methylimidazolium tetrafluoroborate $[EMIM]^+[BF_4]^-$, with acetophenone over the wide range of composition at T= (293.15, 303.15, 313.15, 323.15 and 333.15) K under atmospheric pressure. The excess molar volumes, V^E_m, deviation in isentropic compressibilities ($\Delta\kappa_s$), deviation in viscosities ($\Delta\eta$) and deviation in refractive indexes (Δn_D) were derived from experimental results. The V^E_m, $\Delta\kappa_s$ and Δn_D values for the mentioned systems are both negative and positive over the entire composition range while the $\Delta\eta$ values are negative under the same experimental conditions. The derived properties were fitted to the Redlich-Kister polynomial equation to check the accuracy of experimental results. Furthermore, the inter-ionic interactions between the cations and anions of the ILs both *in vacuo* and in acetophenone (using continuum solvation) were confirmed using quantum chemical technique such as Density Functional Theory (DFT). The quantum chemical results are in good agreement with the results obtained from experimental suggesting that there exist appreciable interactions between the ILs and acetophenone. The theoretical and measured data were interpreted in terms of intermolecular interfaces and structural effects between similar and dissimilar molecules upon mixing. It is a well-known fact that reliable experimental data ensure a higher degree of accuracy than correlations used to estimate unknown properties. Thus, the results from these studies can be utilized in optimizing the process parameters for the effective design of separation process on an industrial scale. These results can also be used to enhance the applications of ionic liquids in certain aspects of research or industrial application.

TABLE OF CONTENTS

LIST OF ABBREVIATIONS

AILs	:	Aprotic ionic liquids.
ILs	:	Ionic liquids.
DFT	:	Density Functional Theory.
FT-IR	:	Fourier transform infrared.
IEFPCM	:	Integral formalism variant of the polarized continuum model.
PILs	:	Protic ionic liquids.
RTILs	:	Room temperature ionic liquids.
$[TBA]^+[PF_6]^-$:	:	Tetrabutylammonium hexafluorophosphate.
$[BMIM]^+[Tf_2N]^-$	:	1-Butyl-3-methylimidazolium bis(trifluoromethysulfonyl)imide
$[BMIM]^+[PF_6]^-$	:	1-Butyl-3-methylimidazolium hexafluorophosphate.
$[BMIM]^+[HSO_4]^-$	:	1-Butyl-3-methylimidazolium hydrogen sulfate.
$[BMIM]^+[MeSO_4]^-$	:	1-Butyl-3-methylimidazolium methylsulfate.
$[BMIM]^+[BF_4]^-$	:	1-Butyl-3-methylimidazolium tetrafluoroborate.
$[BMIM]^+[SCN]^-$	:	1-Butyl-3-methylimidazolium thiocyanate.
$[BDMIM]^+BF_4]^-$	:	1-Butyl-2,3-dimethylimidazolium tetrafluoroborate.
$[EMIM]^+[EtSO_4]^-$	:	1-Ethyl-3-methylimidazoium ethyl sulfate.
$[EMIM]^+[MeSO_4]^-$	:	1-Ethyl-3-methylimidazolium methyl sulfate.
$[EMIM]^+[BF_4]^-$	:	1-Ethyl-3-methylimidazolium tetrafluoroborate.
$[HMIM]^+[BF_4]^-$	:	1-Hexyl-3-methylimidazolium hexafluorophosphate.
$[OMIM]^+[PF_6]^-$	:	1-Octyl-3-methylimidazolium hexafluorophosphate.
$[HeMIM]^+[BF_4]^-$	:	1-(2-hydroxyethyl)-3-methylimidazolium tetrafluoroborate.

LIST OF FIGURES

Figure 4.7 Viscosity deviation ($\Delta\eta$) *vs* mole fraction of IL for IL (1)+ acetophenone (2): (a) $[BMIM]^+[BF_4]^-$, (b) $[BMIM]^+[PF_6]^-$, (c) $[EMIM]^+[BF_4]^-$ and (d) $[EMIM]^+[EtSO_4]^-$ at T= (293.15, 303.15 313.15, 323.15 and 333.15) K. The dotted lines were generated using Redlich-Kister curve-fitting with parameter given in Table 4.2.

Figure 4.8 Refractive index deviation (Δn_D) *vs* mole fraction of IL for IL (1)+ acetophenone (2): (a) $[BMIM]^+[BF_4]^-$, (b) $[BMIM]^+[PF_6]^-$, (c) $[EMIM]^+[BF_4]^-$ and (d) $[EMIM]^+[EtSO_4]^-$ at T= (293.15, 303.15 313.15, 323.15 and 333.15) K. The dotted lines were generated using Redlich-Kister curve-fitting with parameters given in Table 4.2.

Figure 4.9 Optimized structures of ionic liquids (a) $[BMIM]^+[BF_4]^-$, (b) $[BMIM]^+[PF_6]^-$, (c)$[EMIM]^+[BF_4]^-$, (d) $[EMIM]^+[EtSO_4]^-$.

Figure 4.10 Schematic representation of interactions of the cations $[BMIM]^+$ and $[EMIM]^+$ with acetophenone.

LIST OF TABLES

LIST OF SYMBOLS AND NOTATIONS

ρ	density of mixture.
ρ_1	density of 1st component.
ρ_2	density of 2nd component.
u	sound velocity of mixture.
K_s	isentropic compressibility.
κs_1	isentropic compressibility of component 1.
κs_2	isentropic compressibility of component 2.
Δks	isentropic compressibility deviation.
η	viscosity of mixture.
$\Delta \eta$	viscosity deviation.
η_1	viscosity of the pure components 1.
η_2	viscosity of pure component 2.
n_1	refractive index of 1st component.
n_2	refractive index of 2nd component
n	refractive index of mixture.
Δn	refractive index deviation.
x_1	mole fraction of 1st component.
x_2	mole fraction of 2nd component.
M_1	molar mass of ionic liquid.
M_2	molar mass of solvent.
V^E_m	excess molar volume.
T	temperature.

Ai	polynomial coefficient.
k	number of coefficients used in the Redlich-Kister correlation.
N	number of experimental points.
σ	standard deviation.
M_0	true mass.
V	volume.
λ	wavelength.
ν	frequency.
π	pi.
εr	material's relative permittivity.
μ_r	relative permeability.
τ	shear stress.
D	diameter.
L	length.
r_s	radius of the sphere.
U_t	terminal velocity of the falling body.
H	height.
F	force
Q	fluid volume-flow rate.
ΔE_{int}	interaction energies.
$E\ (a)$	energies of the pure anion.
$E(c)$	energies of the pure cation.
$E\ (ac)$	energy of ionic liquid system.

CHAPTER ONE

INTRODUCTION

1.1. Description of ionic liquids

The term ionic liquid (IL) is used to define a wide group of salts which has a broad liquid range [1]. These are generally molten salts or molten oxides [2], fused salts, organic salts or eutectic mixtures of an organic salts or inorganic salts [3]. As compared to traditional molecular organic solvents, ILs are liquids at ambient temperatures [4], and are composed entirely of cations and anions [1, 4]. There are two categories of ILs: aprotic and protic. Aprotic ILs (AILs) are composed entirely of cations that are not protonated [3]. Protic ILs (PILs) result from a proton transfer from an acid capable of donating a proton to a base that is able to accept a proton [3]. The melting point of ILs is relatively low, fixed at/below 100°C [1], and stay as liquids within a wide temperature window (<300 ◦C) [1, 4]. The low melting point of ILs is due to its chemical composition [5], the relatively large size of one or both ions in ILs and low symmetry account for the lower melting points of these materials [6].

ILs that melts at room temperature are said to be room temperature ionic liquids (RTILs) [7] and may act uniquely in contrast to common molecular liquids when utilized as solvents [1]. RTIL are typically salts with large nitrogen or phosphorous-containing organic cations with linear alkyl chain [3]. Room temperature ionic liquids comprise of bulky and asymmetric organic cations for example 1-alkyl-3-methylimidazolium, 1-alkylpyridinium, 1-methyl-1-alkylpyrrolidinium or ammonium ions [7]. RTILs remain liquid at room temperature due to the reason that their ions do not pack well [8]. The organic cations components of IL/RTIL include imidazolium, pyridinium, pyrrolidinium, phosphonium, guanidinium or/ and ammonium), [1, 9] and the inorganic anion could be Cl^-, PF_6^-, BF_4^- and more while the organic anions could be

trifluoromethylsulfonate $[CF_3SO_3]^-$, bis[(trifluoromethyl) sulfonyl)]imide $[Tf_2N]^-$, trifluoroacetate $[CF_3CO_2]^-$ [1] (see **Figure 1.1**). Scientific literature has reported about 1500 ILs and 300 of these are readily available commercially [2, 3].

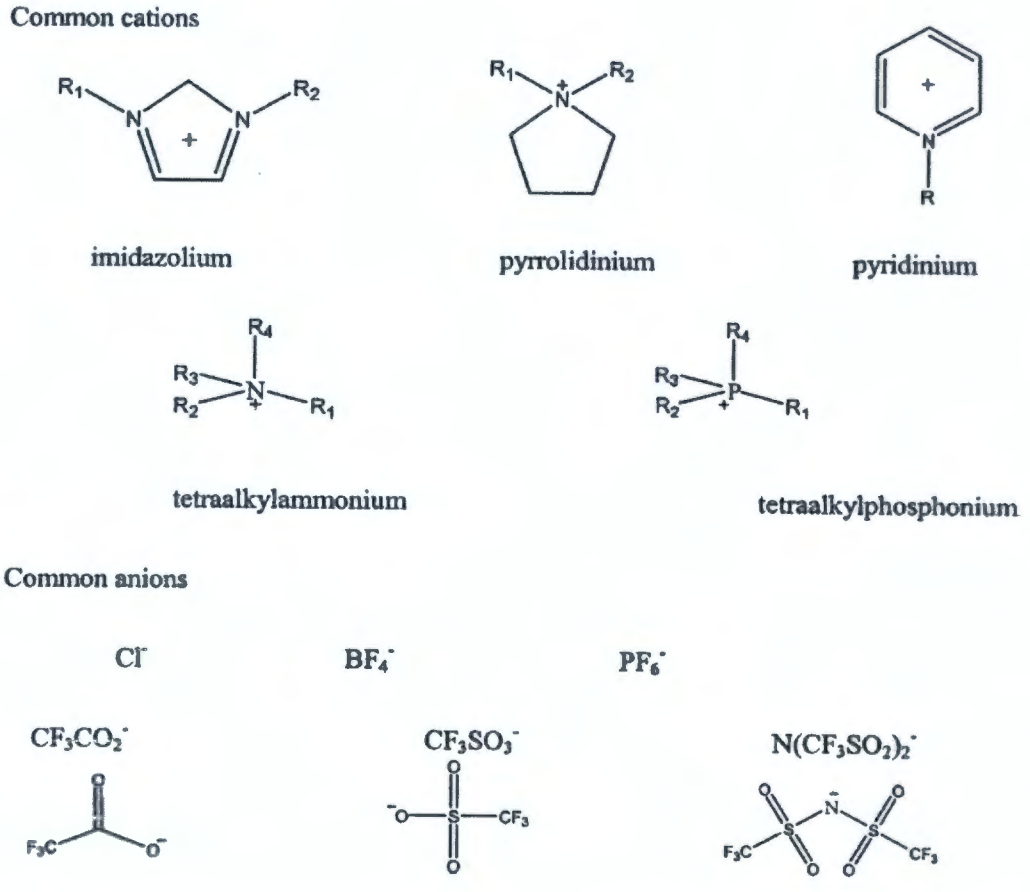

Figure 1.1 Structures of common cations and anions of ionic liquids [1].

1.2. Ionic liquids and its importance

The ILs are completely composed of ions and possess more favourable properties than organic molecular solvents, which includes wide liquid range [10], negligible vapour pressure unlikely to evaporate under normal conditions [3], high thermal stability and non-flammable [3, 10, 11]. They are also non-volatile and are reusable [12]. The pure ILs compounds are found to be

colourless in nature [11], whereas for less pure ionic liquids the colour normally ranges from yellowish to orange [13]. ILs are exceptionally polar [5], and have a more extensive liquid range of solubilities and miscibillities, for instance, some IL are hydrophilic, while others are hydrophobic [3], however ILs are immiscible with numerous natural solvents [5]. ILs have controlled miscibility [14, 15], which results in many possible combinations of cations and anions [16, 17] and allows a large variety of interactions and applications [18].

The ILs have been used as solvents for reactions, absorption media for gas separations, separating agent in extractive distillation, heat transfer fluids, for processing biomass, and as the working fluid in a variety of electrochemical applications (batteries, capacitors, solar cells, etc.) [19–24]. IL could contribute considerably to the improvement of green chemistry and green technology by, for instance (a) substituting toxic and flammable volatile organic solvents (b) reducing or inhibiting chemical wastage or contamination and (c) enhancing the well-being of chemical processes and products. The solvent properties of ILs can be tuned for a particular application by changing the anion and cation combinations [7, 25]. The properties of the ILs can be tuned by altering and varying the length of the alkyl groups that are integrated into the cation and the types of anions [5]. The properties and advantages that the ionic liquids possess enable them to be applicable in a variety of fields and chemical industries.

1.3. Physical properties of ionic liquids

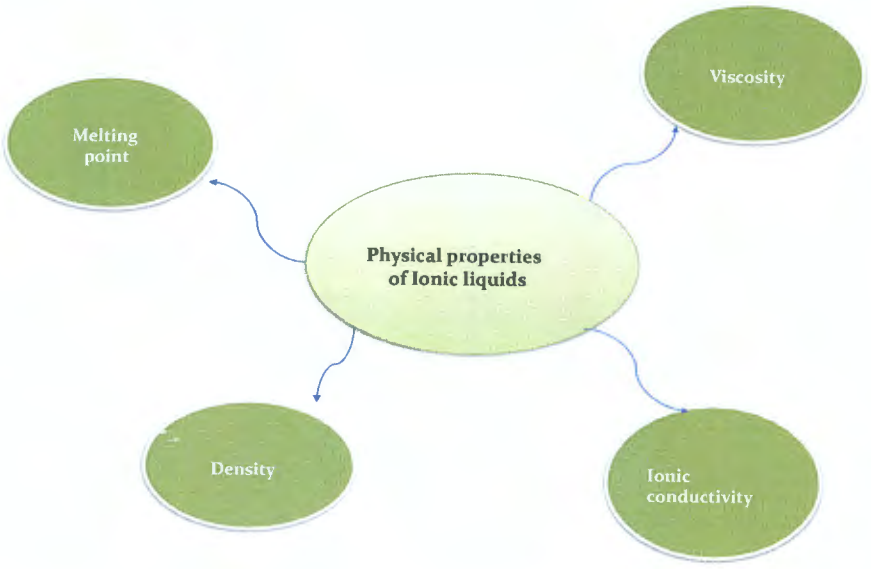

Figure 1.2 Diagram illustrating the physical properties of ionic liquids.

1.3.1. Melting point

ILs have been characterized to have melting point underneath 100 °C and the greater part of them are liquids at room temperature [26]. The primary components that influence the melting point are the charge distribution on the particles, H-bonding capability, the symmetry of the particles and the van der Waals interactions [2]. Both cations and anions contribute to the low meting points of ionic liquids. The increase in anion size leads to a decrease in melting point [27]. Cations size and symmetry make an important effect on the melting points of ionic liquids. Large cations and increased asymmetric substitution results in a melting point reduction [28].

1.3.2. Density

Ionic liquids in general are denser than water with values ranging from 1 to 1.6 g ·cm^{-3}and their densities decrease with increase in the length of the alkyl chain in the cation [2]. The densities of ionic liquids are additionally influenced by the character of anions [26].

Table 1.1

Measured density (ρ) from the literature (ρ^{lit}) at T=298.15 K for $[BMIM]^+[C(CN)_3]^-$, $[BMIM]^+[N(CN)_2]^-$, $[BMIM]^+[OcSO_4]^-$, $[BMIM]^+[SCN]^-$ and $[BMIM]^+[CH_3SO_4]^-$.

Component	ρ/g ·cm^{-3}
$[BMIM]^+[C(CN)_3]^-$	1.0473[30]
$[BMIM]^+[N(CN)_2]^-$	1.0631[30]
$[BMIM]^+[OcSO_4]^-$	1.0684[31]
$[BMIM]^+[SCN]^-$	1.0698[2]
$[BMIM]^+[CH_3SO_4]^-$	1.2124[33]

1.3.3. Viscosity

ILs are more viscous compared to common organic solvents [14]. Most RTILs are viscous fluids, with viscosities more practically identical to viscosities of oils, being two to three orders of degree greater than those for organic solvents [2]. The viscosity of ionic liquids is determined by van der waals forces and hydrogen bonding. Electrostatic forces may also play an important role. Alkyl chain lengthening in the cation leads to an increase in viscosity [29]. This is due to stronger van der waals forces between cations leading to increase in the energy required for molecular motion. Also, the ability of anions to form hydrogen bonding has a pronounced effect on viscosity.

1.3.4. Ionic conductivity

Ionic liquids have sensibly good ionic conductivities in contrast with those of organic solvents/electrolyte systems. In view of the way that ionic fluids are made exclusively out of ions, it would be predictable that ionic liquids have high conductivities. This is not the case since the conductivity of any solution is influenced not only on the number of charge carriers but also on their mobility. The large fundamental ions of ionic liquids decrease the ion mobility which, in turn, leads to lower conductivities. Moreover, ion pair establishment and/or ion aggregation decrease conductivity. The conductivity of ionic liquids is inversely related to their viscosity. Therefore, ionic liquids of higher viscosity display lower conductivity and increase in temperature, increases conductivity and lowers viscosity [26].

1.4. Importance of thermophysical and thermodynamic properties

Thermophysical and thermodynamic properties of ILs mixtures are vital in various industries namely, oil and gas for flow assurance and oil recovery, pharmaceutical and polymer industries for solvent selection and emission, chemical industry for the design of separation processes, in biotechnology as the origin of several diseases is traced to aggregation of proteins and many protein separations and in the environmental science for the estimation of the distribution of chemicals in various ecosystems [33]. In chemical engineering, density and viscosity data is needed for calculations concerning chemical separations, fluid flow, mass, and heat transfer [34-36]. Moreover, the thermophysical and derived thermodynamic properties also allows for new correlations and/or predictive models to test the solution theories for ILs and their binary mixtures with organic solvents [37-45] and give solute-solute, solute-solvent and solvent-solvent interactions that take place in binary mixtures specifically where hydrogen bonding occurs.

Experimental information on thermodynamic properties of ionic liquids is scarce and fragmenting. These quantities are required for the authentication and improvement of the molecular modelling and are first principle methods towards this new class of solvents [46]. The increasing use of these compounds in numerous industrial processes has greatly stimulated the need for extensive information an investigation on their thermodynamic and thermophysical properties and their mixtures with organic solvents [3]. The understanding of thermophysical properties of mixed solvents of ILs with organic molecular liquid is important for the design of various technological processes and practical applications [21, 47-50].

1.5. Density and excess molar volume

By definition [51-52] the excess molar volume, V_m^E, is given by:

$$V_m^E = V_m - V_m^{id} \tag{1.1}$$

Where V_m is the molar volume if the mixture defined by the following equation:

$$V_m = \frac{x_1 M_1 + x_1 M_2}{\rho} \tag{1.2}$$

where x_1 and x_2 are the mole fractions, M_1 and M_2 are molar masses and ρ is the density

And V_m^{id} is the molar volume of ideal mixture defined by the following equation:

$$V_m^{id} = \frac{x_1 M_1}{\rho_1} + \frac{x_2 M_2}{\rho_2} \tag{1.3}$$

Where ρ_1, ρ_2 are the densities where *1* and *2* refers to the component *1* and *2* respectively.

Finally, the, V_m^E, for a binary mixture is determined from density measurements using equation

$$V_{\mathrm{m}}^{\mathrm{E}} = \frac{x_1 M_1 + x_2 M_2}{\rho} - \frac{x_1 M_1}{\rho_1} - \frac{x_2 M_2}{\rho_2} \tag{1.4}$$

The excess molar volume, $V_m{}^E$, for binary mixtures can be determined experimentally in two ways, namely (i) indirectly and (ii) directly. The indirect methods measurements involve measuring the density of the pure liquid as well as the density of the mixture and calculating, V_m^E, from (pycnometric or densitometer) whereas the direct method involve measuring the resultant volume change upon mixing of the two components from dilatometric methods. Both these experimental methods have been extensively reviewed [53-60].

1.5.1. Indirect methods

The development of the dilatometer was complemented by a larger accuracy from density measurement techniques and the previous methods became less used for determination of $V_m{}^E$. Nonetheless the development of exceedingly accurate vibrating tube densitometers made it promising to determine, $V_m{}^E$, with satisfactory accuracy from density measurements. This technique is also very simple.

1.5.1.1. Pycnometry

Pycnometry includes the determination of the mass for a constant volume. A vessel with a known volume is jam-packed with a liquid mixture of known composition. It is then weighed and this mass, together with the composition and volume of the vessel is used to determine V_m^E. A pycnometer capable of a precision of 5×10^{-6} g $\cdot$cm^{-3} for density measurement translates into a precision of 0.001 cm$^3\cdot$mol^{-1}for V_m^E has been described by Wood and Bruisie [61]. The pycnometer based on the design of [61] is shown in **Figure 1.3**.

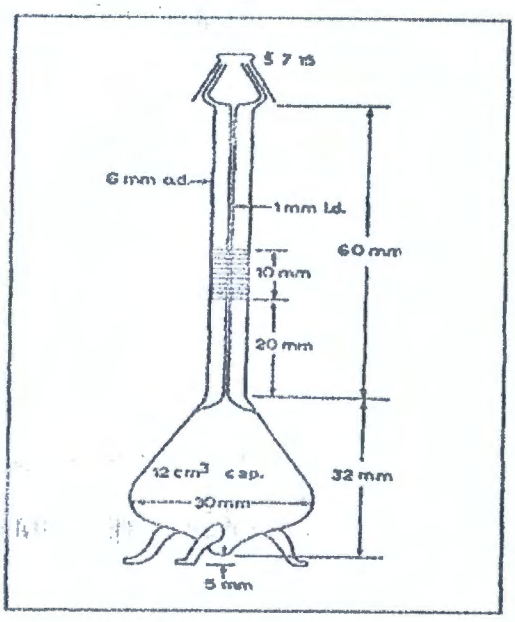

Figure 1.3 Schematic representation of a pycnometer based on the design of Wood and Brusie [61].

1.5.1.2. Magnetic float densimeter

The operation of magnetic float densimeter is centred on the determination of the height of a magnetic float in a liquid mixture. The height of this magnetic float in existence of a known magnetic field is a function of the buoyancy of the liquid. The buoyancy of the liquid is linked to the density of the liquid. An instrument with a precision 3×10^{-6} g $\cdot$cm^{-3}has been stated and this translates to a precision of 0.0008 cm$^3\cdot$mol^{-1} [62]. The magnetic float densimeter based on the design of Franks and Smith 1967 [62] is shown in **Figure 1.4**.

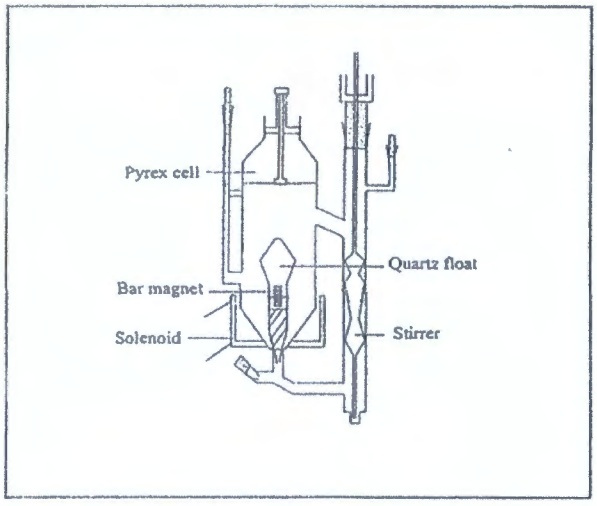

Figure 1.4 Schematic representation of a magnetic float densimeter [62].

1.5.1.3. Mechanical oscillating densitometer

Mechanical oscillating densimeters attached to digital output displays are being broadly utilised in the chemical industry, and in research laboratories to measure densities of liquid and liquid mixtures. The frequency of the vibrating tube containing a liquid that is subjected to a constant electric stimulation is connected to the density of the liquid. According to Handa and Benson [54], the frequency of a vibration of an undamped oscillator (e.g. tube containing a liquid) connected by a spring with a constant elasticity, c, is related to the mass of the oscillator, M, by using the following expression

$$2\pi V = \left(\frac{c}{M}\right)^{\frac{1}{2}} \tag{1.5}$$

Since the oscillator is a hollow tube, M is the sum of the contents in the tube and the true mass, M_0, c is the constant elasticity of a spring and V is the frequency of the vibrating tube, if a liquid with a density, ρ, fills the hollow which has a volume V, then:

$$M = M_0 + \rho V \tag{1.6}$$

Substitution of equation (1.5) into equation (1.6) and solving for ρ

$$\rho = -\frac{M_0}{V} + \left(\frac{c}{4\pi^2}\right)\left(\frac{1}{V^2}\right) \tag{1.7}$$

Where $-\frac{M_0}{V}$ and $\frac{c}{4\pi^2}$ are constants and V^2 is the frequency. Equation (1.7) can therefore be written as:

$$\rho = A + B\left(\frac{1}{v}\right)^2 \tag{1.8}$$

The constants A and B are characteristics of the oscillator. Equation (1.8) can also be written as:

$$\rho = A + B\tau^2 \tag{1.9}$$

Where A and B are determined by calibration, τ is the period and density is known by the symbol. This involves determining the period for two pure substances of known density. Densities are measured in relation to a reference material:

$$\rho - \rho_0 = B\left(\tau^2 - \tau_0^2\right) \tag{1.10}$$

Commercially available vibrating tube densimeters with a precision of 0.001 % are available.

1.5.2. Direct methods

The direct method measures the volume change that happens when the liquids are mixed. Direct methods for estimation of, V_m^E, includes batch dilatometer and continuous dilution dilatometer. Batch dilatometer is described by the determination of a single data point for every loading of the apparatus and continuous dilatometer is described by the determination of numerous information points per loading of the apparatus [54, 63-64].

1.5.2.1. Batch dilatometer

The dilatometer is loaded with known masses of pure liquids, which are isolated by mercury. The height of mercury in the calibrated graduated section is noted. The liquids are mixed by rotating the dilatometer and the volume change on mixing is shown by the adjustment in the height of the mercury in the calibrated capillary. The, V_m^E, is obtained from the volume change and the masses of the segments. It was reported that an accuracy of ± 0.003 $cm^3 \cdot mol^{-1}$ in the, V_m^E, could be accomplished over the temperature scope of (280 to 350) K utilizing this method. A disadvantage of this apparatus is that it is hard to fill the dilatometer and this is typically refined utilizing a narrow needle. A key source of error in this method is the determination of the components as is it important to measure the dilatometer as it contains mercury. This results in large errors in the measured mass. The error associated with taking a difference in expansive masses is typically quiet critical [65]. The Batch dilatometer is shown in **Figure 1.5**.

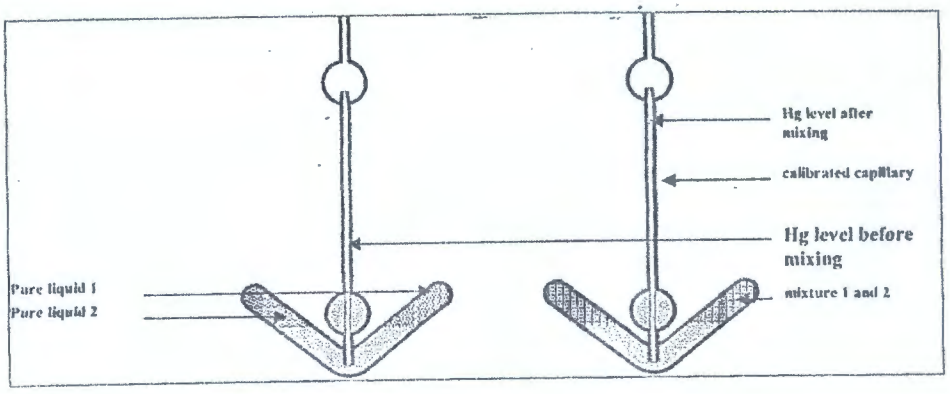

Figure 1.5 Schematic representation of a typical batch dilatometer [63-64].

1.5.2.2. Continuous dilution dilatometer

This method has become more common than the batch method since it is less time consuming and more information is produced per loading. The mode of operation includes the progressive addition of one liquid into the repository, which contains the other liquids and detecting the volume change that goes with the addition.

The dilatometer of [60] which established on the design of Bottomly and Scott is displayed in **figure 1.6**. Both are viewed better to other continuous dilatometer in light of the fact that mercury and the liquids don't go through greased gas. The instrument of Kumaran and McGlashan is viewed as an enhancement on the one created by Bottomly and Scott due to the fact that it is less demanding to load. Kumaran and McGlashan obtained an accuracy of 0.0003 $cm^3 \cdot mol^{-1}$ V_m^E for their apparatus.

A measurement is made by filling the burette (e) with one of the pure liquids and the bulb (d) with the other pure liquid. As the dilatometer is tilted some of the mercury is displaced into the burette through a capillary (c) and collects at the bottom of the burette. This displaced mercury forces some of the pure liquid from the burette into the bulb through the higher capillary *(b)*.

After mixing the change in volume is registered as a change in the level of the mercury in the calibrated capillary (a). The amount of pure liquid that is displaced is determined from the height of the mercury in the burette. Because mercury is used, a capillary pressure effect is possible and the compressibility of mercury has to be considered when determining the excess molar volume.

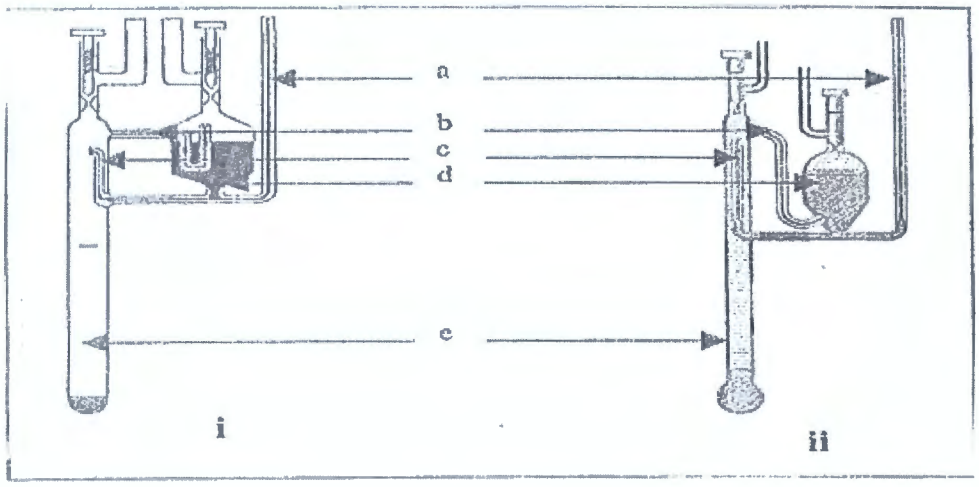

Figure 1.6 Schematic representation of a continuous dilatometer (i) design of Bottomly and Scott [66], (ii) design of Kumaran and McGlashan [60]. a; calibrated capillary from which the volume change is determined, b; liquid capillary, c; mercury capillary, d; bulb that contains mercury, e; burette liquid 2 [60, 66].

1.6. Sound velocity and isentropic compressibility deviation

Measurement of the sound velocity, u, in liquids is a beneficial source of information to identify small changes in gas composition or effects of slight concentration changes [67]. Sound velocity and density are utilised to determine the isentropic compressibility by using the Newton-Laplace equation:

$$\kappa S = \frac{1}{\rho u^2} \tag{1.11}$$

Where ρ the density and u is the sound velocity of the binary mixtures. The isentropic compressibilities deviation is therefore written as:

$$\Delta\kappa_s = \kappa_s - (x_1\kappa_{s1} + x_2\kappa_{s2}) \tag{1.12}$$

Where x_1 and x_2 are the mole fractions, κ_{s1} and κ_{s2} are the isentropic compressibility for component 1 and 2.

1.6.1. Instruments used for the measurement of the sound velocity

1.6.1.1. Mittal Ultrasonic interferometer M-81G

It is not an easy device and the frequency is employed to calculate the ultrasonic velocity in liquids with a high amount of uncertainty. The frequencies for succession of readings are captured and the average reading calculated. It consists of a:

- High frequency generator, that is designed to stimulate the quartz plate fastened at the bottom of the measuring cell at a resonance frequency to produce ultrasonic waves in the investigational liquid in the measuring cell.
- Measuring cell that is uniquely made and consist of double walled cell for sustaining the temperature of the liquid fixed throughout the experiment. A fine micrometer screw is given at the top, and can lower or rise the reflector plate in the cell over a known distance.

  It has a quartz plate at the bottom. A diagram showing the Ultrasonic Interferometer M81G and interferometer is shown in **Figures 1.7**.

Figure 1.7 Photograph of an Ultrasonic interferometer M-81G.

(Taken from Instruction Manual of Mittal Enterprises Ultrasonic Interferometer for Liquids).

The standard utilised in the measurement of velocity, u, is established on the precise determination of the wavelength λ, in the medium. Ultrasonic waves of known frequency, ν, are formed by a quartz plate cell. A mobile plate kept parallel to the quartz plate replicates the waves. When separation between plates is accurately a whole multiple of the sound wavelength, standing waves are produced in the medium. The acoustic resonance gives rise to an electrical response on the generator transporting the quartz plate so that the anode current of the generator develops a maximum if the distance between the reflector and crystal is increased or decreased and the difference is precisely one half wavelength, ($\lambda/2$) or multiple of it, the anode current again becomes a maximum. From the knowledge of wavelength, (λ), the velocity or speed of sound, (u), can be attained by the relation:

$$u = \lambda \times \nu \tag{1.13}$$

1.7 Refractive index and refractive index deviation

By definition, the refractive index, n_D, is given by:

$$n = \frac{Speed\ of\ light\ in\ material\ 1}{Speed\ of\ light\ in\ material\ 2} = \frac{\sin\theta 1}{\sin\theta 2} \tag{1.14}$$

This is written as $n_{1,2}$ and is the refractive index in material 2 relative to material 1. The incident light is in material 1 and the refracted light is in material 2.

If the incident light is in a vacuum this value is called the absolute refractive index of material 2. By definition the refractive index in a vacuum is 1. In practice, air makes little difference to the refraction of light with an absolute refractive index of 1.0008, so the value of the absolute refractive index can be used assuming the incident light is in air. The refractive index is also defined as the ratio of the speed of a wave either light or sound in a reference medium to a second medium.

Commonly is it used in the context of the speed of the wave of light with a vacuum as a reference medium, even though historically other reference media (e.g. air at a standardized pressure and temperature) have been utilised. In the case of light, the refractive index is given by:

$$n_D = \sqrt{\varepsilon_r \mu_r} \tag{1.15}$$

Where ε_r is the material's relative permittivity and μ_r is its relative permeability. For naturally taking place materials, μr is very close to 1 [68]. So n is approximately $\sqrt{\varepsilon r}$. In contrast to a widespread misconception, the real part of a complex n may be lower than one, dependent upon the material and wavelength. This has practical technical applications, such as effective mirrors for X-rays based on total external reflection.

Furthermore, the refractive index is the ratio of the sine of the angle of incidence (medium 1) θ_1 to the sine of the refraction of (medium 2) θ_2 and is given by [69]:

$$n = \frac{\sin \theta 1}{\sin \theta 2} \quad (1.16)$$

The angles are determined to the normal of the surface. This meaning is based on Snell's law [69] and is equivalent to the meaning above if the lights pass in from the reference medium (a vacuum).

1.7.1. Instruments used for the determination of refractive index

1.7.1.1. ATAGO RX 5000 refractometer

The ATAGO RX-5000 digital refractometer provides rapid and precise measurements. The RX-5000 measures sample for refractive index with an accuracy and resolutions of ± 0.00004 and 0.00001/0.01 in four seconds the instrument ranges from 132700-1.5800 n. All results, including date, time, current temperature, measurement result, measurement temperature, etc., are electronically showed. It is utilised for testing and developing medicines, or chemical products, or processed foods, by inspecting the refractive index and concentration of materials as an auxillary means of analysis.

The instrument consist of a printer output, RS-232C output, AC adapter (AD-11), power cable, keyboard mask, 3 plastic spoons, and 2 meters of tubing for connecting to separate circulating constant temperature bath, 10 tube tie bands, test report and instruction manual with Overall Dimensions is 37 × 20 × 12 cm. **Figure 1.8** shows the diagram of an ATAGO RX 5000 Refractometer.

Figure 1.8 Photograph of an ATAGO RX 5000 Refractometer.

(Taken from Instruction Manual ATAGO RX 5000 Refractometer).

1.7.1.2. Abbemat digital refractometer

Abbemat digital refractometers permit fast but less precise refractive index measurements. They are factory calibrated with official standards from the Physikalisch-Technische Bundesanstalt (PTB, National Metrology Institute of Germany). Refractive index results from an Abbemat 300/350 are accurate to ± 0.0001 n_D and for an Abbemat 500/550 ± 0.00002. Abbemat 350/550 refractometers are set up with touchscreen. The instrument has a coloured LCD monitor and membrane keys which are resistant to leakage and dirt. Instrument produces automatic warning if the sample is not enough. There is a quick wipe system which wipes the prism after each measurement. Abbemat 350/550 measures turbid, coloured or opaque samples and all samples from liquids to pastes and polymers to solids. There is no effect from humidity, temperature or vibrations. A wide range of scales are kept in the Abbemat for converting refractive index into concentrations. **Figure 1.9** shows the diagram of an Abbemat Digital Refractometer.

Figure 1.9 Photograph of an Abbemat Digital Refractometer 350/550.

(Taken from Instruction Manual of Anton Paar Abbemat Digital Refractometer 350/550)

1.8 Viscosity and viscosity deviation

Viscosity is defined as the internal friction of a fluid. The microscopic nature of internal friction in a liquid is similar to the macroscopic theory of mechanical friction in the system of an object moving on a stationary planar surface. Since viscosity involves the transport of mass within a certain velocity, the viscous response is called a momentum transport process. There are two forms of viscosity, the shear dynamic viscosity and the kinematic viscosity. The shear dynamic viscosity is more concerned with a shear force that produces the fluid motion (see equation 1.17), whereas kinematic viscosity is more concerned with the diffusion of momentum where the motion of a fluid is considered without reference to force. Diffusion of momentum is a more useful description of viscosity (see equation 1.18).The mathematical expression describing the shear dynamic viscosity is simply:

$$\tau_{zx} = \frac{\eta dU_x}{d_z} = \eta\gamma_{zx} \qquad (1.17)$$

Where τzx, the shear stress, is the force per unit area exerted on the upper plate in the x-direction (and hence is equal to the force per unit area exerted by the fluid on the upper plate in the x -direction under the assumption of a no-slip boundary layer at the fluid–upper plate interface) and dUx/dz is the gradient of the x -velocity in the z-direction in the fluid.

The kinematic viscosity is given by the following expression:

$$\upsilon = \frac{\eta}{\rho} \tag{1.18}$$

Where ν is the velocity, η is the kinematic viscosity and ρ is the density of the fluids.

1.8.1 Instruments used for the determination of viscosity

The instruments for viscosity measurements are designed to determine a fluid's resistance to flow, a fluid property defined above as viscosity. The basic principle of all viscometers is to deliver as simple flow kinematics as possible, preferably one-dimensional (isometric) flow, in order to determine the shear strain rate accurately, easily, and independent of fluid type.

1.8.1.1 Capillary viscometer

The capillary viscometer is based on the well-developed laminar tube flow theory (Hagen–Poiseuille flow) shown in **Figure 1.10.** The capillary tube length is many times larger than its small diameter, so that entrance flow is neglected or accounted for in more accurate measurement or for shorter tubes. The expression for the shear stress at the wall is:

$$\tau_W = \left[\frac{\Delta P}{L}\right]\cdot\left[\frac{D}{4}\right] \tag{1.19}$$

Where τ_w is the shear stress exerted on the w-direction, D is the diameter, L is the length of the capillary tube and ΔP referrers to the change between the inlet and outlet.

and

$$\Delta P = (P_1 - P_2) + (z_1 - z_2) - \frac{[C\rho V^2]}{2} \tag{1.20}$$

Where, C > 1.1, P, z, V = $\frac{4Q}{\pi D^2}$ and Q are correction factor, pressure, elevation, the mean flow velocity, and the fluid volume-flow rate, respectively. P_1 and P_2 refer to the inlet and outlet, respectively.

The expression for the shear rate at the wall is:

$$\gamma = \left\{\frac{[3n+1]}{4n}\right\} o \left\{\frac{8V}{D}\right\} \tag{1.21}$$

Where $n = \frac{d[\log \tau_w]}{d[\log \frac{8V}{D}]}$ is the slope of the measured log (τ_w) – log (8V/D) curve. Then, the viscosity is simply calculated as:

$$\eta = \frac{\tau_w}{\gamma} = \left\{\frac{4n}{[3n+1]}\right\} \circ \left\{\frac{\Delta P D^2}{[32LV]}\right\} = \left\{\frac{4n}{[3n+1]}\right\} \circ \left\{\frac{[\Delta P D^4 \pi]}{[128QL]}\right\} \tag{1.22}$$

The advantages of capillary is that they cost low, high accuracy (particularly with longer tubes), and the ability to achieve very high shear rates, even with high viscosity samples. The main

disadvantages are high residence time and variation of shear across the flow, which can change the structure of complex test fluids, as well as shear heating with high-viscosity samples [70].

Figure 1.10 Photograph of a capillary viscometer.

(Taken from Instruction Manual of LAUDA DR. R. WOBSER GMBH & CO. KG capillary viscometer).

1.8.1.2 Falling Sphere viscometer

The falling sphere viscometer is one of the earliest and least involved methods to determine the absolute shear viscosity of a Newtonian fluid. In this method, a sphere is allowed to fall freely a measured distance through a viscous liquid medium and its velocity is determined. The viscous drag of the falling sphere results in the creation of a restraining force, F, described by Stokes' law [67]:

$$F = 6\pi\eta r_s U_t \tag{1.23}$$

Where r_s is the radius of the sphere and U_t is the terminal velocity of the falling body. If a sphere of density ρ_2 is falling through a fluid of density ρ_1 in a container of infinite extent, then by balancing equation 1.23 with the net force of gravity and buoyancy exerted on a solid sphere, the resulting equation of absolute viscosity is:

$$\eta = 2gr_r^2 \frac{(\rho_2 - \rho_1)}{9U_t} \tag{1.24}$$

Equation 1.24 shows the relation between the viscosity of a fluid and the terminal velocity of a sphere falling within it. Having a finite container volume necessitates the modification of equation 1.24 to correct for effects on the velocity of the sphere due to its interaction with container walls (*W*) and ends (*E*). Considering a cylindrical container of radius *r* and height *H*, the corrected form of equation 1.24 can be written as:

$$\eta = 2gr_r^2 \frac{(\rho_2 - \rho_1)W}{(9U_tE)} \tag{1.25}$$

Figure 1.11 is a schematic diagram of the falling sphere method and demonstrates the attraction of this method. This method is useful for liquids with viscosities between 10^{-3} Pa·s and 105 Pa·s. Due to the simplicity of design, the falling sphere method is particularly well suited to high pressure–high temperature viscosity studies [70].

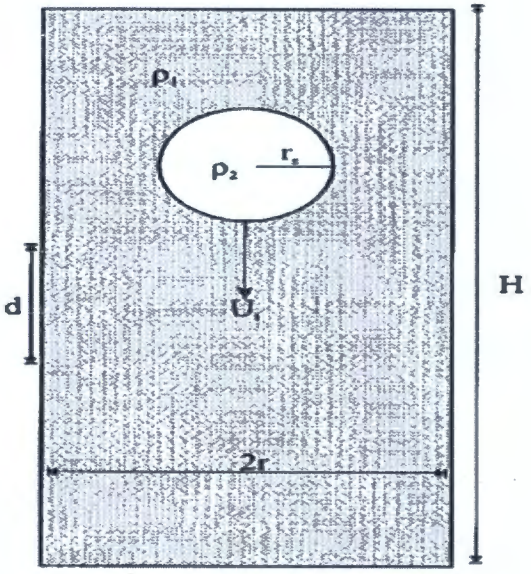

Figure 1.11 Schematic diagram of the failing sphere viscometer [71].

1.9. Quantum chemistry

Quantum chemistry can model molecular properties and changes, and in combination with experiment [72], lead to an improved understanding of mechanism reacting species containing cations and anions. As of late, the quantum chemistry computing technique has turned into a viable approach to investigate the correlation of the atomic structure and its restraint properties and a lot has been achieved in this direction [73-78]. The quantum chemistry computing method is regularly used to examine simple basic systems [79] and the advantage of utilizing quantum-chemical calculations is that they give direct data on the coupling or binding energetics of the distinctive species, which are moderately hard to extract from electrochemical estimations [80]. Thus, quantum-chemical calculations give important data to complement and effectively analyse experimental results, regardless of the calculated systems considered may appear rather idealized compared with the experimental data [80].

1.9.1. Density function theory

Amongst quantum chemical methods, density function theory, (DFT) has shown significant promise in evaluation of corrosion inhibitors [81] is suitable for investigating the changes in electronic structure accountable for inhibitory action. Density Functional Theory (DFT) [72], focuses on the electron density of the system, which depends on only three variables. DFT methods have become very popular in the last decade due to their accuracy and take less time as compared to other methods. In agreement with the DFT, the energy of the fundamental stateof polyelectronic systems can be expressed through the total electronic density, and in fact the use of the electronic density instead of the wave function for the calculation of the energy constitutes the fundamental base of DFT [82]. In most recent years, theoretical quantum chemical calculations have turn out to be complementary for experimental methods in many fields [83-86].

1.10. Scope of present work

In the present work, density, ρ , sound velocity , u, viscosity, η, and refractive index, n, of alkyl imidazolium based ionic liquids, (namely 1-butyl-3-methylimidazolium tetrafluoroborate $[BMIM]^+[BF_4]^-$, 1-butyl-3-methylimidazolium hexafluorophosphate $[BMIM]^+[PF_6]^-$, 1-ethyl - 3-methylimidazoium ethyl sulphate $[EMIM]^+[EtSO_4]^-$, 1-ethyl-3-methylimidazolium tetrafluoroborate $[EMIM]^+[BF_4]^-$) and their binary mixtures with acetophenone at various temperatures and concentrations were presented. The results, obtained in the study are used to derive the thermodynamic data; excess molar volume, isentropic compressibility deviation, refractive indexes deviation and viscosity deviation. The intermolecular interactions of the ILs and their binary mixtures are also evaluated. Furthermore, the influence of changes in temperature and concentration, as well as the variance in the anion, cation and alkyl group of the IL and their binary mixtures is discussed. The chemical structures of the studied alkyl imidazolium based ionic liquids are given in **Figure 1.11**. The present work is a part of an ongoing comprehensive investigations on physicochemical properties of alkyl imidazolium/ammonium-based ILs with solvents at different temperatures [87-98].

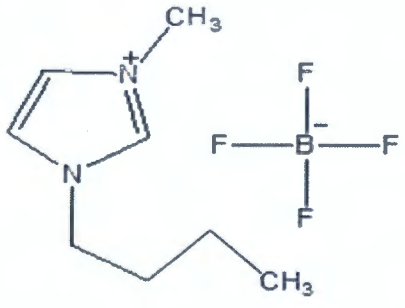

(a)

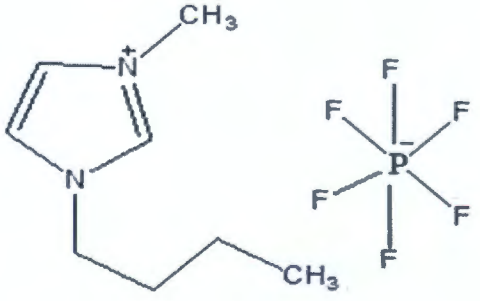

(b)

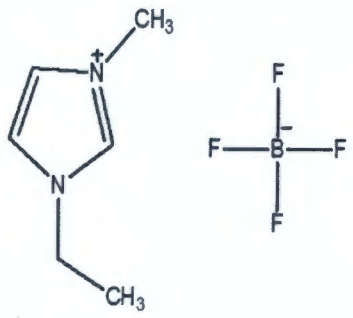

(c)

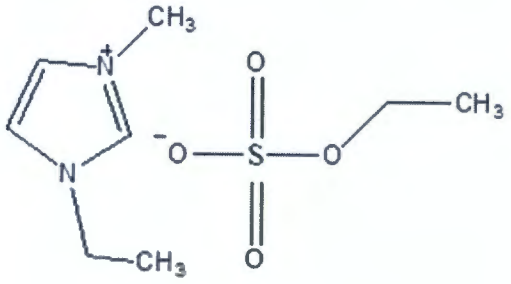

(d)

Figure 1.11 Chemical structure of (a) $[BMIM]^+[BF_4]^-$ (b) $[BMIM]^+[PF_6]^-$ (c) $[EMIM]^+[BF_4]^-$ and (d) $[EMIM]^+[EtSO_4]^-$.

1.11. Problem statement

In the synthesis of ILs the important aspect is the variation of cations and anions, which determines their use in various systems. Nonetheless, in practical applications, ILs are mixed with other substances especially molecular organic solvents which results in modified properties, due to interactions at molecular level between the ILs and other substances. Therefore, there is a need for studying the properties of ILs and their binary mixtures.

Although nowadays a lot of thermophysical and structural IL data are available, little data has been found on thermodynamic properties of ILs and they have not been used in industrial scale. Therefore the main purpose of this study is to obtain information or data related to thermophysical and thermodynamic properties of ILs and their binary mixtures in order to contribute to a data bank of thermodynamic properties of IL mixtures, so to establish principles for the molecular design of suitable ILs for chemical separation processes and for utilization for large scale of applications.

1.12. Aim and objectives

The aim of the proposed research is to carry out an extensive investigation of thermophysical and thermodynamic properties of alkyl imidazolium-based ionic liquids with acetophenone at various concentrations and temperatures.

The aim and objectives will be achieved in the following steps:

- To measure the thermophysical properties such as density, sound velocity, viscosity and refractive index of ionic liquids and their binary mixtures with acetophenone at various temperatures and concentrations.
- To calculate the thermodynamic properties (excess/ derived properties) such as excess molar volume, deviation in isentropic compressibility, deviation in refractive viscosity and deviation in refractive index from the thermophysical properties of ionic liquids and their binary mixtures with acetophenone at various temperatures and concentrations
- To investigate the effect of temperature, concentration and alkyl group on these properties and their derived properties.
- To investigate the effect of cations, anions and alkyl group of the cation on intermolecular interactions.
- To study the intermolecular interactions occurring between the ILs with acetophenone.

CHAPTER TWO

LITERATURE REVIEW

Countless ionic liquids which are of interest to chemists and researchers are binary mixtures of an organic salt or inorganic salt [3]. Ionic liquids are new compounds therefore experimental data on the thermophysical properties, which include viscosity, density, refractive index and sound velocity of the pure ionic liquids and their binary mixtures with other organic solvents are needed in order to design future technological processes and equipment [99]. In the 20 years, there has been a significant increase in the number of studies on thermophysical and thermodynamic properties of ionic liquids and their binary mixtures with molecular organic solvents [3]. Some of the binary mixtures have been studied [100-149].

Rao *et al.* [100] evaluated density, refractive index and sound velocity for the binary mixture of 1-butyl-3-methylimidazolium tetrafluoroborate $[BMIM]^+[BF_4]^-$ and 2-pyrrolidone over the whole composition range at T= (298.15 to 323.15) K and atmospheric pressure. In addition, the molecular interactions in the binary mixtures were scrutinised utilizing the experimental. The Fourier transform infrared (FT-IR) spectrum taken at room temperature. The results found that excess molar volume displays a inversion in the sign from negative to positive deviation. The FT-IR spectra investigation shows the ion-dipole interactions between of $[BMIM]^+[BF_4]^-$ and 2-pyrrolidone.

Pal *et al.* [101] reported density and sound velocity for ILs, $[BMIM]^+[BF_4]^-$, $[BMIM]^+[TF_2N]^-$ and $[BMIM]^+[MeSO_4]$- with 1,2-propanediol over the full composition range at T= (293.15 to 318.15) K. The excess properties and spectroscopic results were evaluated in terms of the effect of temperature and the change of the anion of ionic liquid. All the investigated systems

displayed positive deviation from the ideality. Studies of spectroscopic results indicated that the multiple hydrogen bonding interactions transpired at microscopic level in the studied systems.

Reddy *et al.* [102] investigated density, sound velocity and refractive index for pure $[EMIM]^+[BF_4]^-$, 2-methoxyethanol and their binary mixtures are measured over the complete composition range at T= (298.15–328.15) K under atmospheric pressure. A qualitative investigation of these properties shows strong intermolecular interactions between the liquid. This was additionally reinforced by IR spectroscopy.

Reddy *et al.* [103] reported density, sound velocity and refractive index for pure $[EMIM]^+[EtSO_4]^-$, 2-ethoxyethanol and their binary mixtures over the complete composition range and at T= (298.15–328.15) K under atmospheric pressure. The negative results for excess molar volumes, excess values of partial molar volumes, isothermal compressibility, free volume, isobaric thermal expansion coefficient and positive data for speed of sound, refractive index, internal pressure showed dominance of strong attractive forces.

Krishna *et al.* [104] measured densities, ultrasonic speeds, and refractive index for binary mixtures of $[BMIM]^+[PF_6]^-$ with 2-propoxyethanol, including the pure liquids over the whole range of composition at T= (298.15-323.15) K under atmospheric pressure. The IR spectra of these mixtures have also been investigated 298.15 K. The FT-IR spectra of these mixtures were analyzed in terms of intermolecular interactions. The differences of these parameters with composition and temperature were deliberated in terms of intermolecular interactions predominant in these mixtures. The results displayed the establishment of strong ion–dipole and hydrogen bonding interactions occurring between $[BMIM]^+[PF_6]^-$ and 2-propoxyethanol

molecules and the geometrical effect due to interstitial fitting of 2-propoxyethanol molecules into the interstices of ionic liquids.

Fan *et al.* [105] investigated density and viscosity for three binary mixtures comprising of IL EMIM]$^{+}$[BF_4]$^{-}$ and organic solvents dimethylacetamide, dimethylformamide, and dimethyl sulfoxide under atmospheric pressure and at T= (303.15 to 333.15) K over the whole composition range. Excess molar volume and viscosity deviations exhibited negative trend.

Krishna *et al.* [106] reported measurements of densities and sound velocity for the binary systems of pure ionic liquid [BMIM]$^{+}$[BF_4]$^{-}$ and an alkanediol at T= (298.15 to 323.15) and found the negative excess molar volumes for the systems.

Rao *et al.* [107] reported the thermophysical properties; density, refractive index and sound velocity of [BMIM]$^{+}$[BF_4]$^{-}$ and its binary mixture with *N*-octyl-2-pyrrolidone at temperatures from T= (298.15 to 323.15) K under atmospheric pressure. Furthermore, the molecular interactions analyses of the binary mixtures were done using the experimental FTIR spectrum at room temperature. Negative values up to 0.2 mole fraction of [BMIM]$^{+}$[BF_4]$^{-}$ were obtained for the excess properties which includes excess isentropic compressibility, excess molar isentropic compressibility and excess intermolecular free length, due to the solvation of the ions in the mixture credited to the strong attractive interactions, and positive values were obtained over the residual composition range all at temperatures. For the excess molar volume positive values were obtained and this indicated that there is a volume expansion upon mixing the IL. The FT-IR spectra also showed the ion-dipole interactions between [BMIM]$^{+}$[BF_4]$^{-}$ and *N*-octyl-2-pyrrolidone.

Rao *et al.* [108] evaluated densities, refractive indexes and sound velocity of 1-butyl-3methylimidazolium tetrafluoroborate $[BMIM]^+[BF_4]^-$ + vinyl- 2-pyrrolidinone binary mixture, over the whole range of mole fractions at T= (298.15 to 323.15) K under atmospheric pressure. In addition, the molecular interactions in the binary system were analysed using the FT-IR spectrum. The excess isentropic compressibility, excess intermolecular free length, and excess molar volume values are negative over the complete composition range and at all considered temperatures. The analysis given by the FT-IR spectra showed the ion-dipole interactions between the binary mixtures of $[BMIM]^+[BF_4]^-$ and vinyl- 2-pyrrolidinone.

Rao *et al.* [109] measured the sound velocity, density and refractive index values for the binary mixture of $[BMIM]^+[BF_4]^-$ with *N*-methyl-2pyrrolidinone over the whole range of mole fraction at temperatures from T= (298.15 to 323.15) K. In addition, the experimental FT-IR spectrum was analysed and recorded at room temperature. Negative values were obtained for excess isentropic compressibility and these values were attributed to the strong attractive interactions, structural readjustments, and efficient packing upon mixing of the liquids. The analysis obtained from the FT-IR spectra indicated ion-dipole interactions between $[BMIM]^+[BF_4]^-$ and *N*-methyl-2-pyrrolidinone.

Wu *et al.* [110] evaluated the densities and viscosities of IL (1-butyl-3-methylimidazolium tetrafluoroborate and its binary mixtures with acetonitrile, *N,N*-dimethylacetamide, methanol, and *N*-methyl-2-pyrrolidone) over the mole fraction range from 0.1 to 0.9 measured at T= (303.15 to 333.15) K under atmospheric pressure. The excess molar volume and viscosity deviations were calculated from the new experimental density and viscosity data, respectively and found to be negative values.

Vercher *et al.* [111] measured densities, sound velocity, viscosities and refractive indexes for binary mixture of $[BMIM]^+[BF_4]^-$ or $[EMIM]^+[BF_4]^-$ with methanol and also of all the pure solvents. These thermophysical properties were measured over the full scope of compositions at T= (278.15 to 318.15) K and under atmospheric pressure. In the entire range of composition at all temperatures, negative values were obtained for both excess molar volume and the excess isentropic compressibility as the temperature increases. The values for deviation on viscosity were constantly negative over the entire composition at all temperatures. Positive values were obtained for deviations on refractive index over the entire range of composition with rise in temperature.

Rafiee and Frouzesh [112] reported density measurement of IL $[EMIM]^+[EtSO_4]^-$ and their binary and ternary mixtures with alkyl alcohol and 1, 3-dichloro-2-propanol at T= (298.15–318.15) K and p=0.087 MPa pressure. The values obtained for excess molar volumes of the binary mixture $[EMIM]^+[EtSO_4]^-$ with alkyl alcohol were negative while positive values were obtained for binary mixture $[EMIM]^+[EtSO_4]^-$ with 1,3-dichloro-2-propanol. For all the investigated binary mixture, these properties decreased with increasing temperature, due to intermolecular interaction and steric effects. Negative values for excess thermal expansion coefficients were obtained for all investigated binary mixtures and the values increased by increasing temperature.

Vaid *et al.* [113] evaluated densities, sound velocity, and refractive indices for, $[BMIM]^+[PF_6]^-$, $[HMIM]^+[PF_6]^-$ and $[OMIM]^+[PF_6]^-$ and their binary mixtures with tetrahydrofuran over the complete composition range at T= (293.15 to 323.15) K under atmospheric pressure. Excess molar volume, excess molar isentropic compressibility and refractive index deviations on volume fraction basis data were calculated and found to be positive for refractive index deviations and negative for both excess molar volumes and excess molar isentropic

compressibilities and became more negative as temperature increases, whereas for refractive index deviation the opposite trend was observed.

Vaid *et al.* [114] reported of densities, sound velocity, and refractive indices for pure ionic liquids, $[BMIM]^+[PF_6]^-$, $[HMIM]^+[PF_6]^-$ and $[OHIM]^+[PF_6]^-$ and their binary mixtures with propylamine at T= (293.15 to 313.15) K and at p= 0.1 MPa. Negative results for excess molar volumes, excess molar isentropic compressibilities were obtained and decreased as temperature increased and positive results for refractive index deviations and increased as temperature increased for all investigate systems.

Wua *et al.* [115] determined the densities and viscosities for the binary liquid mixture of $[BMIM]^+[BF_4]^-$ with acetone, methyl ethyl ketone and *N,N*-dimethylformamide, at T= (303.15 to 333.15) K. The values of both the excess molar volume and the viscosity deviation were negative for all systems.

Singh *et al.* [116] evaluated density and sound velocity for $[EMIM]^+[EtSO_4]^-$ and its binary mixtures with acetic and propionic acid measured at T= (293.15-313.15) K under atmospheric pressure. The values obtained for excess molar volumes and deviations in isentropic compressibility are negative for all the systems at all temperatures over the entire range of composition. It indicated that ion–dipole and hydrogen bonding interactions are predominantly responsible of the mixtures.

Singh *et al.* [117] evaluated density and sound velocity for ILs: $[EMIM]^+[EtSO_4]^-$ and $[BMIM]^+[SCN]^-$and its binary mixtures with acetonitrile measured at T= (293.15-313.15) K and at p = 0.1 MPa. Negative deviations were observed for both excess properties for investigated systems at all temperatures.

Chaudhary *et al.* [118] evaluated the thermophysical which includes density, refractive index, sound velocity and specific conductivity for aqueous mixtures of $[BMIM]^+[BF_4]^-$ with water at T= (293.15–323.15) K over the full composition of range. NMR and FT-IR were used to understand the nature of molecular interactions stirring between $[BMIM]^+[BF_4]^-$ and water, and also to find the moieties in which the interactions are taking place. The results obtained showed that temperature has a substantial effect on the thermophysical properties. Thermophysical studies demonstrated the existence of dispersion forces between $[BMIM]^+[BF_4]^-$ and water and the greatness of dispersion force is more protruding at higher temperatures.

Ciocirlan *et al.* [119] evaluated density and refractive index for the binary systems of $[BMIM]^+[BF_4]^-$ with 1,4-dioxane and $[EMIM]^+[BF_4]^-$ with 1,4-dioxane and ethylene glycol (EG). The experiments for the binary systems with ethylene glycol were made over the complete composition range under atmospheric pressure and at T= (293.15 to 353.15) K for densities and from T= (298.15 to 323.15) K for refractive indices. Negative results for excess molar volumes were obtained for both mixtures with 1,4-dioxane and positive for both mixtures containing ethylene glycol over the complete composition range with deviation refractive index displaying an opposite sign.

Bhagour *et al.* [120] recorded the densities and sound velocity of $[EMIM]^+[BF_4]^-$ with acetone or dimethylsulphoxide binary mixtures at T= (293.15-308.15) K also excess molar enthalpies of the binary mixtures at 298.15 K. The measured results were used to calculate excess molar volumes and excess isentropic compressibilities. The Graph theory was used to calculate state of components of ionic liquid mixtures in their pure and mixed state; nature and extent of interactions existing in mixtures; and excess molar volumes, excess isentropic compressibilities and excess molar enthalpies values.

Iulian and Ciocirlan [121] reported the densities for the binary systems of ILs, 1 $[EMIM]^+[BF_4]^-$ and $[HMIM]^+[BF_4]^-$, with the molecular solvents dimethyl sulfoxide and acetonitrile at atmospheric pressure over the entire range of composition and temperatures from T= (298.15 to 353.15) K. The obtained excess molar volumes were negative for all investigated systems over the entire range of composition at all investigated temperatures.

Rilo *et al.* [122] measured the experimental density for pure ionic liquids of the 1-ethyl-3methylimidazolium alkyl sulphate family, with the alkyl group being ethyl $[EMIM]^+[ES]^-$, butyl $[EMIM]^+[BS]^-$, hexyl $[EMIM]^+[HS]^-$, and octyl $[EMIM]^+[OS]^-$, and their binary mixtures with water and ethanol over whole composition range, at T= (288 to 318) K and under atmospheric pressure. The excess molar volumes values observed were very small for all of the measured systems.

Pal and Kumar [123] reported the experimental densities and sound velocity for binary mixtures of the room temperature ionic liquid $[BMIM]^+[BF_4]^-$ in ethylene glycol monomethyl ether, diethylene glycol monomethyl ether and triethylene glycol monomethyl ether over the whole composition range and at T= (288.15 to 318.15) K. It was found that the excess molar volumes were negative over the whole composition range.

Taib and Murugesan [124] measured the refractive indexes and densities for a binary mixture comprising of $[BMIM]^+[BF_4]^-$ with water and monoethanol amine at T= (293.15 to 353.15) K within the whole range of composition. The excess molar volumes and thermal expansion coefficient data were calculated from new experimental density. Positive values of excess molar volumes were obtained for the whole mole fraction range.

Bhattacharjee *et al.* [125] measured densities and viscosities for binary mixtures of 1-alkyl-3-methylimidazolium alkyl sulphates with water at T= (278 to 343) K and under atmospheric

pressure. Experimental density and viscosity data was reported for four alkyl sulphate ILs, which includes; $[BMIM]^+[HSO_4]^-$, $[BMIM]^+[MeSO_4]^-$, $[EMIM]^+[MeSO_4]^-$ and 1-ethyl-3-methylimidazolium ethyl sulphate $[EMIM]^+[EtSO_4]^-$. Higher values for viscosity and density were obtained for the pure ILs and decreased by increasing mole fraction of water. The density and viscosity of the binary mixtures also decreased when the alkyl side chain of the cation and anion of the IL increased. The excess molar volume and viscosity deviation were calculated and found negative and this showed that denser molecular packing than in pure liquids. The excess molar volume values decreased by increasing temperature. Deviation in viscosity decreases in size as the temperature increases. The deviation in viscosity increased when the cation alkyl chain length increases however only a minimal effect of the anion alkyl chain length was detected.

Chaudhary *et al.* [126] measured the thermophysical properties, density, sound velocity and specific conductivity of $[BMIM]^+[PF_6]^-$ and its binary mixtures with Triton X-45 and Triton X-100 over the whole composition range at temperatures between T= (293.15 to 323.15) K. The excess molar volume, deviation in isentropic compressibility, partial molar excess volume, deviation in partial molar isentropic compressibility and deviation in specific conductivity were calculated. In addition, the spectroscopic properties IR, NHR and NMR of the mixtures were investigated to understand the structural and interactional behaviour of the mixtures.

Ciocirlan *et al.* [127] reported the densities and the dynamic viscosities for selected binary mixtures of the ionic liquid $[BMIM]^+[BF_4]^-$, with polar solvents, dimethyl sulfoxide, and ethylene glycol, in the temperature range from T= (293.15 to 353.15) K. The excess molar volumes were negative for the $[BMIM]^+[BF_4]^-$ with dimethyl sulfoxide system and positive for $[BMIM]^+[BF_4]^-$ with ethylene glycol system over the whole composition range at the investigated temperatures.

Lehmann *et al.* [128] reported densities and excess molar volumes for binary mixtures of ionic liquid $[EMIM]^+[EtSO_4]^-$ with acetone, acetonitrile, propylene carbonate, dichloromethane, methanol, ethanol, and water. The excess molar volumes determined from density measurements for binary mixtures of the $[EMIM]^+[EtSO_4]^-$ with various solvents showed negative values indicating denser molecular packing than in the pure liquids.

Li *et al.* [129] measured densities for $[BMIM]^+[BF_4]^-$ and its binary mixture with aromatic compound aniline at T= (298.15 to 313.15) K and atmospheric pressure over the whole composition range. Furthermore, partial molar volumes, apparent molar volumes and partial molar volumes at infinite dilution were calculated for each component. The values obtained for excess molar volume were negative, this shows that the effects due to ion-dipole interactions and to packing between aniline and $[BMIM]^+[BF_4]^-$ dominate over the disruption of dipolar orders. The excess molar volume values decreased with increase in temperature.

Singh and Kumar [130] measured the thermophysical properties, density and refractive index for $[BMIM]^+[PF_6]^-$ and their binary mixtures with ethylene glycol derivatives: diethylene glycol monomethyl ether, triethylene glycol monomethyl ether, triethylene glycol dimethyl ether and tetraethylene glycol dimethyl ether over the entire composition range. The excess molar volumes, apparent molar volumes, partial molar volumes, excess partial molar volumes, their limiting values at infinite dilution were calculated using the density data obtained respectively. The excess molar volume values obtained became more negative when moving from an alkoxyalkanol to poly ether and it decreased with the increase in temperature for all investigated systems. The experimental refractive index data were used to calculate deviations in refractive index and deviation from additivity on volume fraction basis were positive for all the investigated mixtures over the entire composition range.

Pal *et al.* [131] evaluated densities, sound velocity and refractive indices for the binary mixtures of $[BMIM]^+[PF_6]^-$ with diethylene glycol monomethyl ether, propylene glycol monomethyl ether and propylene glycol monoethyl ether over the entire composition range at atmospheric pressure. Excess molar volume values were calculated from density data, while sound velocity and density data were used to calculate changes in isentropic compressibilities and the experimental refractive indices values were used to calculate the deviation in refractive indices and molar fraction. Solute-solvent interactions were gained from the calculated apparent molar volume and apparent molar compressibility at infinite dilution data.

Han *et al.* [132] measured the densities for a pure $[BMIM]^+[BF_4]^-$ and its binary mixture with ethanol, benzene and acetonitrile at T= (313.2 to 473.2) K. Values for excess molar volumes calculated from the density data are negative, which shows more efficient packing or attractive interactions between the ionic liquid and organic compounds.

Fan *et. al* [133] investigated densities and viscosities for ionic liquid binary mixtures of methyl methacrylate and $[BMIM]^+[PF_6]^-$ over the full concentration range at T= (283.15 to 353.15) K under atmospheric pressure. The excess molar volumes were obtained by utilising the measured experimental densities and fitted to the Redlich-Kister type equation. All the excess molar volume data were negative and turn out to be further and further negative when temperature increases.

Gao *et al.* [134] determined the densities of the binary mixture of $[BMIM]^+[BF_4]^-$ with aromatic compound benzaldehyde over the wide range of compositions at T= (298.15 to 313.15) K and at atmospheric pressure. Excess molar volume values obtained were negative and decreased with an increase in temperature, this displayed the effect due to the ion-dipole interactions and

packing between benzaldehyde and $[BMIM]^+[BF_4]^-$ are dominating over the disruption of dipole orders of benzaldehyde.

Tian *et al.* [135] evaluated experimental densities and viscosities for binary mixtures of IL $[BMIM]^+[BF_4]^-$ + methyl formate or methyl acetate or ethyl formate or acetone at T= 298.15 K. Negative values were obtained for V_m^E in all systems, due to the ion-dipole interactions that dominates. Large negative values for viscosity deviations were found, this is because of the big variance between ionic liquid and the viscosity of the other compound.

Malham and Turmine [136] reported viscosities and refractive indexes for binary mixtures of ILs $[BMIM]^+[BF_4]^-$ and $[BDMIM]^+[BF_4]^-$ with water at T= 298.15 K over the entire composition range. The Lorentz– Lorenz, Wiener, and Gladstone–Dale equations were used to predict the refractive indexes of the pure IL and the binary mixture. Positive values were obtained for refractive index deviation, while negative values were obtained for viscosity deviation.

Dománska and Laskowska [137] reported densities for binary mixtures of 1-ethyl-3methylimidazolium ethyl sulphate $[EMIM]^+[EtSO_4]^-$ with alcohols (1-propanol or 1-butanol or 1-pentanol or 1-hexanol or 1-heptanol or 1-octanol or 1-nonanol or 1-decanol) at T= 298.15 K and ambient pressure. The excess molar volume data were obtained from experimental the density data were both positive and negative. Excess molar volume values obtained for 1-propanol and 1-butanol were negative and these attributed to hydrogen bonding occurring between the short chain alcohols and ionic liquid, and high packing effects.

González *et al.* [138] measured the densities, viscosities, and sound velocity for a binary mixture of $[EMIM]^+[EtSO_4]^-$ with methanol, 1-propanol, and 2-propanol, at T= (298.15 to 328.15) K and measured the refractive index of the binary mixtures at 298.15 K. Density and

sound velocity data measured were used to calculate excess molar volumes, V_m^E and excess molar isentropic compressions, K^E_s for all the binary systems and the values obtained were negative due to ion-dipole interactions. The values for viscosity deviations found were negative in all binary systems over the whole composition range and as the temperature increases the values became less negative, while at T= 298.15 K the refractive index deviations for all three studies systems over a whole temperature range indicates positive values.

Huo *et al.* [139] evaluated densities of the binary mixture of ILs: $[BMIM]^+[PF_6]^-$ $[BMIM]^+[BF_4]^-$ with acetonitrile, benzene and 1-propanol at T= (293.15 to 343.15) K over a whole composition range. The values obtained for the excess molar volume were negative for all the investigated systems, and for benzene binary mixtures the values were furthermost negative. The values became more negative by increasing temperature.

Iglesias-Otero *et al.* [140] measured densities and refractive indexes for $[BMIM]^+[BF_4]^-$ and their binary mixtures with methanol or 1,3-dichloropropane or dimethyl carbonate at T= (293.15 to 318.15) K over the entire composition range. Values obtained for excess molar volume and excess isobaric thermal expansivity were negative for all investigated systems. The values for both deviations of refractive index and excess molar volume came to be more negative with increasing temperature.

Zafarani-Moattar and Majdan-Cegincara [141] investigated viscosity and refractive index of $[BMIM]^+[PF_6]^-$ with tetrahydrofuran, dimethylsulfoxide, methanol, and acetonitrile and also density and sound velocity for solutions of $[BMIM]^+[PF_6]$- with tetrahydrofuran or dimethylsulfoxide over the complete range of composition at T= 298.15 K. The experimental viscosity, refractive index, density, and speed of sound results, the viscosity deviation, refractive index deviation, excess molar volume, and deviation in isentropic compressibility

were estimated, individually. It was established that all of these estimated properties were negative. The Redlich-Kister equation was utilised effectively to correlate viscosity deviation, refractive index deviation, excess molar volume, and deviation in isentropic compressibility data.

Zhong *et al.* [142] reported densities for binary mixtures of IL $[BMIM]^+[PF_6]^-$ with benzyl alcohol or benzaldehyde over the entire composition range at T= (298.15 K to 313.15) K under atmospheric. The excess molar volumes for all the investigated systems were calculated from the density data and correlated using the fourth-order Redlich-Kister equation. Negative values were obtained for excess molar volumes and increased slightly with an increase in temperature. The negative values indicated that the effects due to the ion–dipole interactions and packing between organic molecular liquids benzyl alcohol or benzaldehyde and $[BMIM]^+[PF_6]$- are dominating over the disruption of dipolar orders in benzyl alcohol or benzaldehyde. The excess molar volumes values are for the benzyl alcohol mixtures are more negative this shows that benzaldehyde mixture have stronger ion-dipole interactions.

Gómez *et al.* [143] measured the densities, sound velocity and refractive indexes for binary mixtures of $[EMIM]^+[EtSO_4]^-$ with water and ethanol at T= 298.15 K and 313.15 K. The values for excess molar volume and viscosity deviations were negative and decreased as temperature increased for both systems. The values for deviations in the refractive indexes were positive for both systems.

Arce *et al.* [144] reported experimental densities, viscosities, refractive indices, and sound velocity for binary mixtures of IL: $[EMIM]^+[EtSO_4]^-$ with ethanol or 2-ethoxy-2-methylpropane and ternary mixture of $[EMIM]^+[EtSO_4]^-$ with ethanol + 2-ethoxy-2-methylpropane at T= 298.15 K and atmospheric pressure. The excess molar volumes values calculated from density data for both the ternary and binary system were found negative. The

deviation in viscosity was negative for all system because of the great difference occurring between ionic liquid and the viscosity of other compounds. The isentropic compressibility values for all systems calculated from the density and sound velocity data were found to be negative.

Zhou *et al.* [145] investigated the densities and viscosities of water [H_2O] [BMIM]$^+$[BF_4]$^-$ binary mixture, at temperatures range from T= (303.15 to 353.15) K. The excess molar volume and deviation in viscosity were calculated using the experimental density data and viscosity data, respectively. The results obtained showed that the water content in the binary mixture has a stronger influence on the thermophysical and excess properties.

Zafarani-Moattar and Shekaari [146] reported the density and sound velocity for [BMIM]$^+$[PF_6]$^-$and [TBA]$^+$[PF_6]$^-$and their binary mixtures with organic solvents methanol, acetonitrile, tetrahydrofuran, *N,N*-dimethylacetamide, and dimethylsulfoxide, having an extensive range of dielectric constants. The limiting apparent molar volume and compressibility values were used to obtain data regarding ion–solvent interactions in the studied systems. In addition, the limiting apparent molar volumes for the cation 1-butyl- 3-methyimidazolium were calculated.

Zafarani-Moattar and Shekaari [147] evaluated sound velocity for ILs of [BMIM]$^+$[PF_6]$^-$ or [BMIM]$^+$[BF_4]$^-$ and their binary mixtures with methanol and acetonitrile under atmospheric pressure and T = 298.15 to 318.15 K. Excess molar volume, isentropic compressibility and excess isentropic compressibility data were calculated from the experimental speed of sound data.

Zafarani-Moattar and Shekaari [148] measured the densities and sound velocity for binary mixtures $[BMIM]^+[PF_6]^-$ with methanol or acetonitrile over the whole range of their compositions at T= (298.15 to 318.15) K. Negative values of excess molar volume and isentropic compressibility deviations were obtained for all systems, and more negative in methanol mixtures than acetonitrile.

Zhang *et al.* [149] determined the densities and viscosities of IL $[EMIM]^+[BF_4]^-$ with water at T= (293.15 to 323.15) K. This result displayed that the densities and viscosities are depend on the water content and faintly on temperature. The viscosity deviation was more profound for temperature as compared to the excess molar volume. It was concluded that water content has a stronger impact on the physical properties and excess thermodynamic properties for binary system of $[EMIM]^+[BF_4]^-$ with water.

CHAPTER THREE

EXPERIMENTAL METHODS

3.1. Materials

Imidazolium based ILs used in the present study, namely 1-butyl-3-methylimidazolium tetrafluoroborate $[BMIM]^+[BF_4]^-$ (CAS No 174501-65-6), 1-butyl-3-methylimidazoilum hexafluorophosphate $[BMIM]^+[PF_6]^-$ (CAS No 174501-64-5) and 1-ethyl-3-methylimidazolium tetrafluoroborate $[EMIM]^+[BF_4]^-$ (CAS No 143314-16-3) were obtained from Ionic Liquids Technologies Inc., 1-ethyl-3-methylimidazoium ethylsulfate $[EMIM]^+[EtSO_4]^-$ (CAS No 342573-75-5) was purchased from Sigma-Aldrich. The solvent acetophenone (CAS No 98-86-2) was supplied by Sigma-Aldrich. Deionised water was used in the experiments. The pure components are presented in Table 3.1 together with literature [150-154] reported at T=303.15 K. The mass percent water content was determined using a Metrohm 702 SM Titrino Coulometer (**Figure 3.1**) before the experiments, and was found to be ≤ 0.06 % in the chemicals used. Other impurities possibly due to solvent which was used to clean the IL.

Figure 3.1 Picture of the 702 Titrino Coulometer.

(Taken from Instruction Manual of Metrohm 702 Titrino Coulometer).

Table 3.1

Pure component specifications: suppliers, molecular weight (MW), specified purity and density at T=303.15 K and at pressure p = 0.1 MPa.

Solvent	Supplier	MW/g.mo^{l-1}	% purity	ρ^{lit} ρ/g·cm^{-3}	ρ^{exp} ρ/g·cm^{-3}
[BMIM]$^+$[BF_4]$^-$	Ionic Liquids Technologies Inc.	226.022	99	1.20129[150]	1.19804
[BMIM]$^+$[PF_6]$^-$	Ionic Liquids Technologies Inc.	284.182	99	1.36240[151]	1.36277
[EMIM]$^+$[BF_4]$^-$	Ionic Liquids Technologies Inc.	197.970	98	1.28174[152]	1.27936
[EMIM]$^+$[$EtSO_4$]$^-$	Sigma—Aldrich	236.289	≥98	1.23395[153]	1.23127
Acetophenone	Sigma—Aldrich	120.148	>99	1.01942[154]	1.01817

3.2. Methods and procedure

3.2.1. Sample preparation

The binary mixtures were prepared by transferring via syringe the pure liquids into stoppered bottles to prevent evaporation. The components were filled directly into the air-tight stoppard 10 cm^3 glass vial and then weighed. For the determination of mass of each component, Radwag analytical mass balance was used with a precision of ±0.0001 g. The mixtures were shaken in order to ensure complete homogeneity of the compounds. The samples were degassed using ultra sonic bath and rotary evaporator. After mixing the sample, the bubble free homogeneous samples were injected into the vibration tube or sample cell of the densitometer, sound velocity analyzer, viscometer and refractometer slowly using a medical syringe to avoid formation of

bubbles inside the vibration tubes or sample cell. The chemicals were used without any further purification.

3.2.2. Density and sound velocity measurements

Density and sound velocity for various ILs, acetophenone and mixture of ILs with acetophenone were measured using a digital vibrating-tube densitometer and sound velocity analyzer (Anton Paar DSA 5000M) (see **Figure 3.2**) with an accuracy of T= ±0.02 K. The instrument measured simultaneously the density in the range of (0 to 3) g. cm^{-3} and sound velocity from (1000 to 2000) m. s^{-1} in temperature range of T= (293.15 to 333.15) K with pressure variation from p = (0 to 0.3) MPa. The sound velocity was measured using a propagation time technique [67]. The samples were mediated between two piezoelectric ultrasound transducers. One transducer emits sound waves through the sample-filled cavity (frequency around 3 MHz) and the second transducer receives those waves [155]. Thus, the sound velocity was determined by dividing the known distance between transmitter and receiver by the measured propagation time of the sound waves [67]. The instrument was calibrated with dry air and freshly distilled degassed water once a day. The estimated error in density and speed of sound was less than $u(s) = \pm 2 \times 10^{-4}$ g. cm^{-3} and $u(u) = \pm 1$ m.s^{-1}, respectively. The estimated error in excess molar volume and deviation in isentropic compressibility $u(V_E) = \pm 0.005$ cm^3. mol^{-1} and $u(\kappa_s) \pm 1$ TPa^{-1},respectively.

Figure 3.2 Picture of the Density and Sound Velocity Meter (DSA 5000 M) (Taken from (Instruction Manual of Anton Paar DSA 5000 M)

3.2.3. Viscosity measurements

The viscosities measurements for the pure components and their binary mixtures were determined using an Anton Paar Stabinger Viscometer SVM 3000 (**Figure 3.3**) fitted with jacketed small sample adapter (SSA) and a thermosel spindle (SC4-18) with an accuracy of $u\ (T) = \pm 0.02$ K. Prior to each experimental run, the cell was firstly cleaned with deionised water (liquid 1) and next with acetone (liquid 2) using a fully automatic X-sample 452 Module which performed a cleaning routine after each measurement X-sample 452 performs a cleaning routine after each measurement. The estimated error in viscosity was less than $u\ (T) = \pm 0.02$ K The instrument measured viscosity at temperature range of T= (293.15 to 333.15) K.

Figure 3.3 Picture of the Stabinger Viscometer (SVM 3000)

(Taken from Instruction Manual of Anton Paar SVM 3000)

3.2.4. Refractive index measurements

Measurement of the refractive index for pure components and their binary mixtures were measured by an Abbemat digital automatic refractometer (Anton Paar RXA 156) (see **Figure 3.4**) with an accuracy $u\ (T) = \pm 0.03$ K. The estimated error in refractive index was less than u $u\ (n_D) = \pm 0.005$. The instrument measured refractive index at temperature range of (293.15 to 333.15) K.

Figure 3.4 Picture of the Abbemat digital automatic refractometer (RXA 156)

(Taken from Instruction Manual of Anton Paar RXA 156)

3.2.5. Quantum Chemical Calculations

In other to validate our experimental results on the study, quantum chemical calculations were used to investigate the inter-ionic interactions between the cations and anions of the ionic liquids studied both in gaseous state and in continuum solvation with acetophenone by utilizing the integral formalism variant of the polarized continuum model (IEFPCM) [156].

Geometry optimizations of the molecular structures of $[BMIM]^+[BF_4]^-$, $[BMIM]^+[PF_6]^-$, $[EMIM]^+[BF_4]^-$ and $[EMIM]^+[EtSO_4]^-$ were done using the Density Functional Theory (DFT) method. The Perdew-Wang hybrid exchange-correlation functional (B3PW91) [157-158] and Pople-type split-valence triple-zeta basis set [159] augmented with diffuse and polarization functions on both the hydrogen and heavier atoms (6-311++G (d,p)) were selected for all the calculations. The B3PW91 (/6-311++G (d,p) was selected because its adequate prediction of ionic liquids properties has been reported [160-162]. Frequency calculations were carried out on the optimized structures and the absence of imaginary frequencies confirmed that the optimized structures are true energy minima. Both geometry optimizations and frequency calculations were performed with ultrafine grid (99 radical and 590 angular points) to increase the accuracy of the results [163]. All the quantum chemical calculations were performed using Windows based Gaussian 09 suite version D.01 [164].

CHAPTER FOUR

RESULTS

4.1. Density (ρ), sound velocity (u), viscosity (η), refractive index (n_D), excess molar volumes (V^E_m), isentropic compressibility deviation ($\Delta\kappa_s$), viscosity deviation ($\Delta\eta$), refractive index deviation (Δn_D)

The density, speed of sound, viscosity, refractive index, excess molar volume, isentropic compressibility deviation , viscosity deviations and refractive index deviation for the binary mixtures of alkyl imidazolium-based ILs $[BMIM]^+[BF_4]^-$ or $[BMIM]^+[PF_6]^-$ or $[EMIM]^+[BF_4]$ or $[EMIM]^+[EtSO_4]^-$ with acetophenone were measured at temperature range from T= (293.15 to 333.15) K as a function of IL concentration under atmospheric pressure are presented in Table 4.1.

The viscosity deviations, $\Delta\eta$ for the studied mixtures were calculated using the expression in (4.1)

$$\Delta\eta = \eta - x_1\eta_1 - x_2\eta_2 \qquad (4.1)$$

where x_1 and x_2 are the mole fractions of the pure components (1 and 2), η_1 and η_2 is the viscosity of the pure components (1 and 2) and η is the viscosity of the mixture.

Equation 4.5 was used to calculate refractive indexes deviation, Δn of the studied systems

$$\Delta n = n - x_1 n_1 - x_2 n_2 \qquad (4.2)$$

where x_1 and x_2 are the mole fractions of the pure components (1 and 2), n_1 and n_2 are the refractive indexes of the pure components (1 and 2) and n is the refractive index of the mixture.

Table 4.1

Mole fraction (x_1) of IL, density (ρ), sound velocity (u), viscosity (η), refractive index (n_D), excess molar volumes (V^E_m), isentropic Compressibility deviation ($\Delta\kappa_s$), viscosity deviation ($\Delta\eta$), and refractive index deviation (Δn_D) for IL+ acetophenone binary mixtures $[BMIM]^+[BF_4]^-$or $[BMIM]^+[PF_6]^-$or $[EMIM]^+[BF_4]^-$or $[EMIM]^+[EtSO_4]^-$ at T= (293.15, 303.15, 313.15. 323.15 and 333.15) K and at pressure p = 0.1 MPa.

x_1	ρ/g·cm^{-3}	u/m·s^{-1}	η/mPa·s	n_D	V^E_m /cm^3·mol^{-1}	κ_s/TPa^{-1}	$\Delta\kappa$s/TPa^{-1}	$\Delta\eta$/ mPa·s	Δn
				{$[BMIM]^+[BF_4]^-$ (1) + acetophenone (2)}					
T=293.15 K									
0.0000	1.0279	1497	1.91	1.533	0.000	217948	00000	0.000	0.0000
0.0484	1.0348	1506	7.00	1.526	0.755	219056	16482	-1.275	-0.0020
0.0974	1.0430	1513	11.77	1.518	1.320	219505	26452	-2.948	-0.0043
0.1946	1.0566	1524	22.32	1.501	2.572	219938	41628	-5.162	-0.0103
0.2935	1.0701	1533	26.01	1.488	3.691	219638	49673	-14.469	-0.0132
0.3921	1.0846	1542	29.49	1.475	4.457	219227	56572	-23.943	-0.0145
0.4936	1.1013	1551	34.38	1.464	4.794	218364	59273	-32.389	-0.0143
0.6024	1.1227	1561	41.70	1.454	4.383	216973	57523	-39.366	-0.0129
0.6940	1.1403	1568	42.42	1.447	3.882	215511	53135	-50.687	-0.0097
0.7954	1.1598	1572	43.58	1.442	3.127	213134	40687	-62.838	-0.0038
0.8999	1.1842	1578	55.66	1.437	1.451	210188	22891	-64.488	0.0025
0.9487	1.1940	1578	78.88	1.432	0.836	208557	12038	-47.696	0.0036
1.0000	1.2052	1579	133.31	1.423	0.000	206780	00000	0.000	0.0000
T= 303.15 K									
0.0000	1.0192	1460	1.65	1.528	0.000	209110	00000	0.000	0.0000
0.0484	1.0261	1469	5.00	1.522	0.777	210222	14622	-0.319	-0.0012
0.0974	1.0342	1477	8.04	1.514	1.362	210978	25712	-1.002	-0.0033
0.1946	1.0480	1489	11.65	1.498	2.656	211674	39691	-4.756	-0.0094
0.2935	1.0614	1500	13.72	1.484	3.814	211900	49081	-10.184	-0.0127
0.3921	1.0759	1510	16.94	1.472	4.615	211815	55348	-14.440	-0.0139
0.4936	1.0926	1520	21.29	1.461	4.981	211423	58753	-17.785	-0.0136
0.6024	1.1140	1531	25.87	1.451	4.589	210375	56119	-21.453	-0.0118
0.6940	1.1316	1539	28.63	1.444	4.102	209240	51380	-25.638	-0.0090

0.7954	1.1511	1544	30.80	1.439	3.360	207196	38259	-31.156	-0.0033
0.8999	1.1755	1551	38.61	1.434	1.685	204589	19729	-31.267	0.0031
0.9487	1.1853	1552	50.37	1.430	1.073	203253	9890	-23.210	0.0038
1.0000	1.1980	1555	77.46	1.421	0.000	201894	0000	0.000	0.0000
$T = 313.15$ K									
0.0000	1.0104	1423	1.37	1.523	0.000	200506	00000	0.000	0.0000
0.0484	1.0173	1432	3.65	1.518	0.801	201598	12573	-0.029	-0.0007
0.0974	1.0255	1441	5.67	1.510	1.407	202486	23127	-0.346	-0.0026
0.1946	1.0392	1455	7.13	1.494	2.745	203739	38972	-3.517	-0.0088
0.2935	1.0538	1467	8.33	1.480	3.792	204144	46403	-7.039	-0.0124
0.3921	1.0672	1477	9.85	1.469	4.783	204537	53696	-10.213	-0.0130
0.4936	1.0838	1488	10.79	1.459	5.180	204413	55918	-14.119	-0.0125
0.6024	1.1052	1501	11.83	1.449	4.809	203945	54955	-18.261	-0.0110
0.6940	1.1229	1510	16.90	1.442	4.339	203038	49014	-17.565	-0.0079
0.7954	1.1423	1516	18.98	1.437	3.613	201293	35020	-20.317	-0.0021
0.8999	1.1668	1524	21.57	1.432	1.941	198962	15285	-22.713	0.0034
0.9487	1.1766	1527	30.48	1.427	1.333	198147	8799	-16.127	0.0037
1.0000	1.1910	1532	49.05	1.418	0.000	197092	0000	0.000	0.0000
$T = 323.15$ K									
0.0000	1.0017	1387	1.17	1.519	0.000	192156	00000	0.000	0.0000
0.0484	1.0087	1396	2.80	1.513	0.816	193260	10900	0.093	-0.0006
0.0974	1.0167	1406	3.81	1.506	1.454	194337	21532	-0.454	-0.0024
0.1946	1.0304	1421	4.79	1.491	2.839	195841	36294	-2.567	-0.0078
0.2935	1.0450	1433	5.43	1.476	3.929	196557	43176	-5.069	-0.0118
0.3921	1.0584	1445	6.54	1.466	4.961	197312	50440	-7.095	-0.0120
0.4936	1.0751	1458	7.62	1.456	5.392	197693	53960	-9.245	-0.0118
0.6024	1.0965	1472	9.74	1.446	5.045	197575	52477	-10.587	-0.0100
0.6940	1.1141	1482	12.22	1.440	4.592	197073	47193	-11.022	-0.0071
0.7954	1.1336	1489	13.65	1.435	3.884	195676	32931	-12.809	-0.0012
0.8999	1.1580	1498	15.40	1.429	2.222	193733	13208	-14.390	0.0036
0.9487	1.1678	1501	20.37	1.425	1.619	192893	4659	-10.974	0.0042
1.0000	1.1839	1509	32.97	1.415	0.000	192441	00000	0.000	0.0000
$T = 333.15$ K									
0.0000	0.9928	1352	1.02	1.514	0.000	184161	0.000	0.000	0.0000
0.0484	0.9997	1361	2.22	1.508	0.854	185285	9474	0.124	-0.0004
0.0974	1.0079	1370	3.23	1.502	1.506	186352	18307	0.035	-0.0021
0.1946	1.0255	1390	4.54	1.487	2.412	188370	34822	-0.812	-0.0069
0.2935	1.0362	1401	4.82	1.474	4.077	189298	40383	-2.741	-0.0105
0.3921	1.046	1413	5.66	1.463	5.156	190347	47161	-4.096	-0.0116
0.4936	1.0662	1427	6.22	1.453	5.623	191031	50190	-5.802	-0.0107
0.6024	1.0876	1443	6.73	1.444	5.303	191496	50738	-7.715	-0.0089
0.6940	1.1053	1454	9.21	1.438	4.872	191298	45314	-7.270	-0.0061
0.7954	1.1247	1462	10.25	1.433	4.184	189953	28044	-8.497	-0.0004
0.8999	1.1491	1472	11.48	1.427	2.525	188583	10415	-9.590	0.0041
0.9487	1.1590	1477	12.85	1.422	1.929	188170	4453	-9.309	0.0045
1.0000	1.1769	1487	23.30	1.413	0.000	187918	0.000	0.000	0.0000

{$[BMIM]^+[PF_6]^-$ (1) + acetophenone (2)}

$T = 293.15$ K									
0.0000	1.0279	1497	1.91	1.533	0.000	217948	00000	0.000	0.0000
0.0500	1.0550	1510	8.38	1.526	0.258	215996	-10397	-8.116	-0.0068
0.0998	1.0806	1523	16.17	1.518	0.428	214687	-14397	-14.840	-0.0132
0.2001	1.1199	1545	28.17	1.502	1.626	213250	-10469	-32.087	-0.0251
0.3030	1.1500	1565	35.57	1.486	3.425	213107	6873	-54.677	-0.0326
0.4001	1.1749	1583	49.32	1.473	5.075	213384	27359	-69.216	-0.0361
0.5027	1.1996	1598	59.76	1.461	6.569	212978	42027	-88.713	-0.0360

0.6092	1.2301	1615	73.27	1.450	6.968	211912	50806	-106.25	-0.0325
0.7001	1.2569	1626	80.80	1.444	6.800	210308	51349	-125.21	-0.0268
0.8017	1.2898	1636	88.37	1.437	5.770	207568	42482	-147.27	-0.0191
0.9087	1.3290	1646	128.92	1.429	3.556	203951	25842	-137.91	-0.0095
0.9496	1.3458	1649	176.23	1.424	2.314	202105	14836	-102.51	-0.0055
1.0000	1.3712	1655	293.44	1.411	0.000	199701	00000	0.000	0.0000
T = 303.15 K									
0.0000	1.0191	1460	1.65	1.528	0.000	209110	00000	0.000	0.0000
0.0500	1.0463	1473	4.64	1.521	0.258	207279	-10397	-5.033	-0.0013
0.0998	1.0719	1486	7.66	1.512	0.428	206075	-14398	-9.996	-0.0037
0.2001	1.1112	1509	14.34	1.497	1.642	205054	-10470	-19.409	-0.0074
0.3030	1.1413	1529	18.50	1.481	3.469	204882	68730	-31.745	-0.0104
0.4001	1.1662	1547	22.93	1.468	5.146	205343	27360	-42.875	-0.0121
0.5027	1.1910	1565	32.38	1.456	6.665	205535	42027	-49.894	-0.0120
0.6092	1.2214	1583	40.88	1.445	7.076	205154	50806	-58.465	-0.0100
0.7001	1.2482	1596	45.05	1.439	6.911	204130	51350	-68.870	-0.0054
0.8017	1.2811	1607	48.50	1.432	5.875	201667	42482	-81.711	0.0001
0.9087	1.3203	1617	67.92	1.424	3.641	198158	25843	-79.459	0.0051
0.9496	1.3371	1622	88.86	1.419	2.387	196845	14837	-65.067	0.0049
1.0000	1.3628	1630	162.01	1.408	0.000	195074	00000	0.000	0.000
T=313.15K									
0.0000	1.0104	1423	1.37	1.523	0.000	200506	00000	0.000	0.0000
0.0500	1.0375	1435	3.57	1.517	0.258	198518	-11280	-2.610	-0.0009
0.0998	1.0632	1449	5.62	1.508	0.428	197447	-16335	-5.339	-0.0033
0.2001	1.1024	1473	8.03	1.493	1.660	196889	-12460	-12.556	-0.0068
0.3030	1.1326	1494	12.30	1.478	3.516	197107	257	-18.161	-0.0096
0.4001	1.1575	1514	16.51	1.465	5.221	198017	18487	-23.266	-0.0114
0.5027	1.1822	1532	21.57	1.453	6.768	198544	34816	-28.060	-0.0115
0.6092	1.2127	1551	28.28	1.443	7.190	198480	45953	-31.576	-0.0086
0.7001	1.2395	1566	32.30	1.437	7.030	197799	48472	-36.284	-0.0040
0.8017	1.2724	1578	35.02	1.430	5.988	195732	38103	-43.311	0.0008
0.9087	1.3114	1592	45.80	1.422	3.751	193217	18026	-42.808	0.0061
0.9496	1.3283	1598	62.26	1.417	2.485	192161	10634	-30.266	0.0058
1.0000	1.3544	1608	97.37	1.406	0.000	190808	00000	0.000	0.0000
T=323.15 K									
0.0000									
0.0500	1.0017	1387	1.17	1.519	0.000	192156	00000	0.000	0.0000
0.0998	1.0288	1399	1.89	1.512	0.259	190261	-15026	-2.345	-0.0007
0.2001	1.0544	1413	4.34	1.505	0.429	189288	-20912	-2.955	-0.0020
0.3030	1.0937	1436	6.00	1.489	1.680	188541	-16766	-7.439	-0.0060
0.4001	1.1238	1458	8.01	1.474	3.567	189174	-4602	-11.747	-0.0090
0.5027	1.1487	1479	11.57	1.462	5.303	190424	13911	-14.135	-0.0103
0.6092	1.1735	1499	15.22	1.450	6.879	191500	29139	-16.786	-0.0103
0.7001	1.2039	1521	20.06	1.441	7.316	192202	38828	-18.469	-0.0076
0.8017	1.2307	1537	23.24	1.435	7.161	191826	40828	-20.872	-0.0027
0.9087	1.2636	1549	26.47	1.428	6.115	189856	30012	-23.865	0.0022
0.9496	1.3028	1564	30.22	1.421	3.843	187702	15242	-26.686	0.0070
1.0000	1.3196	1571	40.99	1.416	2.566	187017	8641	-18.418	0.0067
	1.3460	1585	62.50	1.403	0.000	186647	0000	0.000	0.0000
T=333.15 K									
0.0000	0.9928	1352	1.09	1.514	0.000	184156	0.0000	0.000	0.0000
0.0500	1.0199	1364	1.62	1.508	0.261	182403	-16190	-1.529	-0.0005
0.0998	1.0456	1378	3.48	1.501	0.433	181495	-23180	-1.726	-0.0016
0.2001	1.0848	1400	4.67	1.486	1.706	180693	-25118	-4.667	-0.0049
0.3030	1.115	1424	8.28	1.471	3.629	181845	-13124	-5.290	-0.0085
0.4001	1.1399	1446	9.34	1.459	5.398	183383	47260	-8.229	-0.0094
0.5027	1.1646	1467	10.24	1.447	7.007	184754	21141	-11.559	-0.0093

0.6092	1.1950	1490	14.21	1.438	7.461	185763	34028	-11.975	-0.0066
0.7001	1.2219	1506	17.72	1.433	7.315	185695	35279	-12.215	-0.0017
0.8017	1.2548	1522	18.62	1.426	6.267	184531	21170	-15.495	0.0036
0.9087	1.2940	1539	20.25	1.419	3.980	182996	5526	-18.281	0.0079
0.9496	1.3107	1546	27.58	1.414	2.691	182311	932	-12.633	0.0074
1.0000	1.3379	1563	42.29	1.400	0.000	182623	0.000	0.000	0.0000

{[EMIM]$^+$[BF$_4$]$^-$ (1) + acetophenone (2)}

T=293.15 K

0.0000	1.0279	1497	1.91	1.533	0.000	217948	0.000	0.000	0.0000
0.0502	1.0477	1509	2.45	1.527	-0.362	217378	-1778	-1.508	-0.0002
0.1082	1.0680	1522	3.20	1.519	-0.557	216942	-1595	-3.122	-0.0009
0.1993	1.0960	1543	4.74	1.507	-0.579	217264	8744	-5.294	-0.0027
0.2995	1.1201	1564	6.79	1.492	-0.028	218510	29049	-7.328	-0.0054
0.4021	1.1398	1583	8.73	1.478	0.918	219838	50352	-9.565	-0.0073
0.5011	1.1573	1598	12.34	1.466	1.859	220590	65623	-10.990	-0.0076
0.5997	1.1715	1608	16.03	1.456	3.043	220581	73246	-12.320	-0.0053
0.7001	1.1901	1618	19.74	1.449	3.618	220013	75413	-14.698	-0.0011
0.8050	1.211	1628	21.73	1.440	3.779	218705	70544	-16.978	0.0025
0.9060	1.2407	1638	25.54	1.429	2.837	216263	54035	-14.792	0.0035
0.9584	1.2616	1640	32.13	1.421	1.560	213206	27558	-8.840	0.0017
1.0000	1.2826	1642	42.66	1.414	0.000	210125	00000	0.000	0.0000

T =303.15K

0.0000	1.0191	1460	1.65	1.528	0.000	209110	0.000	0.000	0.0000
0.0502	1.0390	1471	2.03	1.522	-0.364	208332	-5932	-0.950	-0.0001
0.1082	1.0592	1485	2.56	1.515	-0.554	208259	-4524	-1.959	-0.0009
0.1993	1.0873	1507	3.61	1.503	-0.571	208936	5598	-3.327	-0.0022
0.2995	1.1076	1528	4.97	1.488	0.440	210675	26682	-4.622	-0.0051
0.4021	1.1273	1546	6.53	1.474	1.422	212033	44043	-5.782	-0.0069
0.5011	1.1448	1561	8.85	1.463	2.398	212818	55531	-7.096	-0.0067
0.5997	1.1590	1571	11.03	1.454	3.624	212842	59406	-7.524	-0.0047
0.7001	1.1776	1581	12.90	1.446	4.229	212275	57428	-8.313	0.0000
0.8050	1.1995	1591	14.27	1.437	4.412	211033	48875	-9.727	0.0028
0.9060	1.2282	1601	16.90	1.426	3.470	208686	29125	-8.783	0.0040
0.9584	1.2491	1608	21.22	1.419	2.178	206998	14173	-5.846	0.0022
1.0000	1.2750	1618	28.17	1.412	0.000	205428	00000	0.000	0.0000

T=313.15 K

0.0000	1.0104	1423	1.37	1.523	0.000	200506	0000	0.000	0.0000
0.0502	1.0303	1435	1.68	1.518	-0.366	199806	-7132	-0.634	0.0000
0.1082	1.0505	1449	2.09	1.510	-0.554	199800	-7349	-1.307	-0.0006
0.1993	1.0785	1472	3.09	1.498	-0.560	200827	2677	-2.007	-0.0023
0.2995	1.0988	1491	3.84	1.484	0.479	202327	17413	-3.125	-0.0048
0.4021	1.1185	1511	5.23	1.471	1.490	203992	33796	-3.650	-0.0065
0.5011	1.1360	1527	6.02	1.460	2.496	205270	46316	-4.717	-0.0060
0.5997	1.1503	1538	8.15	1.451	3.755	205679	50140	-5.421	-0.0040
0.7001	1.1689	1550	9.45	1.443	4.385	205476	47844	-6.001	0.0000
0.8050	1.1907	1560	10.91	1.435	4.588	204298	35788	-6.495	0.0034
0.9060	1.2195	1572	12.35	1.424	3.649	20255	18108	-5.949	0.0043
0.9584	1.2404	1581	15.35	1.416	2.349	201604	8447	-3.921	0.0027
1.0000	1.2674	1595	20.05	1.409	0.000	200770	0000	0.000	0.0000

T=323.15 K

0.0000	1.0017	1387	1.17	1.519	0.000	192156	0.000	0.000	0.0000

0.0502	1.0215	1398	1.42	1.513	-0.368	191258	-11030	-0.438	-0.0001
0.1082	1.0417	1413	1.76	1.506	-0.552	191589	-10086	-0.900	-0.0002
0.1993	1.0698	1437	2.36	1.495	-0.547	193020	510	-1.550	-0.0016
0.2995	1.0901	1457	3.10	1.481	0.522	194755	13762	-2.189	-0.0043
0.4021	1.1098	1477	4.14	1.468	1.565	196448	26509	-2.563	-0.0058
0.5011	1.1273	1493	4.73	1.457	2.602	197807	36049	-3.334	-0.0056
0.5997	1.1415	1506	6.29	1.448	3.897	198721	41162	-4.129	-0.0034
0.7001	1.1601	1519	7.25	1.441	4.553	198778	37638	-4.551	0.0005
0.8050	1.1820	1530	8.09	1.432	4.777	198180	27378	-5.158	0.0041
0.9060	1.2107	1544	9.43	1.422	3.844	197024	11686	-4.210	0.0048
0.9584	1.2316	1555	11.61	1.414	2.534	196455	3851	-2.748	0.0031
1.0000	1.2600	1572	14.93	1.407	0.000	196239	0000	0.000	0.0000
T = 333.15 K									
0.0000	0.9928	1352	1.09	1.514	0.000	184155	00000	0.000	0.0000
0.0502	1.0126	1363	1.23	1.508	-0.368	183334	-12069	-0.382	0.0003
0.1082	1.0329	1377	1.52	1.502	-0.548	183454	-15315	-0.701	0.0000
0.1993	1.0609	1400	2.00	1.490	-0.531	184686	-9986	-1.168	-0.0017
0.2995	1.0812	1422	2.58	1.477	0.573	186950	4959	-1.636	-0.0041
0.4021	1.1009	1442	3.39	1.464	1.650	188960	17186	-1.897	-0.0053
0.5011	1.1184	1462	3.49	1.454	2.721	191153	31524	-1.837	-0.0052
0.5997	1.1326	1476	5.03	1.446	4.055	192431	36738	-2.321	-0.0025
0.7001	1.1513	1490	5.77	1.438	4.740	192935	34074	-2.333	0.0009
0.8050	1.1705	1502	7.18	1.430	5.335	192735	24021	-2.320	0.0046
0.9060	1.2019	1520	7.45	1.419	4.063	192202	10935	-2.100	0.0050
0.9584	1.2228	1531	9.09	1.412	2.746	191717	2059	-1.009	0.0034
1.0000	1.2525	1550	11.53	1.404	0.000	191830	0000	0.000	0.0000

{$[EMIM]^+[EtSO_4]^-$ (1) + acetophenone (2)}

T = 293.15 K									
0.0000	1.0279	1497	1.91	1.533	0.000	217948	0000	0.000	0.0000
0.0498	1.0454	1511	3.04	1.531	-0.118	218494	-1526	-3.648	0.0012
0.1001	1.0623	1526	3.67	1.528	-0.250	219062	-2902	-7.856	0.0008
0.2027	1.0935	1552	4.30	1.521	-0.480	220261	-5298	-17.085	-0.0017
0.3079	1.1240	1577	6.86	1.513	-0.948	221197	-10686	-24.622	-0.0036
0.4001	1.1480	1596	10.10	1.507	-1.337	221962	-15968	-30.246	-0.0044
0.4994	1.1699	1615	14.88	1.502	-1.543	223080	-18696	-34.988	-0.0047
0.5998	1.1886	1634	22.57	1.497	-1.549	224627	-17308	-36.946	-0.0045
0.6992	1.2016	1652	30.24	1.493	-1.020	227135	-6170	-38.825	-0.0033
0.8000	1.2101	1669	40.28	1.490	0.021	230063	8983	-38.463	-0.0008
0.9003	1.2190	1684	55.87	1.487	0.593	232551	19803	-32.511	0.0016
0.9495	1.2278	1691	68.31	1.485	0.573	232912	16503	-24.804	0.0019
1.0000	1.2382	1695	97.96	1.480	0.000	231969	00000	0.000	0.0000
T = 303.15 K									
0.0000	1.0192	1460	1.65	1.528	0.000	209110	0000	0.000	0.0000
0.0498	1.0367	1474	2.48	1.527	-0.101	209705	-2741	-2.081	0.0014
0.1001	1.0536	1489	2.88	1.524	-0.231	210413	-4453	-4.633	0.0011
0.2027	1.0848	1516	5.31	1.517	-0.437	211877	-7745	-8.211	-0.0013
0.3079	1.1153	1542	6.60	1.509	-0.885	213177	-13120	-13.082	-0.0031
0.4001	1.1393	1562	8.39	1.504	-1.254	214271	-18287	-16.686	-0.0042
0.4994	1.1612	1583	11.85	1.499	-1.434	215703	-21297	-19.034	-0.0043
0.5998	1.1799	1602	16.37	1.494	-1.410	217547	-20406	-20.395	-0.0042
0.6992	1.1927	1621	21.33	1.490	-0.818	220359	-9653	-21.263	-0.0028
0.8000	1.2014	1640	27.09	1.487	0.244	223784	6992	-21.403	-0.0005
0.9003	1.2103	1656	35.33	1.484	1.137	226537	17007	-19.027	0.0017
0.9495	1.2191	1663	43.94	1.482	0.850	226910	12129	-13.308	0.0022
1.0000	1.2313	1670	60.20	1.478	0.000	226579	00000	0.000	0.0000

$T = 313.15$ K

0.0000	1.0104	1423	1.37	1.523	0.000	200506	0000	0.000	0.0000
0.0498	1.0280	1438	2.00	1.523	-0.090	201178	-3650	-1.292	0.0016
0.1001	1.0449	1453	3.32	1.520	-0.209	202096	-4951	-1.905	0.0014
0.2027	1.0761	1481	4.64	1.513	-0.391	203725	-10023	-4.530	-0.0009
0.3079	1.1065	1507	5.65	1.506	-0.815	205356	-15624	-7.572	-0.0028
0.4001	1.1305	1529	7.20	1.500	-1.162	206770	-20686	-9.570	-0.0039
0.4994	1.1525	1550	9.80	1.495	-1.314	208507	-23976	-10.786	-0.0042
0.5998	1.1711	1571	11.89	1.491	-1.258	210640	-23569	-12.564	-0.0037
0.6992	1.1841	1591	14.50	1.487	-0.651	213682	-13852	-13.786	-0.0025
0.8000	1.1926	1610	17.96	1.484	0.486	217442	2769	-14.197	-0.0001
0.9003	1.2017	1628	23.95	1.482	1.425	220672	14179	-12.064	0.0019
0.9495	1.2103	1637	28.98	1.479	1.150	221421	11416	-8.933	0.0020
1.0000	1.2245	1646	39.86	1.475	0.000	221331	0000	0.000	0.0000

$T = 323.15$ K

0.0000	1.0017	1387	1.17	1.519	0.000	192156	0000	0.000	0.0000
0.0498	1.0192	1402	1.68	1.518	-0.079	192845	-5093	-0.815	0.0017
0.1001	1.0361	1417	1.94	1.516	-0.186	193829	-7376	-1.907	0.0018
0.2027	1.0673	1446	2.19	1.509	-0.341	195962	-10766	-4.394	-0.0004
0.3079	1.0978	1473	3.41	1.502	-0.740	197760	-18122	-5.977	-0.0024
0.4001	1.1218	1496	5.80	1.497	-1.064	199484	-23095	-6.053	-0.0034
0.4994	1.1437	1518	7.99	1.492	-1.186	201517	-26664	-6.515	-0.0038
0.5998	1.1624	1540	9.33	1.487	-1.095	203930	-26730	-7.853	-0.0033
0.6992	1.1754	1561	10.72	1.484	-0.445	207228	-17691	-9.125	-0.0021
0.8000	1.1839	1581	13.12	1.482	0.743	211177	-2477	-9.416	0.0001
0.9003	1.1928	1601	17.14	1.479	1.731	214979	11389	-8.075	0.0021
0.9495	1.2016	1611	20.59	1.477	1.469	215911	8840	-5.940	0.0021
1.0000	1.2177	1623	27.88	1.472	0.000	216243	0000	0.000	0.0000

$T = 333.15$ K

0.0000	0.9928	1352	1.02	1.514	0.000	184155	0000	0.000	0.0000
0.0498	1.0103	1365	1.46	1.514	-0.066	184345	-6382	-0.522	0.0021
0.1001	1.0273	1379	1.66	1.511	-0.159	185102	-7237	-1.298	0.0020
0.2027	1.0585	1404	1.86	1.505	-0.285	186342	-11938	-3.084	-0.0002
0.3079	1.0889	1428	3.57	1.498	-0.656	187323	-19682	-3.402	-0.0021
0.4001	1.1129	1448	4.86	1.493	-0.952	188321	-25076	-3.893	-0.0034
0.4994	1.1348	1467	6.76	1.488	-1.041	189620	-28632	-3.915	-0.0035
0.5998	1.1535	1485	8.27	1.484	-0.913	191280	-28786	-4.353	-0.0029
0.6992	1.1665	1503	9.62	1.481	-0.216	193775	-20419	-4.919	-0.0017
0.8000	1.1750	1521	11.90	1.479	1.028	196874	-6237	-4.595	0.0003
0.9003	1.1839	1538	14.22	1.476	2.068	199827	6566	-4.212	0.0023
0.9495	1.1927	1548	16.22	1.474	1.828	200874	8817	-3.165	0.0023
1.0000	1.2110	1560	20.36	1.470	0.000	200834	0000	0.000	0.0000

The density values for all studied binary mixtures increased as concentration of the IL in acetophenone increased and decreased with temperatures as shown in **Figure 4.1 (a, b, c and d)**.

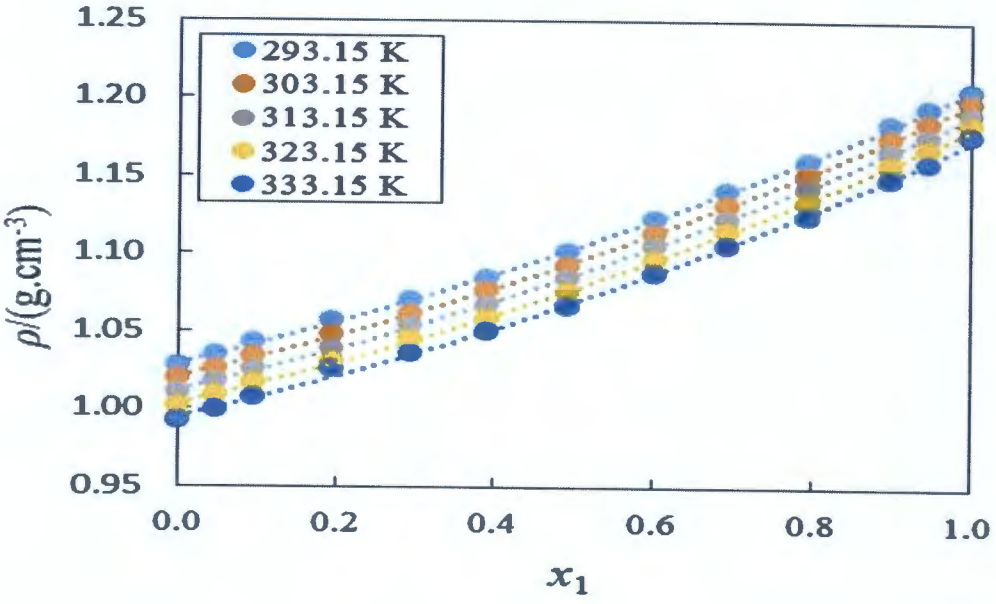

Fig 4.1a

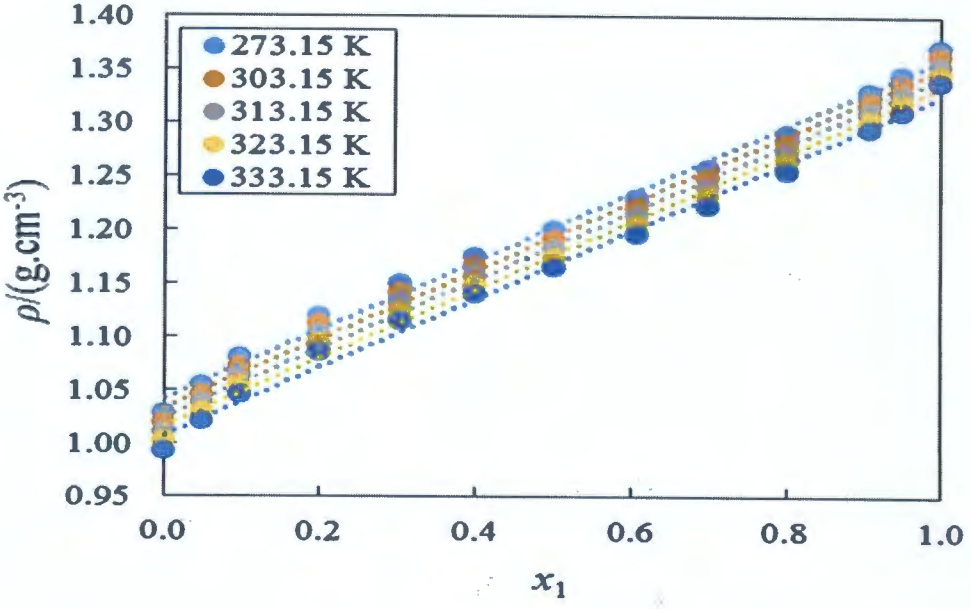

Fig 4.1b

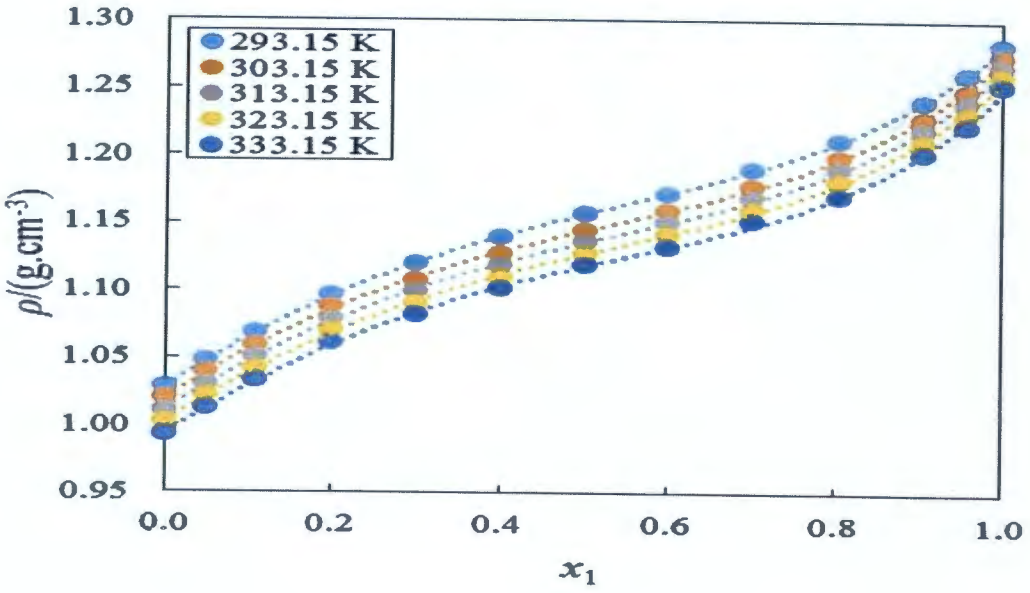

Fig 4.1c

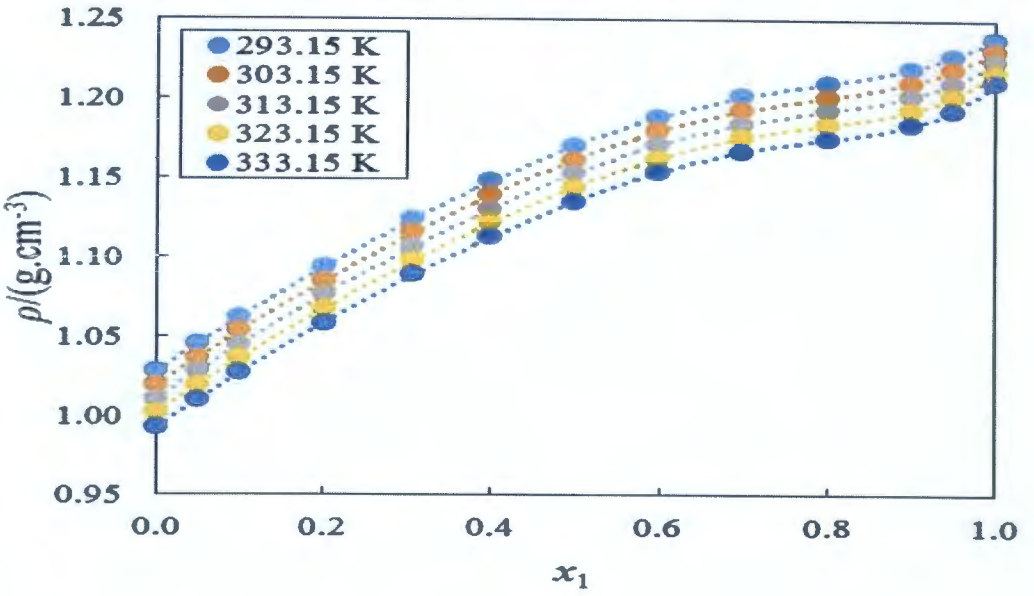

Fig 4.1d

Figure 4.1 Density (ρ) *vs* mole fraction of IL for IL (1)+ acetophenone(2): (a) $[BMIM]^+[BF_4]^-$, (b) $[BMIM]^+[PF_6]^-$, (c) $[EMIM]^+[BF_4]^-$ and (d) $[EMIM]^+[EtSO_4]^-$ at T= (293.15, 303.15, 313.15, 323.15 and 333.15) K. The dotted line represents the smoothness of these data.

At a given temperature, the sound velocity values increased as the concentration of IL increases in the mixture and decreased as the temperature is increasing for all studied systems [see **Figure 4.2 (a, b, c and d)**].

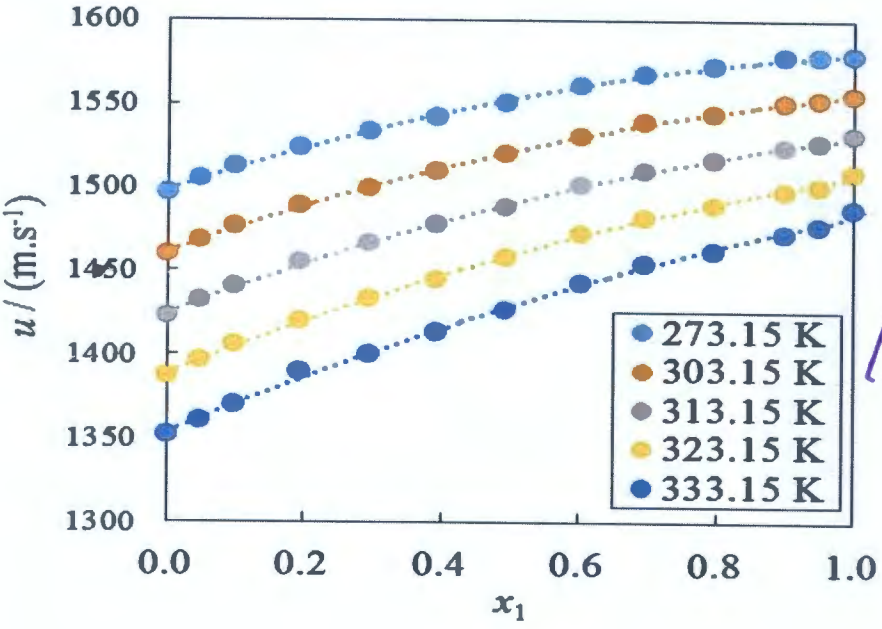

Fig 4.2 a

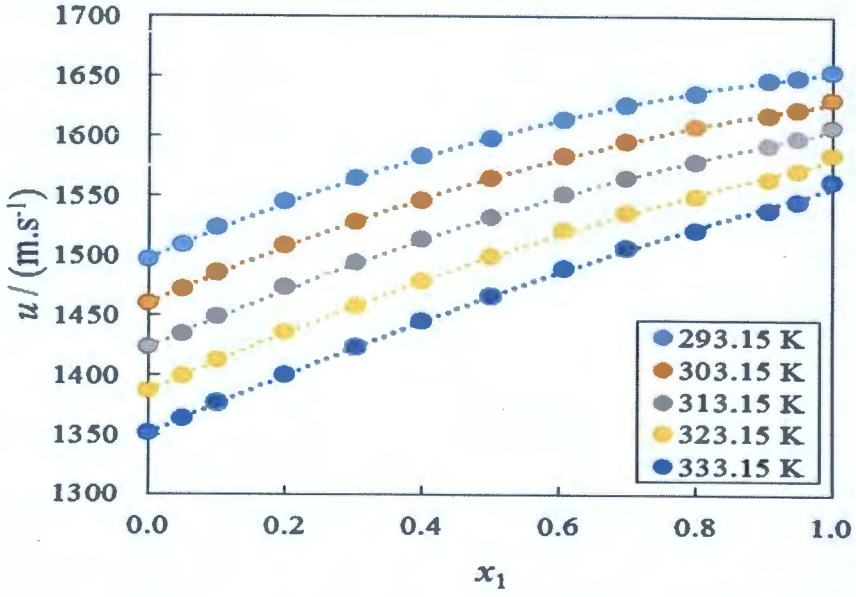

Fig 4.2b

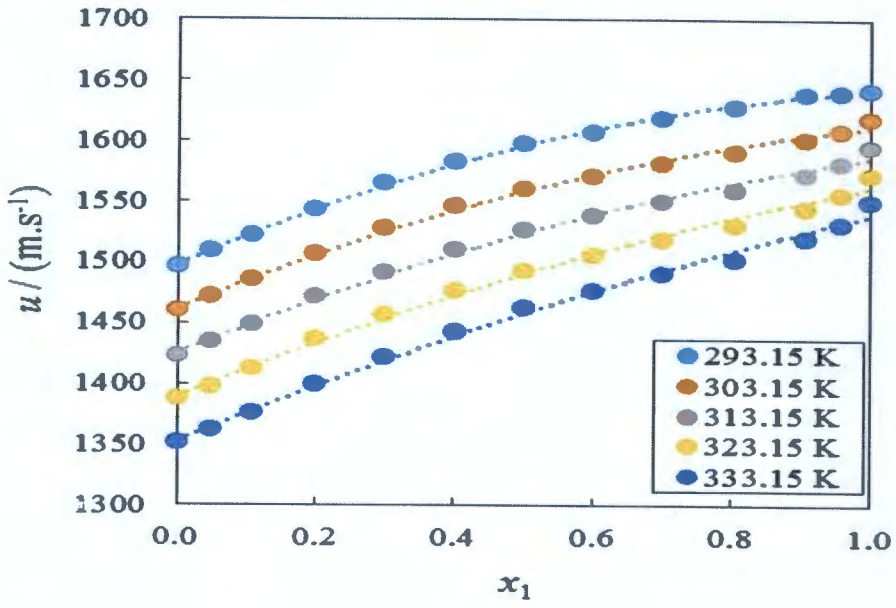

Fig 4.2c

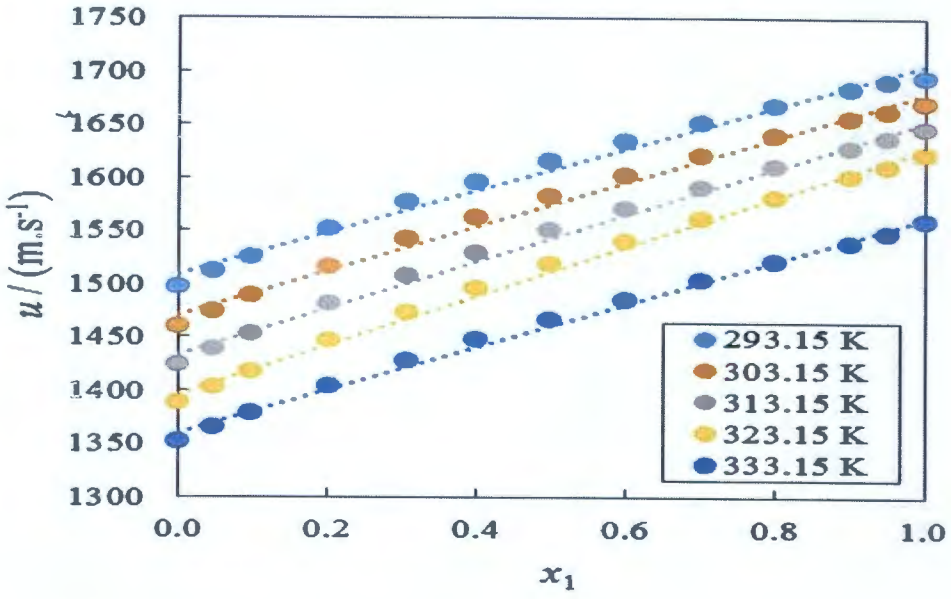

Fig 4.2 d

Figure 4.2 Sound velocity (u) vs mole fraction of IL for IL (1)+ acetophenone (2): (a) $[BMIM]^+[BF_4]^-$, (b) $[BMIM]^+[PF_6]^-$, (c) $[EMIM]^+[BF_4]^-$ and (d) $[EMIM]^+[EtSO_4]^-$ at T= (293.15, 303.15 313.15, 323.15 and 333.15) K. The dotted line represents the smoothness of these data.

For all studied binary mixtures the values of viscosity increased as concentration of the IL increased in acetophenone as seen in **Figure 4.3 (a, b, c and d)**.

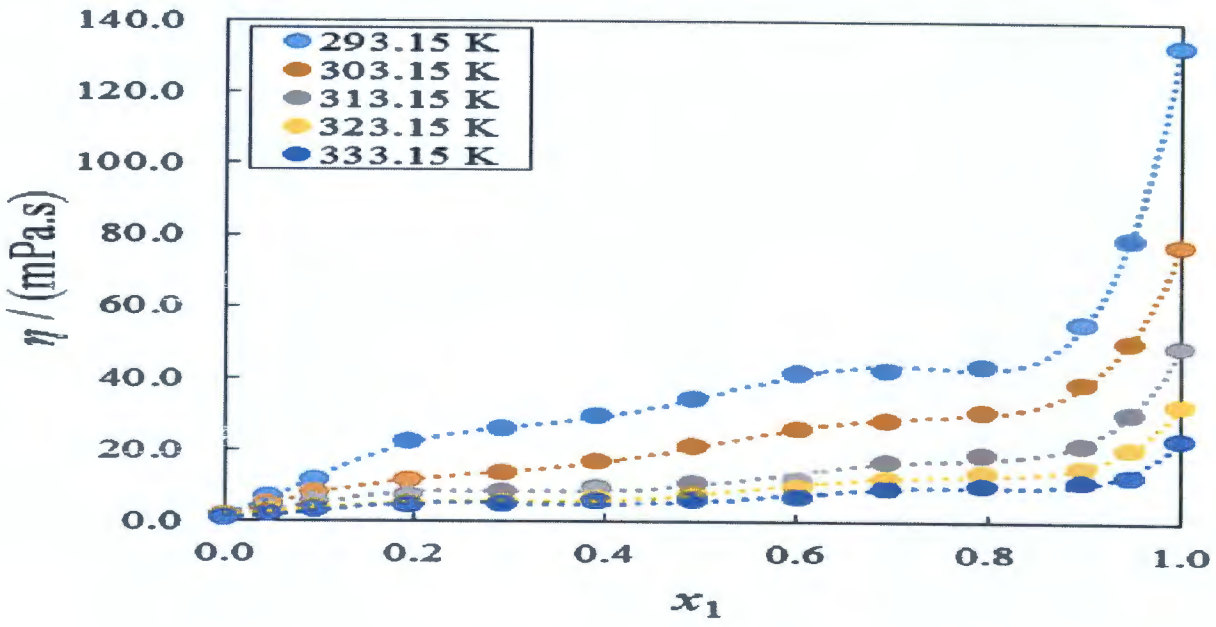

Fig 4.3 a

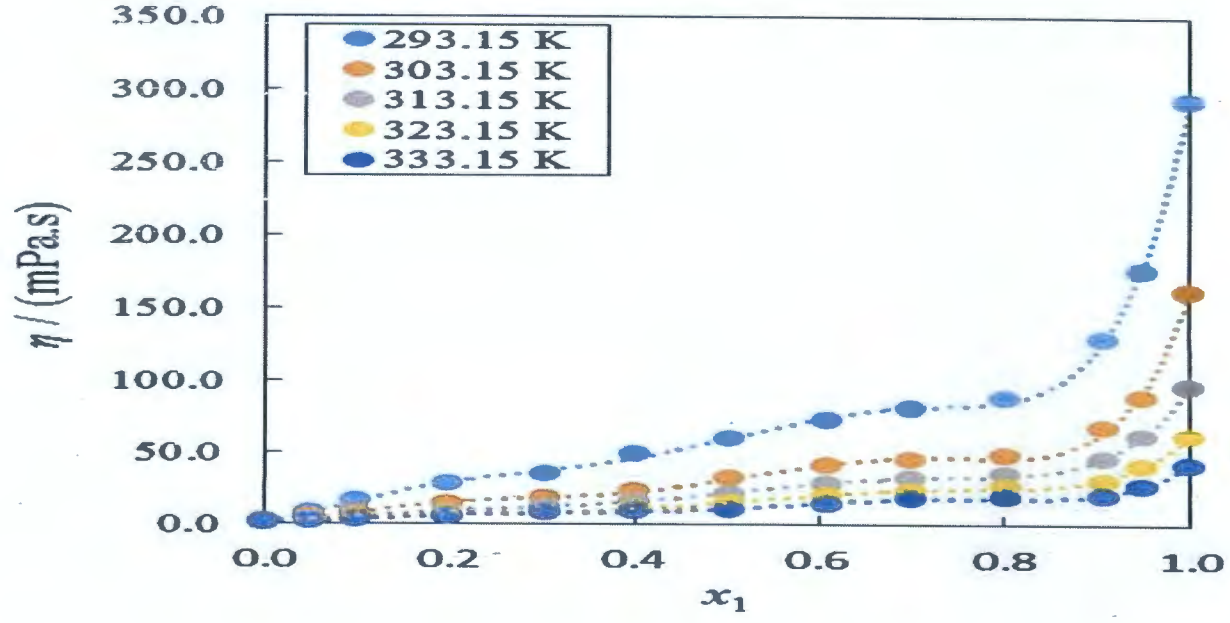

Fig 4.3 b

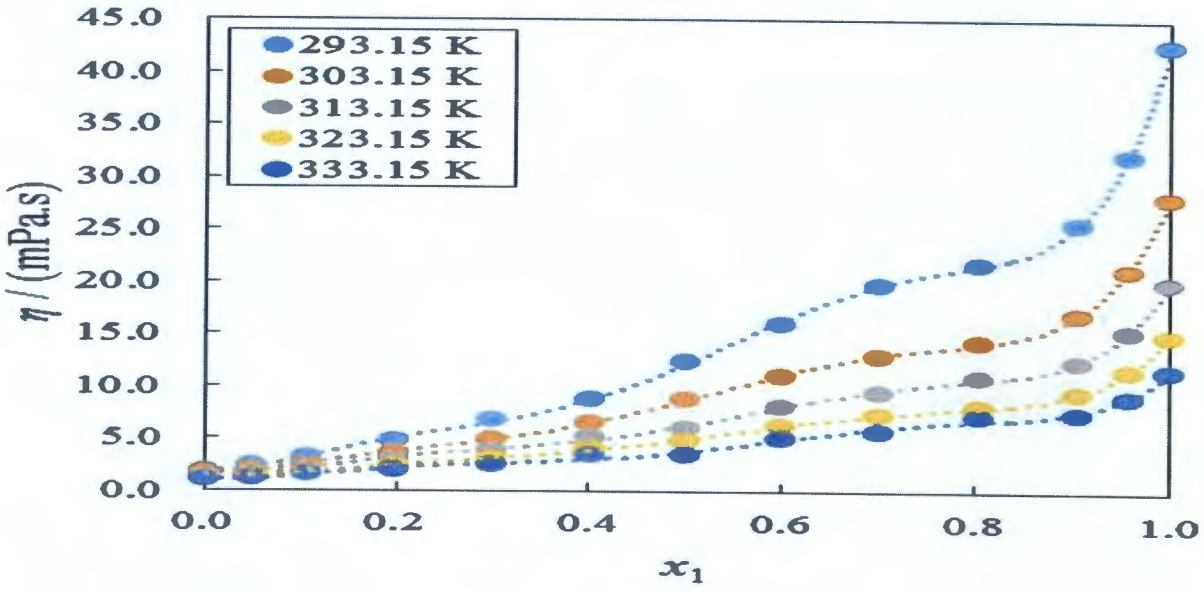

Fig 4.3 c

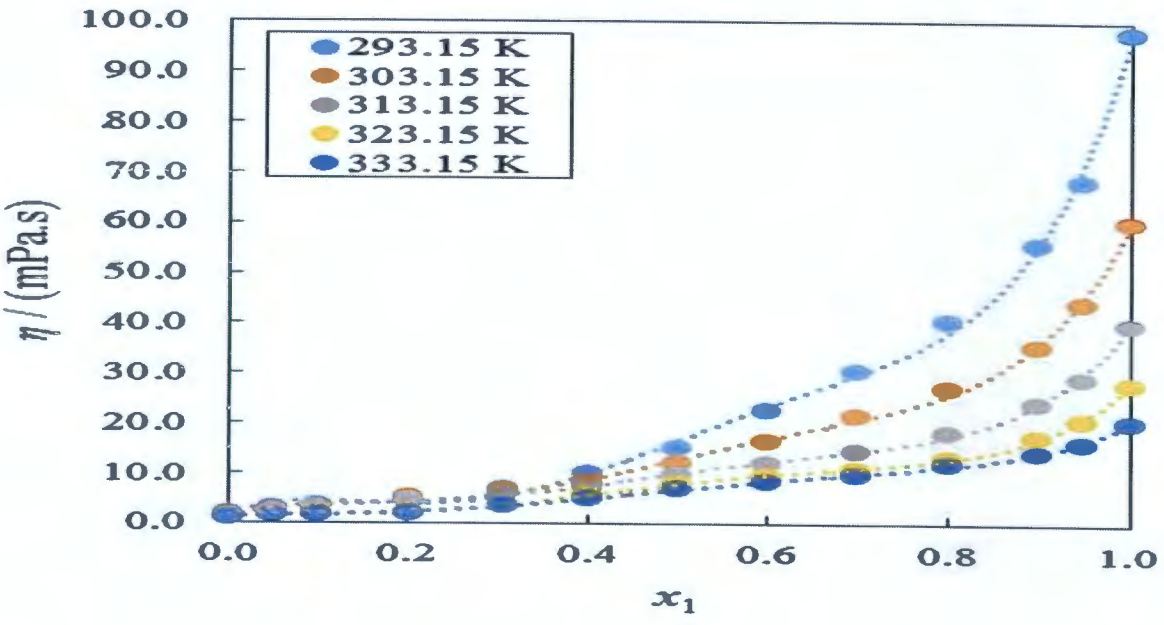

Fig 4.3 d

Figure 4.3 Viscosity (η) *vs* mole fraction of IL for IL(1)+ acetophenone (2): (a) $[BMIM]^+[BF_4]^-$, (b) $[BMIM]^+[PF_6]^-$, (c) $[EMIM]^+[BF_4]^-$ and (d) $[EMIM]^+[EtSO_4]^-$ at *T*= (293.15, 303.15 313.15, 323.15 and 333.15) K. The dotted line represents the smoothness of these data.

Refractive index values decreased as concentration of the IL in acetophenone increased with temperature as shown in **Figure 4.4 (a, b, c and d).**

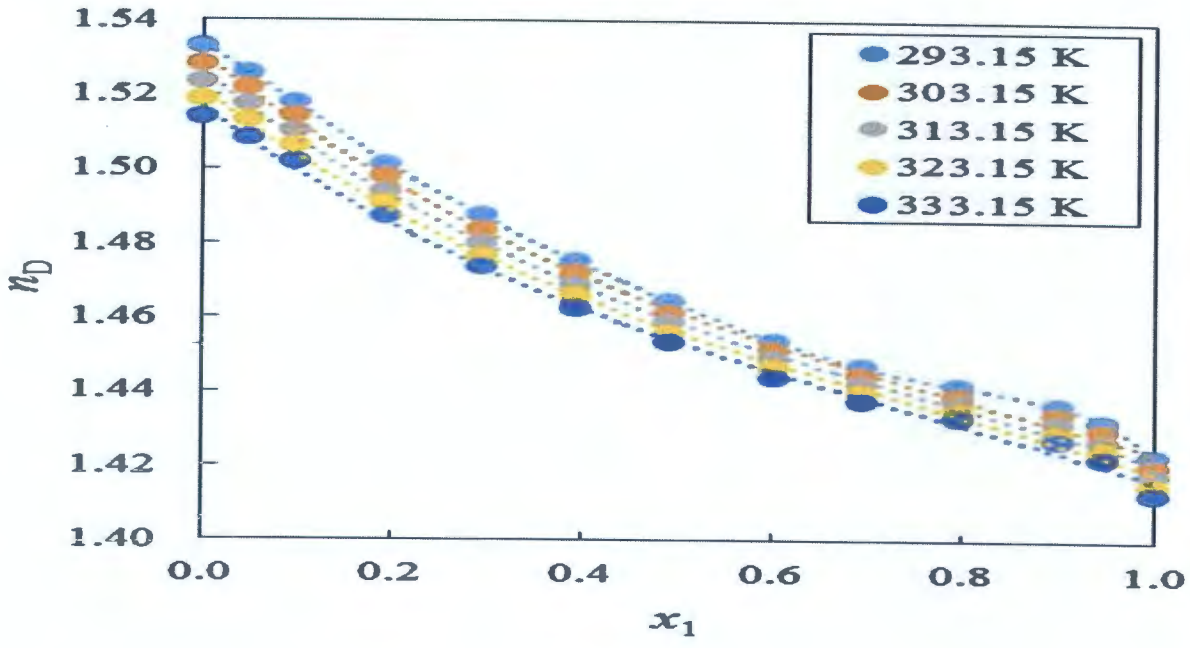

Fig 4.4 a

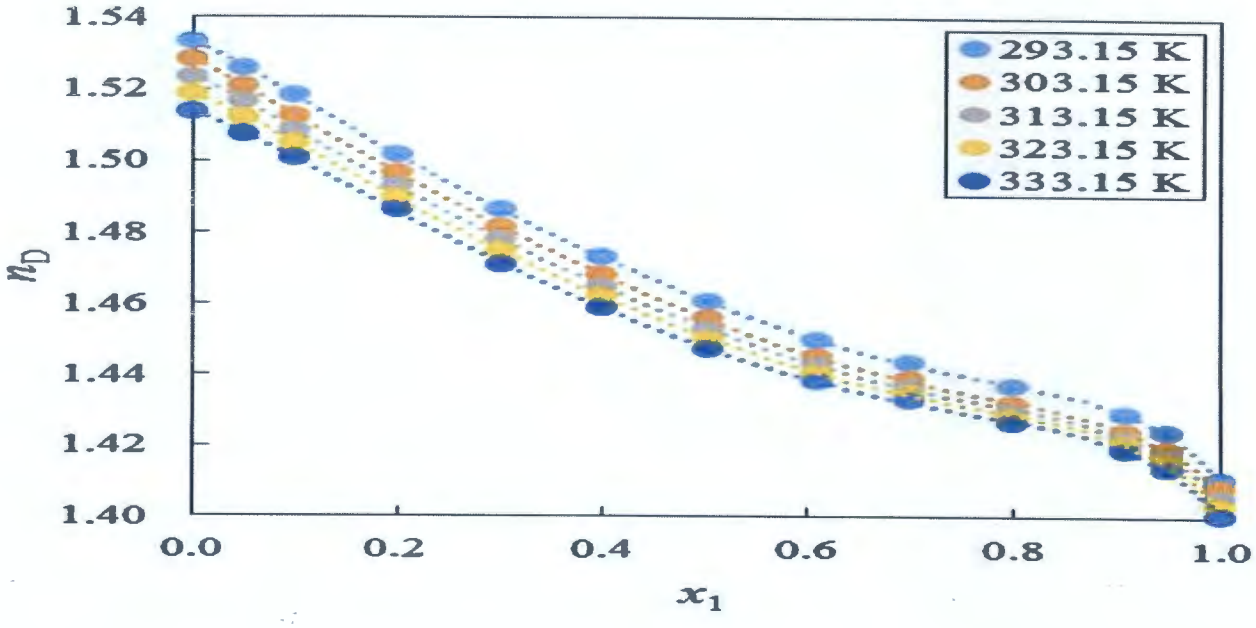

Fig 4.4 b

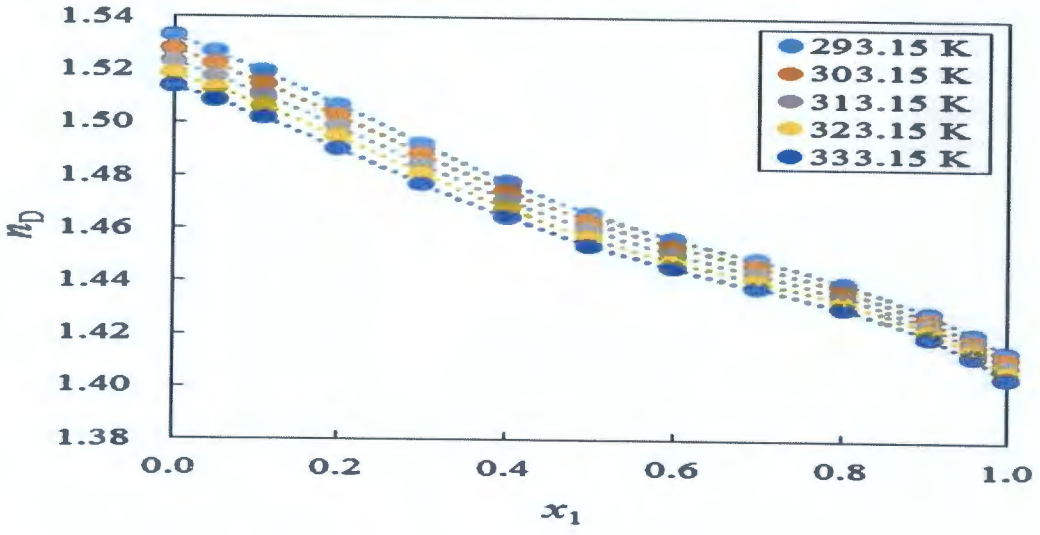

Fig 4.4 c

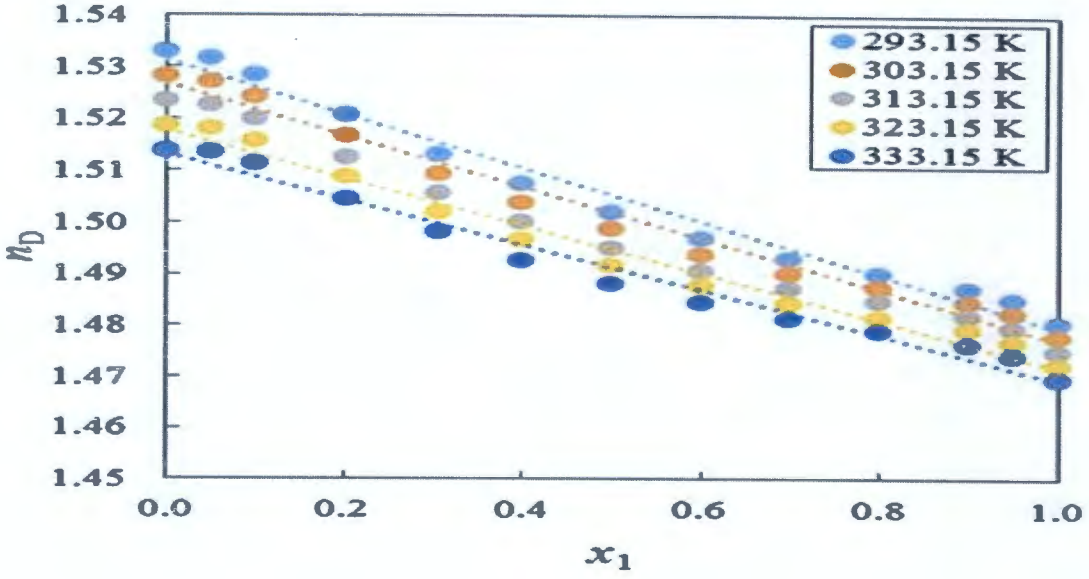

Fig 4.4 d

Figure 4.4 Refractive index (n_D) vs mole fraction of IL for IL (1)+ acetophenone (2): (a) $[BMIM]^+[BF_4]^-$, (b) $[BMIM]^+[PF_6]^-$, (c) $[EMIM]^+[BF_4]^-$ and (d) $[EMIM]^+[EtSO_4]^-$ at T= (293.15, 303.15 313.15, 323.15 and 333.15) K. The dotted line represents the smoothness of these data.

The excess molar volume values were both negative and positive over the entire composition range depending on the IL as a function of mole fraction as seen in **Figure 4.5 (a, b, c and d)**.

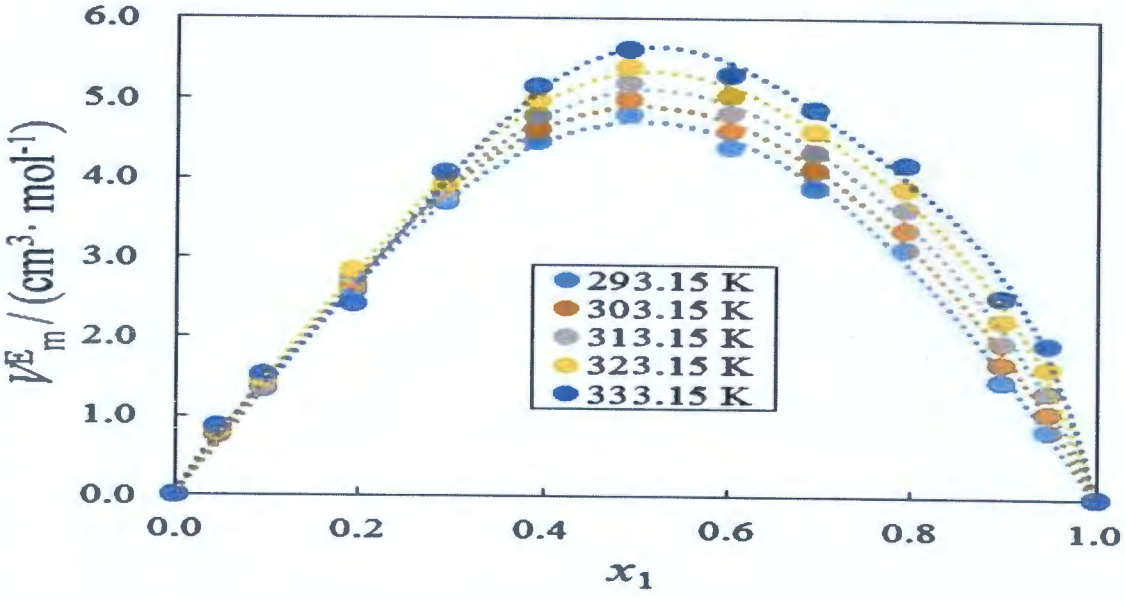

Fig 4.5 a

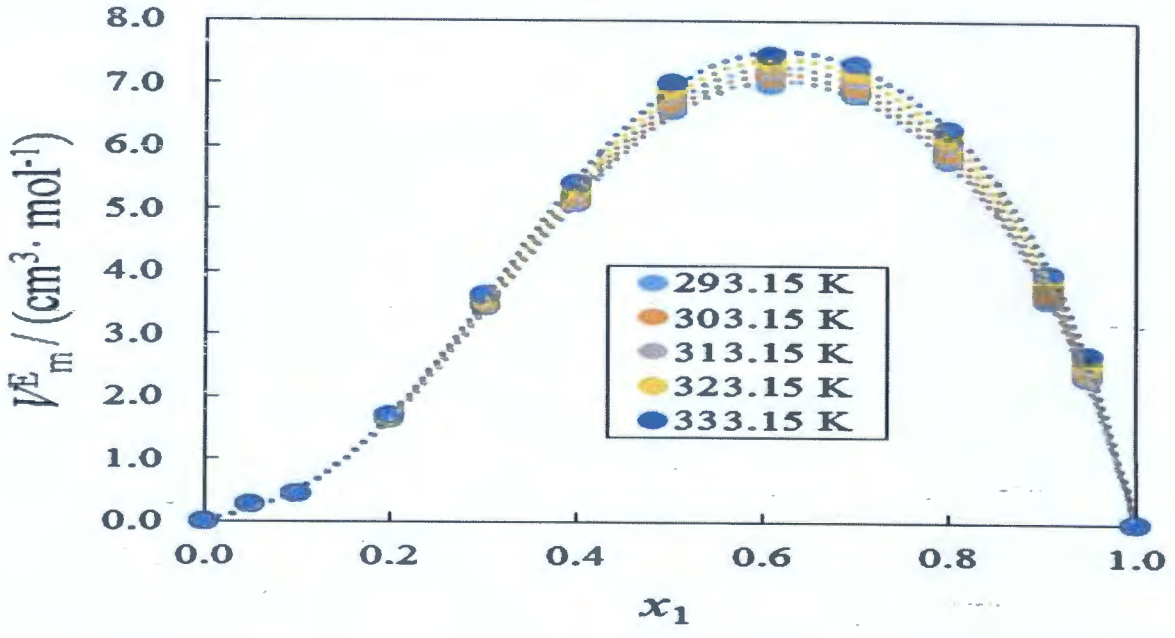

Fig 4.5b

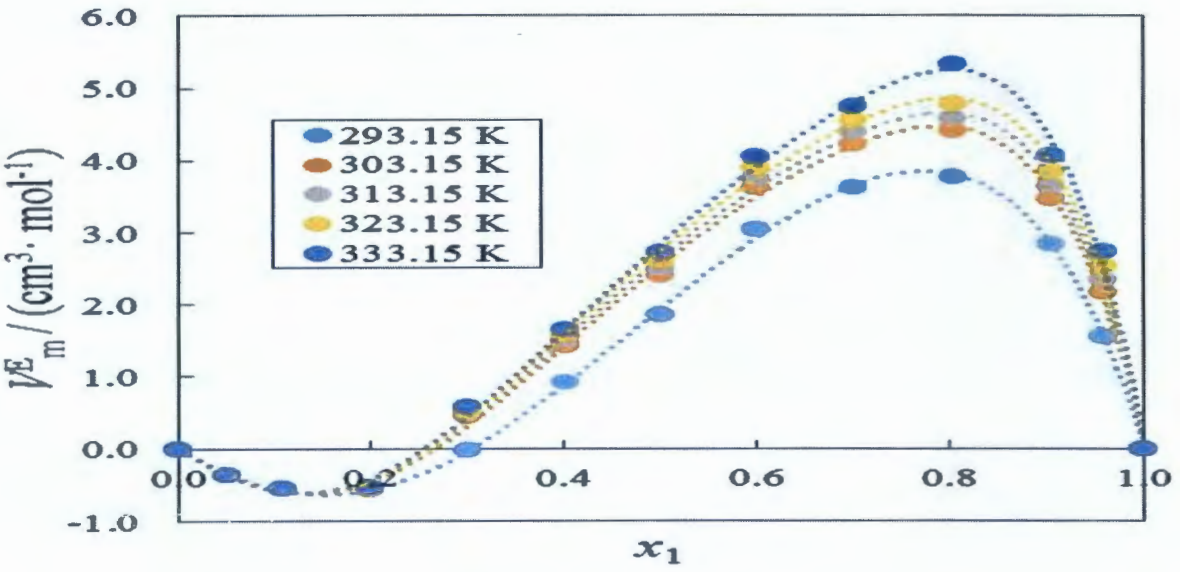

Fig 4.5 c

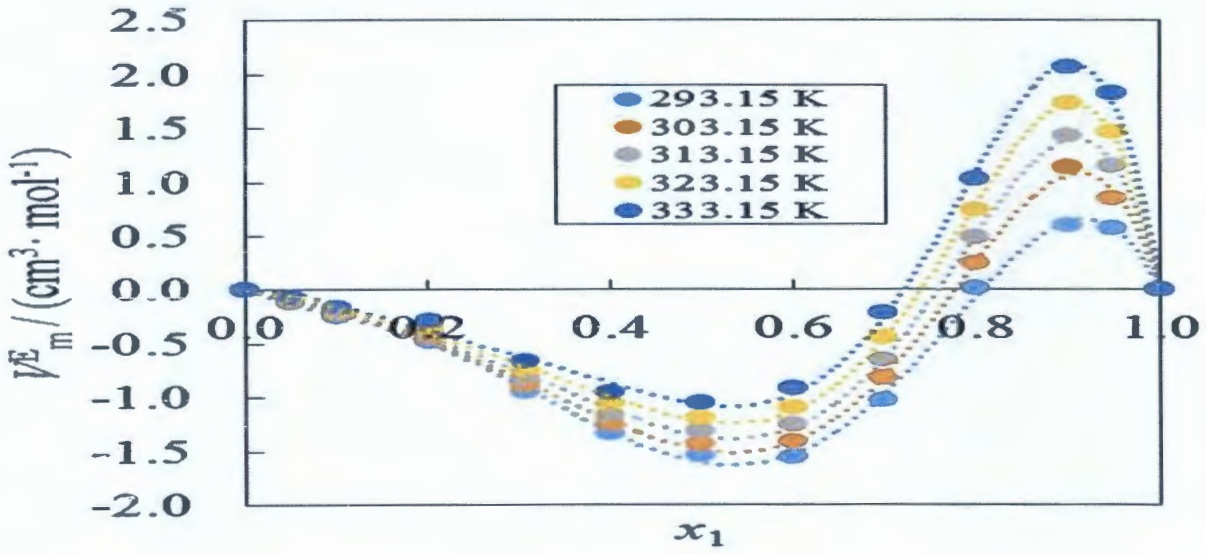

Fig 4.5 d

Figure 4.5 Excess molar volume ($V_m{}^E$) vs mole fraction of IL for IL(1)+ acetophenone (2) (a) $[BMIM]^+[BF_4]^-$, (b) $[BMIM]^+[PF_6]^-$, (c) $[EMIM]^+[BF_4]^-$ and (d) $[EMIM]^+[EtSO_4]^-$ at T= (293.15, 303.15 313.15, 323.15 and 333.15) K. The dotted lines were generated using Redlich-Kister curve-fitting with parameter given in Table 4.2.

The deviation isentropic compressibility deviation values as a function of mole fraction were both negative and positive over the whole composition range [see **Figure 4.6 (a, b, c and d)**].

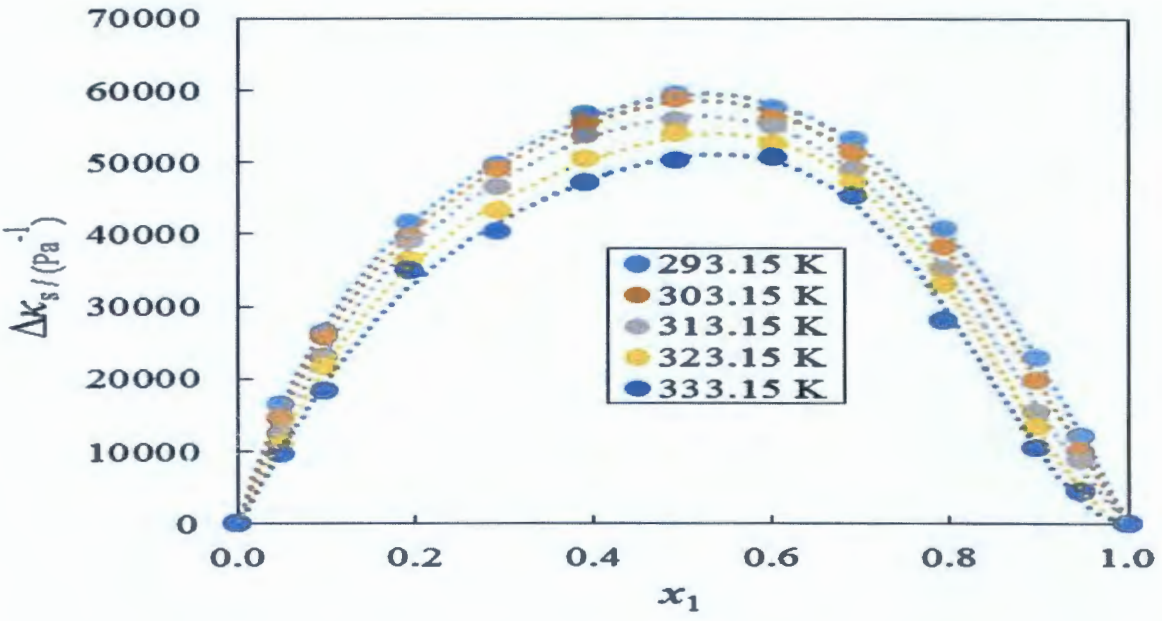

Fig 4.6 a

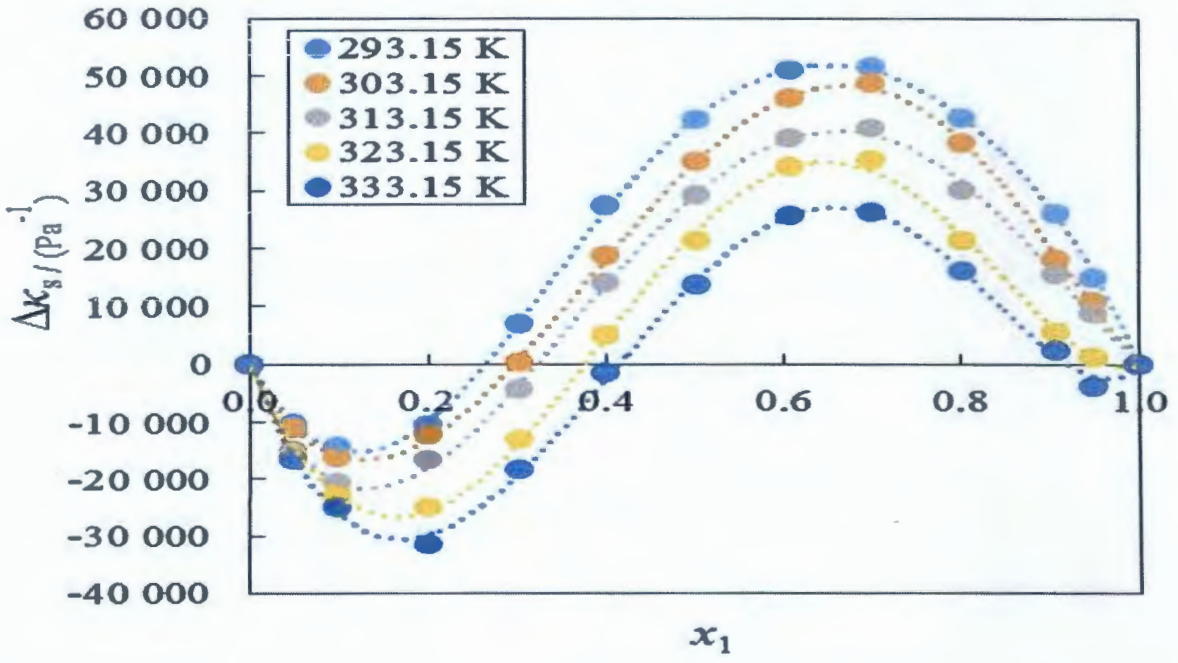

Fig 4.6 b

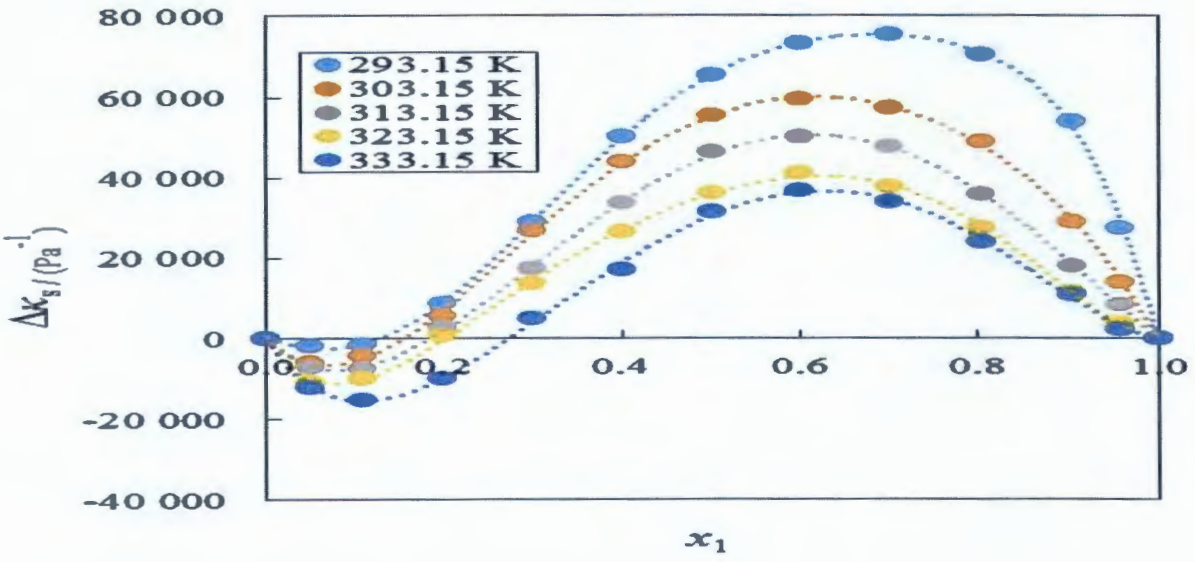

Fig 4.6 c

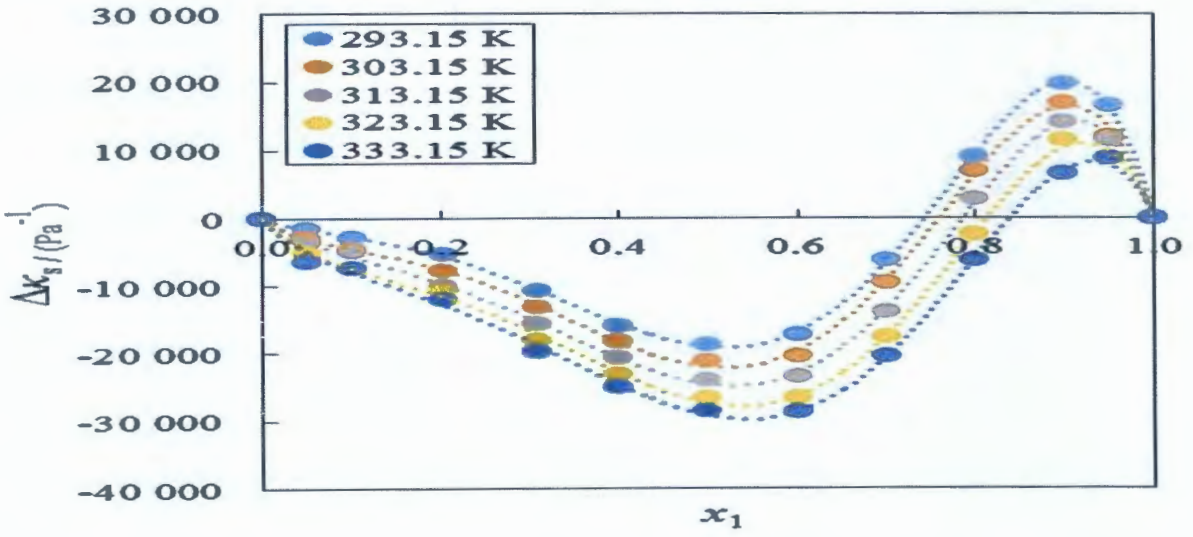

Fig 4.6d

Figure 4.6 Deviation in isentropic compressibility ($\Delta\kappa s$) vs mole fraction of IL for IL (1)+ acetophenone (2): (a) $[BMIM]^+[BF_4]^-$, (b) $[BMIM]^+[PF_6]^-$, (c) $[EMIM]^+[BF_4]^-$ and (d) $[EMIM]^+[EtSO_4]^-$ at T= (293.15, 303.15 313.15, 323.15 and 333.15) K. The dotted lines were generated using Redlich-Kister curve-fitting with parameters given in Table 4.2.

The viscosity deviation values were negative, but decreased with increase in temperature for all binary system over the entire composition range [see **Figure 4.7 (a, b, c and d)**].

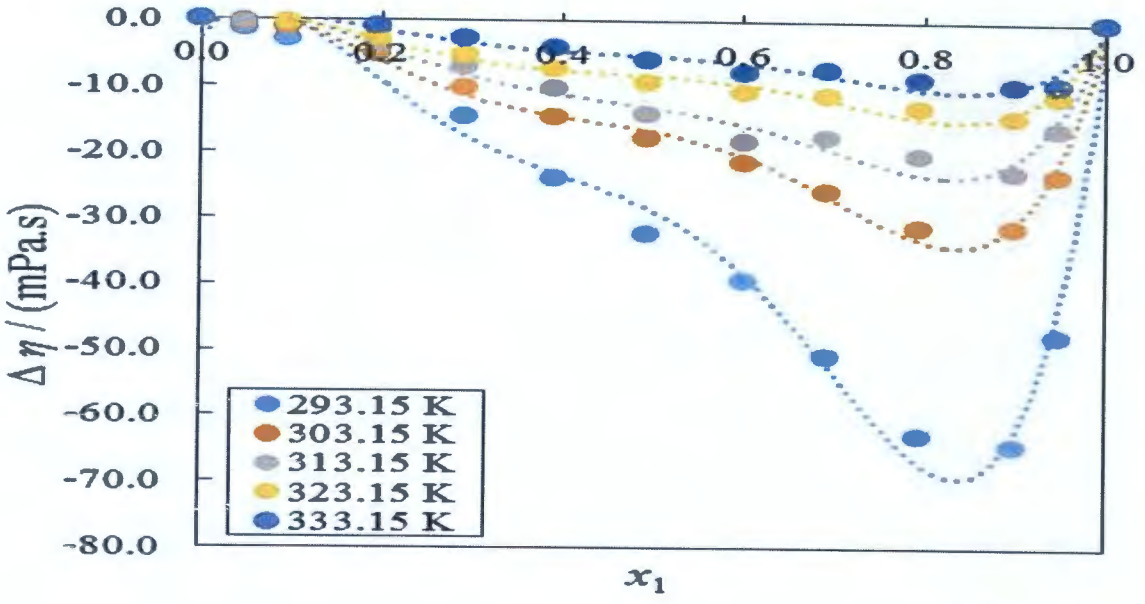

Fig 4.7a

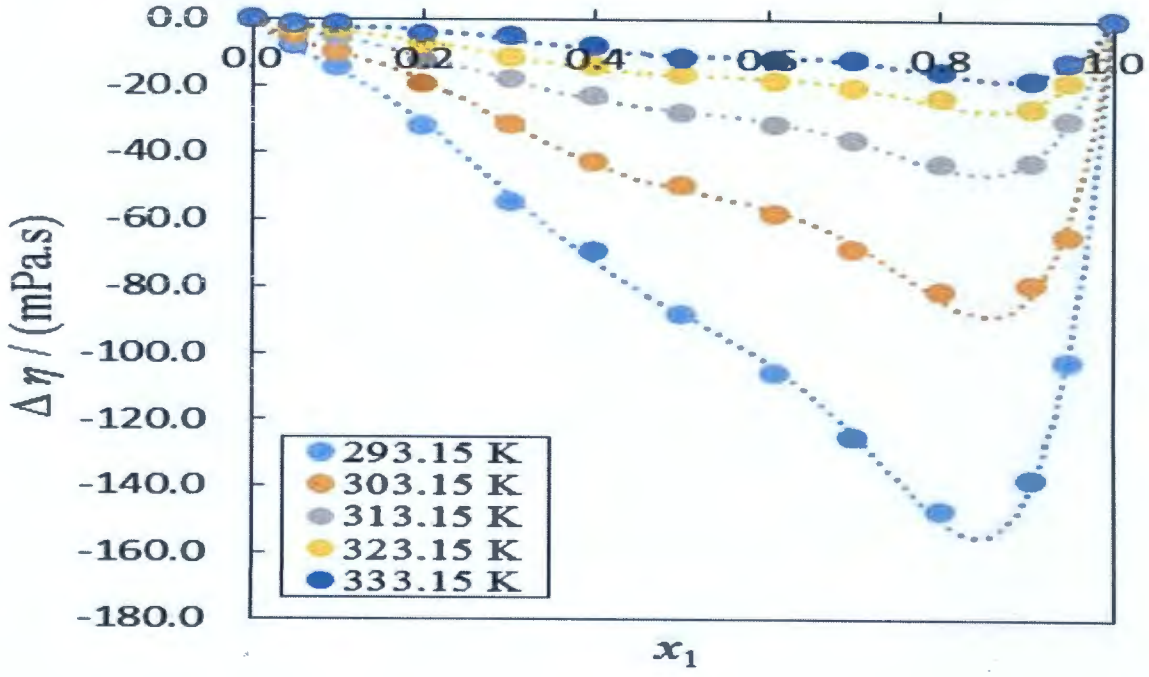

Fig 4.7b

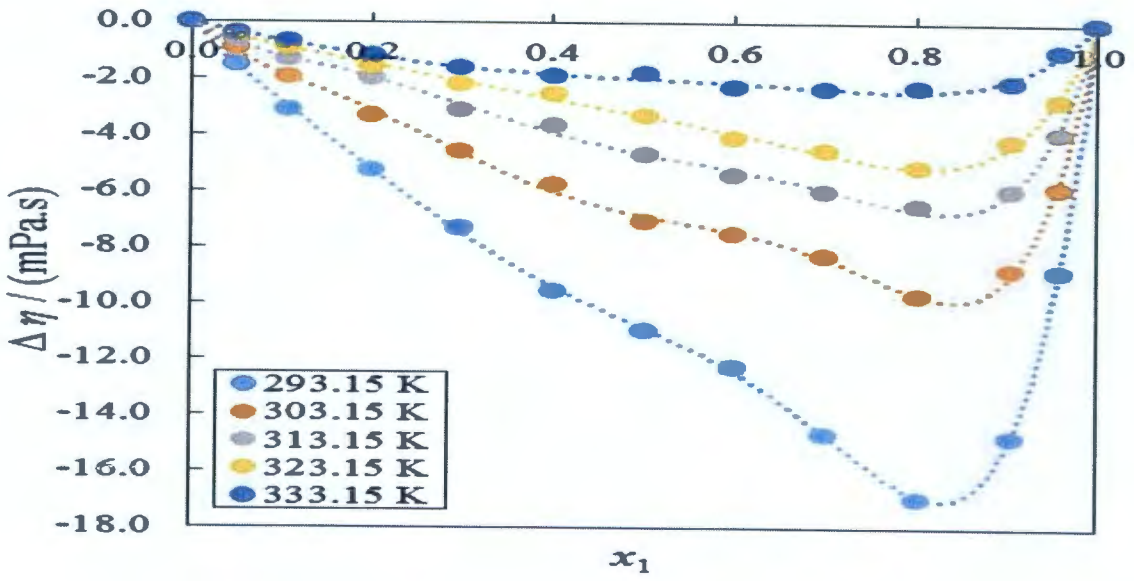

Fig 4.7c

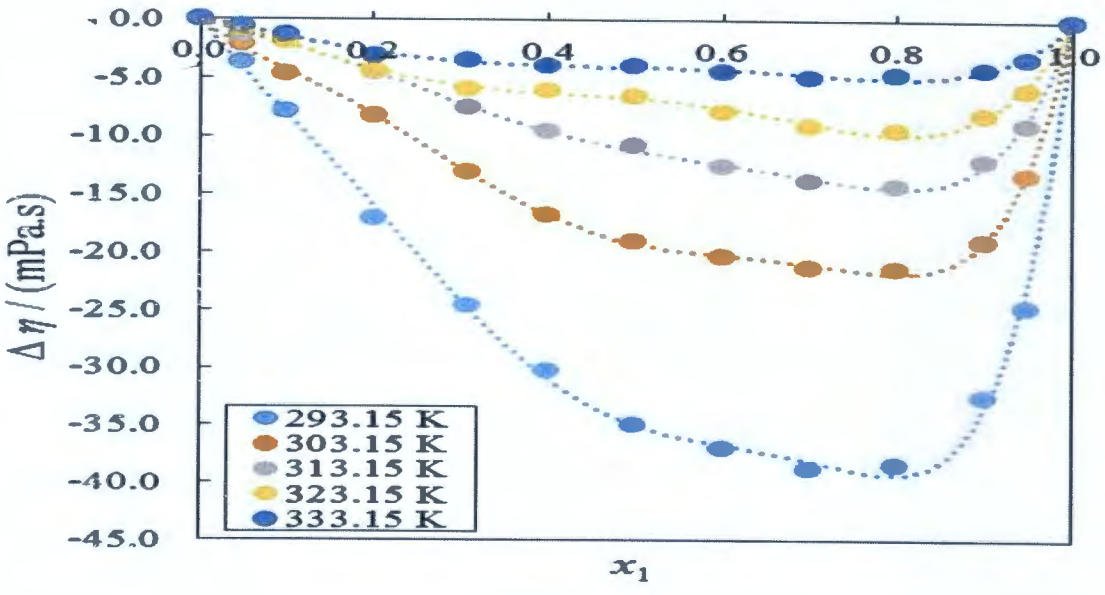

Fig 4.7d

Figure 4.7 Viscosity deviation ($\Delta\eta$) vs mole fraction of IL IL (1)+ acetophenone (2): (a) [BMIM]+[BF_4]-, (b) [BMIM]+[PF_6]-, (c) [EMIM]+[BF_4]- and (d) [EMIM]+[$EtSO_4$]- at T=(293.15, 303.15 313.15, 323.15 and 333.15) K. The dotted lines were generated using Redlich-Kister curve-fitting with parameters given in Table 4.2.

The refractive index deviations values as a function of mole fraction were both negative and positive for all binary system over the entire composition range as shown in **Figure 4.8 (a, b, c and d)**.

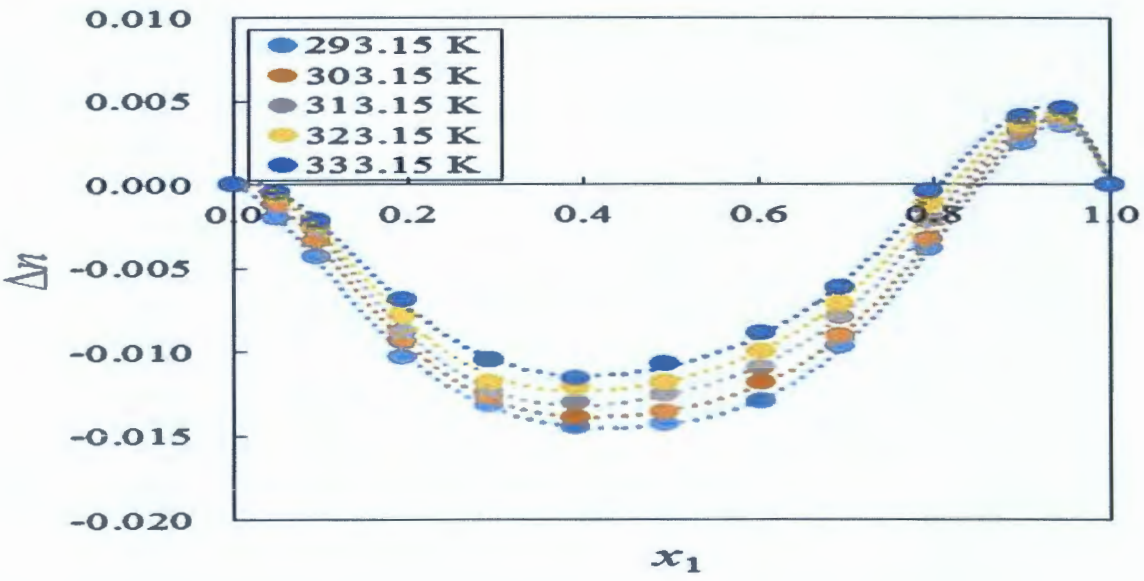

Fig 4.8a

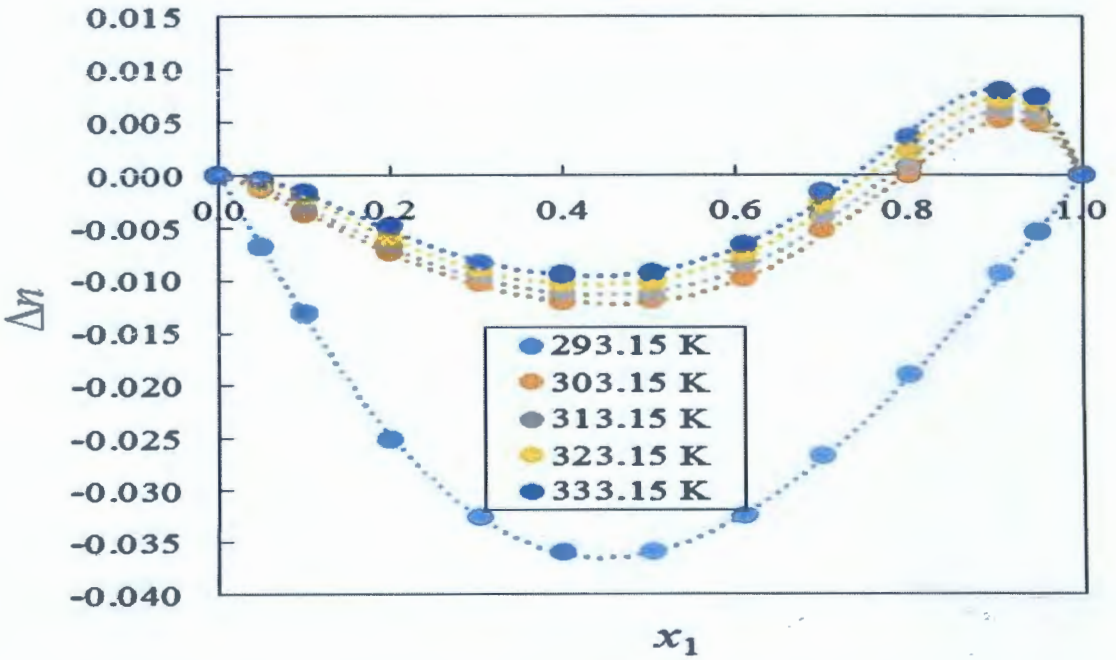

Fig 4.8b

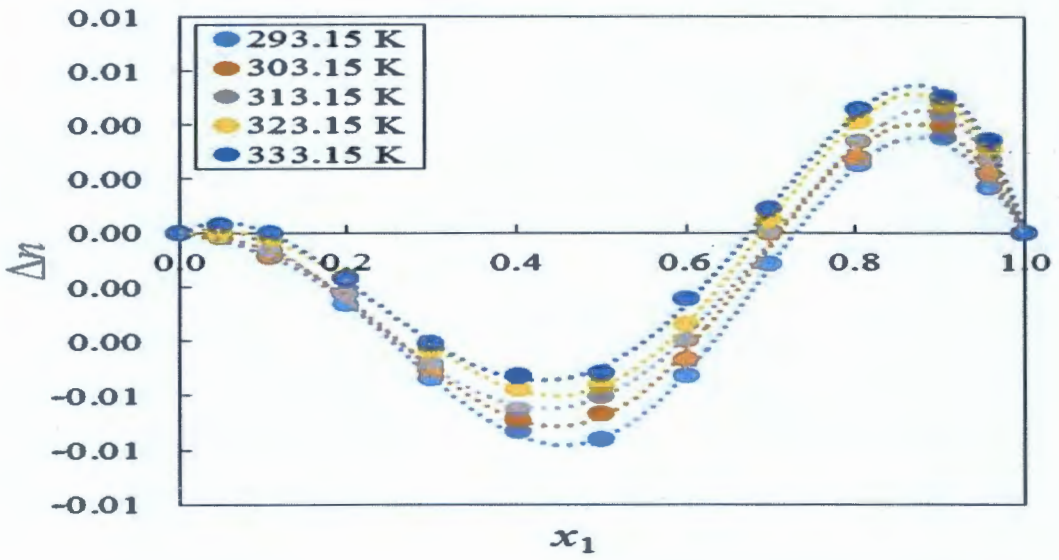

Fig 4.8c

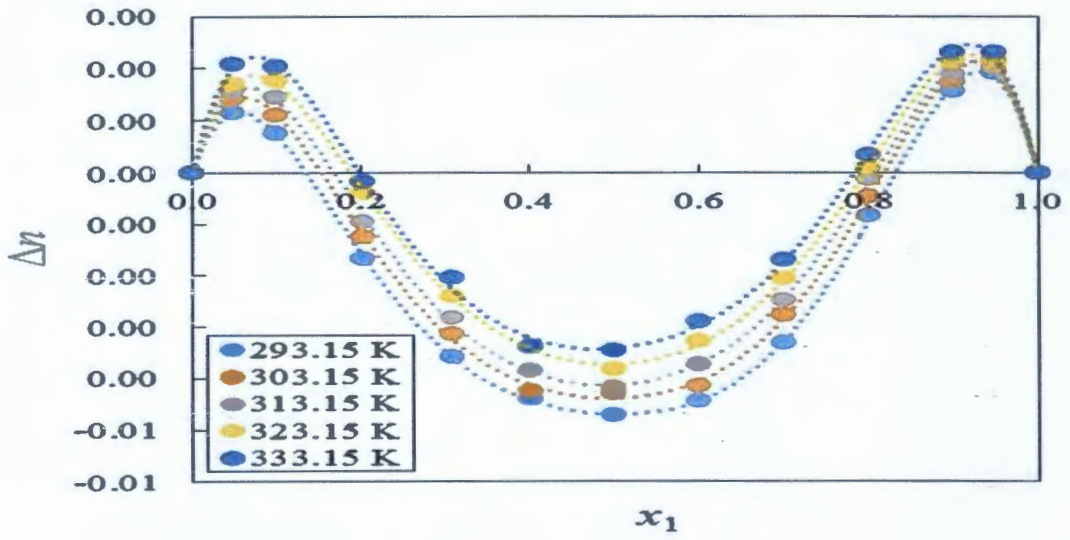

Fig 4.8 d

Figure 4.8 Refractive index deviation (Δn_D) vs mole fraction of IL for IL (1)+ acetophenone (2): (a) $[BMIM]^+[BF_4]^-$, (b) $[BMIM]^+[PF_6]^-$, (c) $[EMIM]^+[BF_4]^-$ and (d) $[EMIM]^+[EtSO_4]^-$ at T= (293.15, 303.15 313.15, 323.15 and 333.15) K. The dotted lines were generated using Redlich-Kister curve-fitting with parameters given in Table 4.2.

4.2. Correlation of excess and derived properties

Experimental excess and derived properties namely ,V_m^E, $\Delta\kappa_s$, $\Delta\eta$ and Δn_D for binary mixtures of $[BMIM]^+[BF_4]^-$ or $[BMIM]^+[PF_6]^-$ or $[EMIM]^+[BF_4]^-$ or $[EMIM]^+[EtSO_4]^-$ with acetophenone were correlated by means of the Redlich-Kister polynomial [165] at the temperatures T= (298.15, 303.15, 313.15, 323.15, 333.15) K in order to give an excellent estimation of the strength of unlike molecular interactions in the solution. The Redlich-Kister equation for binary mixtures is given below:

$$X = x_1 x_2 \sum_{i=1}^{k} A_i \left(1 - 2x_1\right)^{i-1} \tag{4.3}$$

where X is the excess or deviation property, V_m^E or $\Delta\kappa_s$ or $\Delta\eta$ or Δn_D, x_1 is the mole fraction of the ionic liquid, x_2 is the mole fraction of the solvent and A_i is the Redlich-Kister parameters for the system. The fitting parameters are given in Table 4.2, together with the root-mean square deviations, σ given by the following equation:

$$\sigma(X) = \sum_{i=1}^{N} \left[\frac{\left(X_{\text{expt}} - X_{\text{calc}}\right)^2}{(N-k)} \right]^{1/2} \tag{4.4}$$

Where X_{expt}, X_{calc} are the values of the experimental and calculated property, N is the number of experimental points and k is the number of coefficients used in the Redlich–Kister equation.

Table 4.2

Coefficients A_i, and standard deviations, σ, obtained for the IL (1)+ acetophenone (2) binary systems at different temperatures and at pressure p = 0.1 MPa for the Redlich-Kister equation.

	T/K	A_0	A_1	A_2	A_3	A_4	σ
				{$[BMIM]^+[BF_4]^-$ (1) + acetophenone (2)}			
V_m^E / $cm^3 \cdot mol^{-1}$	293.15	18.852	-0.637	-3.972	-1.029	0.131	0.106
	303.15	19.631	-0.803	-4.373	-3.110	3.022	0.103
	313.15	20.449	-1.587	-6.059	-4.431	8.210	0.113
	323.15	21.333	-1.755	-6.516	-7.050	11.654	0.119
	333.15	22.574	-2.933	-13.007	-9.821	22.630	0.170
$\Delta\kappa_S$ /TPa^{-1}	293.15	237330	-22924	37085	89050	44842	543
	303.15	233685	-20053	24521	99867	11297	411
	313.15	225243	-18744	25051	111467	-44855	831
	323.15	214378	-32887	34326	146457	-104398	644
	333.15	203168	-320638	217978	1486978	-1228338	1373
$\Delta\eta$/ mPa·s	293.15	-131.150	136.112	-70.256	466.800	-482.503	0.786
	303.15	-72.971	51.551	-47.655	248.928	-191.642	0.436
	313.15	-59.012	39.132	25.249	168.289	-202.855	1.134
	323.15	-37.538	14.851	14.935	125.530	-133.040	0.537
	333.15	-25.400	13.596	34.790	90.037	-133.621	0.839
Δn_D	293.15	-0.0560	-0.0085	-0.0128	-0.0697	0.1364	0.0002
	303.15	-0.0552	-0.0192	0.0022	-0.0415	0.1291	0.0002
	313.15	-0.0510	-0.0209	-0.0051	-0.0416	0.1159	0.0003

	323.15	-0.0474	-0.0249	-0.0077	-0.0349	0.1213	0.0004
	333.15	-0.0443	-0.0242	0.0211	-0.0349	0.1100	0.0004
			{[BMIM]$^+$[PF$_6$]$^-$ (1) + acetophenone (2)}				
V_m^E / cm^3·mol^{-1}	293.15	25.867	-19.539	-13.925	-5.802	17.259	0.058
	303.15	26.252	-19.848	-14.239	-6.323	18.098	0.060
	313.15	26.668	-20.117	-14.717	-7.167	19.465	0.062
	323.15	27.111	-20.513	-14.953	-7.661	20.216	0.065
	333.15	27.629	-20.878	-15.365	-8.669	21.732	0.069
$\Delta\kappa$s /TPa^{-1}	293.15	169167	-254159	-217659	-58317	92919	656
	303.15	169169	-254157	-217677	-58338	92944	656
	313.15	138325	-290681	-137488	57475	-64931	610
	323.15	115907	-259106	-185707	-213	-50674	998
	333.15	87080	-306315	-225102	151424	-95946	983
$\Delta\eta$/ mPa·s	293.15	-352.733	273.914	-283.830	959.770	-847.274	2.253
	303.15	-204.106	110.791	-83.038	637.389	-652.417	2.346
	313.15	-110.457	54.423	-77.853	323.853	-272.339	0.794
	323.15	-67.379	19.187	-13.282	214.549	-217.628	0.915
	333.15	-43.425	17.276	29.925	139.596	-211.452	0.928
Δn_D	293.15	-0.1436	-0.0381	0.0072	0.0221	0.0241	0.0002
	303.15	-0.0479	-0.0154	0.0554	-0.0678	0.0526	0.0004
	313.15	-0.0455	-0.0195	0.0534	-0.0686	0.0716	0.0005
	323.15	-0.0396	-0.0178	0.0443	-0.0757	0.0959	0.0005
	333.15	-0.0365	-0.0181	0.0681	-0.0841	0.0657	0.0003
			{[EMIM]$^+$[BF$_4$]$^-$ (1) + acetophenone (2)}				
V_m^E / cm^3·mol^{-1}	293.15	7.762	-21.213	4.294	-4.592	6.467	0.056

	303.15	10.164	-21.110	1.146	-12.883	15.145	0.113
	313.15	10.587	-21.508	0.805	-14.441	17.417	0.125
	323.15	11.046	-21.924	0.418	-16.138	19.923	0.140
	333.15	11.393	-22.981	3.878	-18.262	18.181	0.155
$\Delta\kappa_S$ /TPa^{-1}	293.15	261467	-238721	-123000	-234443	264715	1010
	303.15	220921	-167349	-133613	-134309	8675	794
	313.15	182119	-172264	-155579	-23923	-39482	521
	323.15	143344	-135284	-81811	-41407	-200615	793
	333.15	121550	-182071	-169015	925	-98418	1058
$\Delta\eta$/ mPa·s	293.15	-43.545	28.300	-48.306	89.442	-62.857	0.112
	303.15	-27.540	12.528	-11.914	59.761	-63.258	0.195
	313.15	-18.761	12.249	-8.344	34.175	-40.769	0.193
	323.15	-13.309	11.7670	-14.720	20.466	-16.561	0.135
	333.15	-8.046	2.827	-7.386	10.065	-5.082	0.119
Δn_D	293.15	-0.0302	-0.0235	0.0974	-0.0083	-0.0432	0.0002
	303.15	-0.0272	-0.0256	0.0949	0.0086	-0.0374	0.0003
	313.15	-0.0246	-0.0258	0.0826	-0.1185	-0.0157	0.0001
	323.15	-0.0227	-0.0243	0.0900	-0.0176	-0.0207	0.0001
	333.15	-0.0201	-0.0277	0.0804	-0.0130	-0.0043	0.0002
			{[EMIM]$^+$[EtSO$_4$]$^-$ (x_1) + acetophenone (x_2)}				
V_m^E / cm^3·mol^{-1}	293.15	-6.429	2.560	12.560	-13.367	1.413	0.047
	303.15	-5.957	2.654	12.016	-17.958	7.353	0.048
	313.15	-5.445	2.573	11.513	-21.042	11.573	0.042
	323.15	-4.893	2.374	11.120	-24.136	15.689	0.052
	333.15	-4.267	2.165	10.760	-27.585	20.393	0.025
$\Delta\kappa_S$ /TPa^{-1}	293.15	-88483	22626	230019	-262334	17006	706
	303.15	-98751	32880	187116	-262214	61755	583

	313.15	-109962	47012	173265	-265702	36968	782
	323.15	-117269	52626	148852	-246001	41707	941
	333.15	-88483	22626	230019	-262334	17006	706
$\Delta\eta$/ mPa·s	293.15	-139.733	50.296	-22.440	200.521	-190.369	1.098
	303.15	-76.920	31.738	1.307	110.531	-131.677	0.030
	313.15	-44.822	26.386	-17.842	71.022	-60.353	0.348
	323.15	-27.050	10.696	-46.834	51.453	-0.645	0.340
	333.15	-16.167	1.901	-19.639	28.183	-6.702	0.279
Δn_D	293.15	-0.0188	0.0002	0.0055	-0.0102	0.0707	0.0000
	303.15	-0.0175	0.0000	0.0090	-0.0090	0.0694	0.0001
	313.15	-0.0166	-0.0014	0.0161	-0.0040	-0.0612	0.0000
	323.15	-0.0149	-0.0008	0.0178	-0.0032	0.0613	0.0000
	333.15	-0.0138	-0.0028	0.0166	0.0014	0.0676	0.0001

4.3. Quantum chemical studies

Quantum chemical calculations were employed to complement our experimental findings on the interactions existing between the ionic liquids studied and acetophenone. Isolated structures of the anions ($[PF_6]^-$, $[BF_4]^-$ and $[EtSO_4]^-$) and cations ($[BMIM]^+$ and $[EMIM]^+$) as well as molecular structures of the ionic liquids were optimized. Optimized structures of ionic liquids are shown in **Figure 4.9**. The interaction energies (ΔE_{int}) for the ionic liquid systems were calculated from the stabilization energy difference according to equation (4.8):

$$\Delta E_{int} = E(ac) - (E(a) + E(c)) \qquad (4.8)$$

Where E(a) and E(c) are the energies of the pure anion and cation, respectively, and E(ac) the energy of ionic liquid system. All calculated energies are corrected by zero point energy (ZPE), using an empirical scaling factor of 0.972 [166].

Frequency calculations were also done on the optimized structures from which the change in Gibb's free energy (ΔG) for the cation-anion interaction was calculated. The interaction energies and change in Gibb's free energies are given in Table 4.3.

Table 4.3

Interaction energies and change in Gibbs free energies of ionic liquid systems in gaseous state and solvent.

ILs	Gaseous state		Acetophenone	
	ΔE_{int} (kJmol^{-1})	ΔG (kJmol^{-1})	ΔE_{int} (kJmol^{-1})	ΔG (kJmol^{-1})
$[BMIM]^+[BF_4]^-$	-337.79	-294.80	-22.04	11.93
$[BMIM]^+[PF_6]^-$	-310.62	-273.16	-14.05	13.01
$[EMIM]^+[BF_4]^-$	-338.10	-297.64	-25.91	4.27
$[EMIM]^+[EtSO_4]^-$	-350.71	-302.36	-24.92	11.44

The interaction energies for ILs studied are more negative and oddly increase and become less negative in the presence of acetophenone.

The molecular structures of $[BMIM]^+[BF_4]^-$, $[BMIM]^+[PF_6]^-$, $[EMIM]^+[BF_4]^-$ and $[EMIM]^+[EtSO_4]^-$ which were optimized using the Density Functional Theory (DFT) method [see **Figure 4.9 (a, b, c, d)**].

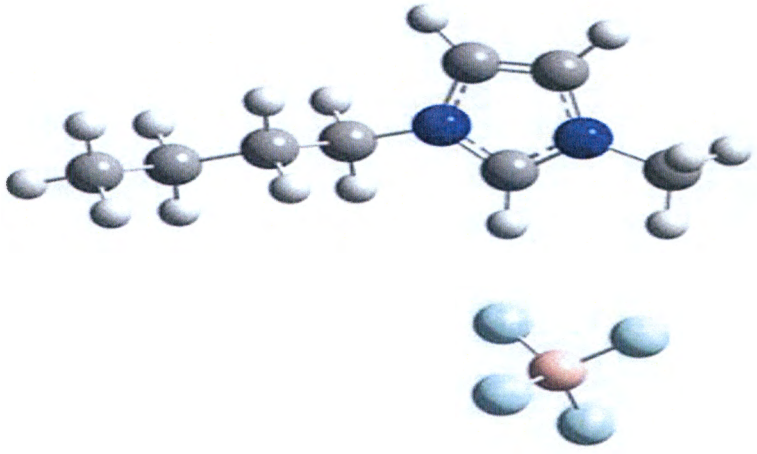

Fig 4.9a

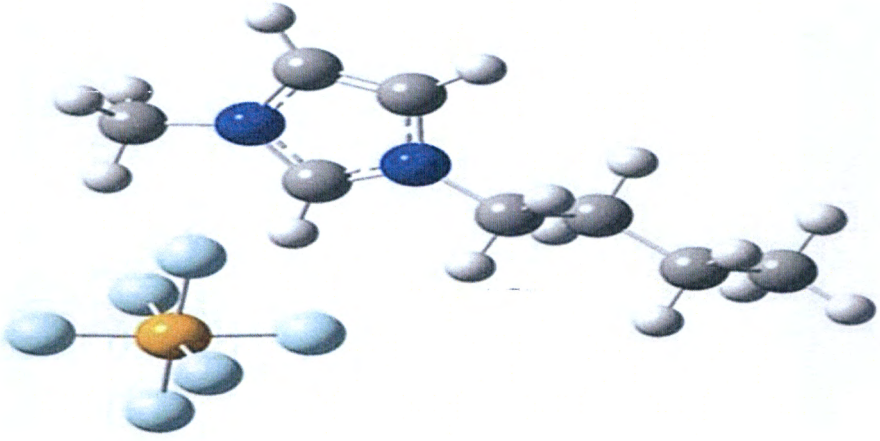

Fig4.9b

Fig 4.9c

Fig 4.9d

Figure 4.9 Optimized structures of ionic liquids (a) $[BMIM]^+[BF_4]^-$, (b) $[BMIM]^+[PF_6]^-$, (c) $[EMIM]^+[BF_4]^-$, (d) $[EMIM]^+[EtSO_4]^-$)

Acetophenone has a tendency to interact with the cation both by ion-dipole interaction and cation-π interaction.

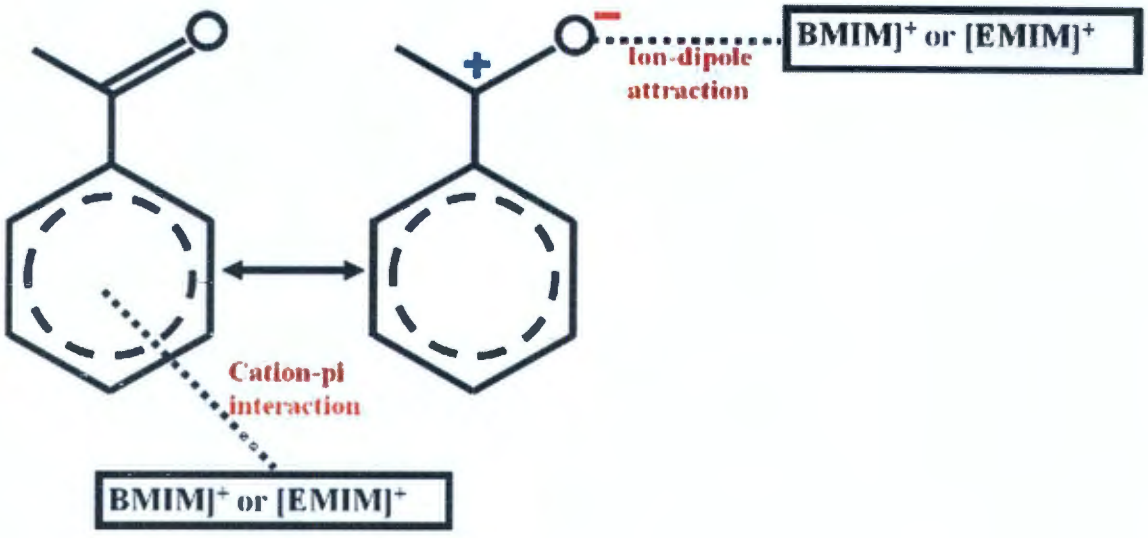

Figure 4.10 Schematic representation of interactions of the cations $(BMIM]^+$ and $[EMIM]^+$) with acetophenone.

CHAPTER FIVE

DISCUSSION

5.1. Physicochemical properties

5.1.1. Density (ρ)

The values of ρ against the mole fraction of the IL at different temperature have been plotted in **Figure 4.1 (a, b, c, d)** for acetophenone and its binary mixtures with $[BMIM]^+[BF_4]$, $[BMIM]^+[PF_6]^-$, $[EMIM]^+[BF_4]^-$ and $[EMIM]^+[EtSO_4]^-$, respectively. Results in **Figure 4.1. (a, b, c and d)** reveals that the ρ values for all studied binary mixtures increased as concentration of the IL in acetophenone increased but decreased with temperature increased. Practically, ILs are completely miscible in solvents having high dielectric constant value and are not completely miscible with solvents having low dielectric constant value [23, 32, 167]. In this study, the ILs were completely miscible with acetophenone (ε = 18.00 at T= 298.15 K) [168] since acetophenone is a high dielectric liquid. The increase in ρ values for IL with actophenone mixtures is possibly due to increase in the ion-pair interactions between IL and acetophenone. As seen in Table 4.1 the values of ρ decreased with an increase in temperature, because the thermal agitation occurring causes molecules in the mixture to accelerate and spread distantly further apart, possessing a larger volume hence a decrease in density [167]. The thermophysical properties of ILs are dependent on the alkyl chain of the cation and nature of the structure of ions. The lower the alkyl chain length of the cation of the IL, the more dense is ILs with higher alkyl chain length, for example (1.20524 $g \cdot cm^{-3}$for $[BMIM]^+[BF_4]^-$ and 1.28258 $g \cdot cm^{-3}$for $[EMIM]^+[BF_4]^-$ at 293.15 K). This is mainly due to increase in dispersive interactions in ILs with increase in chain length, resulting in a nanostructural organization in polar and non-polar regions. The nonpolar regions are build-up of alkyl chains whereas the polar regions contain the cationic head groups and the anions. When the chain length of cation

is enhanced, the nonpolar regions increase and take up more and more space, resulting in lower density in ILs with higher alkyl chain length [170-172]. The ρ values at all temperatures of the alkyl imidazolium-based ILs with acetophenone follow the order: $[BMIM]^+[PF_6]^-$> $[EMIM]^+[BF_4]^-$> $[EMIM]^+[EtSO_4]^-$> $[BMIM]^+[BF_4]^-$. This result show a clear indication of effect of cation and anion on ρ [173]. This order displays the highest ρ values due to the increased size of the anion with the same cation and vice versa. Results obtained gives a clear indication that the ρ of the binary mixtures is affected by the size of the cation and anion of the alkyl imidazolium-based ILs and the composition of the entire binary mixture.

5.1.2. Sound velocity (u)

The sound velocity of the (IL + acetophenone) mixtures, **Figure 4.2 (a, b, c and d)** shows that the size of the ions has an effect on the values of u of the studied binary mixtures. Practically, the u values of ILs mainly depend on the nature and structure of ions and the alkyl chain length of the cation. It can be clearly seen from **Figure 4.2 (a, b, c and d)** that at a given temperature, u values increase as the concentration of IL increased in the mixture but decrease as the temperature is increased for all studied systems. The u values at T= 333.15 K of the alkyl imidazolium-based ILs with acetophenone follow the order: $[BMIM]^+[PF_6]^-$> $[EMIM]^+[EtSO_4]^-$ >$[EMIM]^+[BF_4]^-$> $[BMIM]^+[BF_4]^-$. This order shows that the highest u value is due to the increased size of the anion. Furthermore, the u values decrease as the cation-alkyl chain length of ILs increases as seen in results with same anion [172-175]. This is mainly due to anion accommodation closer to the cation. Apparently, ILs with higher cation side chain it exhibits by lower ρ and lower u. Therefore, our result demonstrates that the influence of the cation and anion is significantly affected by the alkyl imidazolium-based ILs-acetophenone interactions. This may be also be due to the stronger molecular interactions decreasing with

increasing size of alkyl chain length of the cation of alkyl imidazolium-based ILs with acetophenone [173].

5.1.3. Viscosity (η)

Figure 4.3 (a, b, c and d) shows that the η values for all studied binary mixtures increases as concentration and the mole fraction of the IL in acetophenone increases, this may be to the strong coulombic interactions between the ions of ILs which are strengthened upon mixing with acetophenone, leading to lower mobility of ions which is partially based on smaller sizes of ions of ILs. The η values decreases with an increase in temperature due to increased Brownian motion of the constituent molecules of ILs [174]. It is clearly shown in Table 4.1 that the (IL + acetophenone) mixtures are less viscous than pure ILs yet more viscous than acetophenone. In contrary to the η which increases with a decrease in the alkyl chain length of the cation, the values of η increases with an increase in alkyl side chain length of the cation if the system exhibit a common anion. For example, the η values for ($[BMIM]^+[BF_4]^-$ + acetophenone) binary mixture are higher as compared to ($[EMIM]^+[BF_4]$ + acetophenone) binary mixture. This results from an increase in the Van der Waals interactions between alkyl side chains of the cation and the proportion of the charged species in an entire mixture. It is clear that these results possibly imply that the cation size has an effect on the variation of the thermo-physical properties of ILs in mixture with acetophenone. Furthermore, it can be seen that η values for ($[EMIM]^+[EtSO_4]^-$ + acetophenone) binary mixture are higher compared to ($[EMIM]^+[BF_4]$ + acetophenone) binary mixture. This is mainly due to the nature of the anion which also affects the η of ILs for the same cation, particularly through relative basicity and the ability to form the hydrogen bonding. The η values at all temperatures of the alkyl imidazoliumbased ILs with acetophenone follow the order: $[BMIM]^+[PF_6]^- > [BMIM]^+[BF_4]^- > [EMIM]^+[EtSO_4]^- > [EMIM]^+[BF_4]^-$. This order shows that the highest η values are due to the

increased alkyl chain of the cation. According to Kavitha et al. [178], density and viscosity values are relatively sensitive to the ionic size, temperature, and mixture composition. The density and viscosity values of IL mixtures mainly depend on the packaging, size and shape of ions as well as ion–ion interactions. With a higher temperature and lower IL composition, the packing of ions in mixture becomes less efficient, resulting in low density and viscosity values. It can be also concluded that, IL systems that possess a higher cation side chain are accompanied by lower ρ and larger η.

5.1.4. Refractive index (n_D)

Figure 4.4 (a, b, c and d) shows the measured values of n_D for alkyl imidazolium- based ILs with acetophenone at T= (293.15, 303.15, 313.15, 323.15 and 333.15) K over the entire composition range plotted against the mole fraction of the IL. The values of n_D decreased with increasing concentration and temperature of IL in the mixture due to weakened ion–ion pair interactions between the IL and acetophenone and also self-interaction between the ions of IL. The n_D values at T=293.15 K of the alkyl imidazolium-based ILs with acetophenone follow the order: $[EMIM]^+[EtSO_4]^-$> $[BMIM]^+[BF_4]^-$> $[EMIM]^+[BF_4]^-\approx$ $[BMIM]^+[PF_6]^-$. This order clearly shows IL with $[EtSO_4]^-$ anion has higher n_D values with cation $[EMIM]^+$ as compared to $[BF_4]^-$ anion with the same cation this is due to the arrangement of ions and an efficient packing of ions of ILs [173]. The results also indicated that as the alkyl chain of cation decreases the n_D values decrease for ILs with the same anion but different cation. The variations in the values of ρ, u, η and n_D with the concentration and temperature suggest that the physical properties of ILs can be adjusted to meet the need of applications of the ILs by adding acetophenone or changing temperature. There are no previous, ρ, u, η and n_D data reported in the literature for studied systems at various temperatures for comparison.

5.2. Thermodynamic properties

5.2.1. Excess molar volume (V^E_m)

Figure 4.5 (a, b, c and d) representing V^E_m of ILs with acetophenone, shows that the values are positive over a wide mole fraction range at T= (293.15 to 333.15) K and these curves are asymmetric for binary systems ($[BMIM]^+[BF_4]^-$, $[BMIM]^+[PF_6]^-$ + acetophenone), while both positive and negative for the systems ($[EMIM]^+[BF_4]^-$, $[EMIM]^+[EtSO_4]^-$ + acetophenone) with negative values up to $x1 \approx 0.3000$, and ≈ 0.8000 and positive values over the remaining mole fraction indicated in **Figure 4.5 (c and d)**, respectively at all temperatures. As the mole fraction of IL increased the negative V^E_m increased sharply up to $x_1 \approx 0.2000$, and positive V^E_m increased sharply up to $x_1 \approx 0.8000$ for $[EMIM]^+[BF_4]^-$ and as the mole fraction of IL increased the negative V^E_m increased sharply up to $x_1 \approx 0.6000$, and positive V^E_m increased sharply up to $x_1 \approx 0.9000$ for the for $[EMIM]^+[EtSO_4]^-$,while with further addition of the ILs there is a decrease in the excess molar volume graph at all temperature ranges as seen in **Figure 4.5 (c and d)**. This may reveal that more efficient packing is due to the differences in size and shape of molecules in the mixtures or attractive interaction occurs in the region of low mole fraction of IL. Furthermore, the negative V^E_m values of acetophenone-rich region of ($[EMIM]^+[BF_4]^-$ or $[EMIM]^+[EtSO_4]^-$ + acetophenone) becomes positive at higher IL concentration region. This inconsistency may be due to the variation from IL to IL (depending on the cation/anion size) as well as solvent to solvent and also depend on the nature of the structural arrangement of ILs and acetophenone. The positive values shows that there is a volume expansion upon mixing of ILs. There is less volume contraction due to the interactions between unlike molecules which are weaker. The negative values shows that more attractive interactions in the mixtures than in the pure components and the systems have a strong packing effect by associations between ILs and acetophenone molecules through hydrogen bonding. The dependency of V^E_m on temperature and composition for the mixtures can also be elucidated by the difference in

intermolecular forces between the compounds or the difference in the molecular packing, which are due to the changes in size and shape of the molecules forming a binary mixture with other compound [134]. The results in **Figure 4.5 (a, b, c and d)** show that the V^E_m values increased with increasing temperature for all systems at a fixed composition, which indicates the deviation from ideal behavior to become pronounced as the temperature is increased. These observations can be attributed to the natural complexity of the IL with acetophenone systems as far as interactions within the system are concerned. From **Figure 4.5 (a, b, c and d)**, it can be noted that the magnitude of V^E_m values for ILs with acetophenone at studied temperature showed the following order: $[BMIM]^+[PF_6]^-$ > $[BMIM]^+[BF_4]^-$ > $[EMIM]^+[BF_4]^-$ > $[EMIM]^+[EtSO_4]^-$. This order shows the highest V^E_m values is due to the increased alkyl chain of the cation from $[BMIM]^+$ to $[EMIM]^+$. At $T = 333.15$ K the positive values of V^E_m for binary mixture ($[BMIM]^+[BF_4]^-$ + acetophenone) ($V^E_m = 5.623\ V_m^E$ / $cm^3 \cdot mol^{-1}$ at $x_1 = 0.4936$) are more positive than for the system ($[EMIM]^+[BF_4]^-$ + acetophenone) ($V^E_m = 2.721 V_m^E$ / $cm^3 \cdot mol^{-1}$ at $x_1 = 0.5011$) while having the same anion $[BF_4]^-$, therefore V^E_m values become more positive in higher alkyl length of the IL cation under the same experimental condition. The more positive V^E_m values for ($[BMIM]^+[PF_6]^-$ + acetophenone) serves as an evidence that higher alkyl chain molecules decrease the hydrogen bonding tendency between $[BMIM]^+$ with acetophenone. On the other hand, the ($[EMIM]^+[EtSO_4]^-$ + acetophenone) mixture reveals less positive values of V^E_m than other studied systems, which imply that $[EMIM]^+[EtSO_4]^-$ ion–dipole interactions and packing effects with acetophenone are stronger than those in the other systems. Furthermore, it is necessary to note that the anion structure in alkyl imidazolium-based ILs strongly affects the V^E_m values. It was found that $[PF_6]^-$ anion exhibit more positive V^E_m values than the corresponding $[BF_4]^-$ anion with same cation $[BMIM]^+$ and also $[BF_4]^-$ anion more than $[EtSO_4]^-$ anion with same cation $[EMIM]^+$. It has been shown that the values of V^E_m also depend on the basicity as well as size of the anion.

5.2.2. Isentropic compressibility deviation

Figure 4.6 (a, b, c and d) depicts the graphs for $\Delta\kappa s$ against the mole fraction at T= (293.15 K to 333.15) K. The values for $\Delta\kappa s$ are all positive for the whole compositions for the system ($[BMIM]^+[BF_4]^-$ + acetophenone) and both positive and negative for the systems ($[BMIM]^+[PF_6]^-$ or $[EMIM]^+[BF_4]^-$ or $[EMIM]^+[EtSO_4]^-$ + acetophenone), negative up to $x_1\approx$ 0.3000, ≈0.2000 and ≈0.8000 and positive over the remaining mole fraction indicated in **Figure 4.6 (b, c and d)**, respectively at all temperatures. The negative $\Delta\kappa s$ values are attributed to the strong attractive interactions of the ions in the mixture due to the solvation of the ions in the acetophenone. The negative values of $\Delta\kappa s$ implies that acetophenone molecules around the ILs are less compressible than the solvent molecules in the bulk solutions. As the mole fraction of IL increased the negative deviation increased sharply up to $x_1 \approx 0.1000$, 0.0500, and 0.5000, while with further addition of the ILs there is a decrease in the compressibility graph at all temperature ranges. This might be due to a decrease in attraction of acetophenone and IL molecules in the IL-rich concentration region, since the interaction between the IL to IL increases and that between IL to acetophenone decreases. On the other hand, the negative $\Delta\kappa s$ values of acetophenone-rich region of ($[BMIM]^+[PF_6]^-$ or $[EMIM]^+[BF_4]^-$ or $[EMIM]^+[EtSO_4]^-$ + acetophenone) becomes positive values at higher IL concentration region. These inconsistencies vary from IL to IL (depending on the cation/anion size) and solvent to solvent as well as on the nature of the structural arrangement of IL and solvent. The positive values of $\Delta\kappa s$ for binary mixtures of IL with acetophenone are possibly attributed to the repulsive forces due to the electric charge of components and therefore, the molecular interactions between IL and acetophenone molecules weaken. The results in **Figure 4.6 (a, b, c and d)** shows that the $\Delta\kappa s$ values decrease with increasing temperature for all systems at a fixed composition. Moreover, the values followed order $[EMIM]^+[EtSO_4]^- > [EMIM]^+[BF_4]^- > [BMIM]^+[BF_4]^- > [BMIM]^+[PF_6]^-$. The $\Delta\kappa s$ values decreased as alkyl chain length of cation increases and have

higher values for the mixture of $[EMIM]^+$ $[EtSO_4]^-$. These results reveal that $\Delta\kappa s$ values also depend on size of anion with the same cation.

5.2.3. Viscosity deviation ($\Delta\eta$)

Figure 4.7 (a, b, c and d) which is the $\Delta\eta$ graphs of ILs with acetophenone, reveals that the values of $\Delta\eta$ are all negative and become less negative with increasing temperature over a wide mole fraction range at T= (293.15 to 333.15) K under atmospheric pressure, and the minimum existed at IL region; i.e., $x_1 \approx 0.8000-0.9000$ and these curves are asymmetric. The minimum $\Delta\eta$ values are -64.48 mPa·s (at $x_1 \approx 0.8999$), -147.27 mPa·s (at $x_1 \approx 0.8017$), -16.98 mPa·s (at $x_1 \approx 0.8050$) and -38.83 mPa·s (at $x_1 \approx 0.6992$) for ($[BMIM]^+[BF_4]^-$, $[BMIM]^+[PF_6]$, $[EMIM]^+[BF_4]^-$, $[EMIM]^+[EtSO_4]^-$ + acetophenone) systems, respectively. The negative $\Delta\eta$ values indicate that there may be formation of weak hydrogen bonding interactions between the ions of ILs with acetophenone. These results clearly show that the $\Delta\eta$ data is more affected with the alkyl imidazolium cation of ILs, which indicates that the interactions become weaken between the ions of ($[BMIM]^+[PF_6]$ + acetophenone) than ($[BMIM]^+[BF_4]^-$ + acetophenone) and ($[EMIM]^+[EtSO_4]^-$ + acetophenone) than ($[EMIM]^+[BF_4]^-$ + acetophenone) systems because of the weakening of the dipolar association by ILs. The negative $\Delta\eta$ values of $[BMIM]^+$ cation with same anion has higher than $[EMIM]^+$ cation may be due to the steric hindrance of alkyl chain groups in $[BMIM]^+$ cations. When acetophenone is added to the IL, the viscosities of the mixtures decreases faster, mainly at lower temperatures. The strong coulomb interaction between the anions and cations becomes strong upon adding acetophenone, which in turn leads to a higher mobility of the ions and hence a lower viscosity of the mixtures. The $\Delta\eta$ values at all temperatures of the alkyl imidazolium-based ILs with acetophenone follow the order: $[EMIM]^+[BF_4]^-$> $[EMIM]^+[EtSO_4]^-$> $[BMIM]^+[BF_4]^-$>

$[BMIM]^+[PF_6]^-$. This order displays the highest negative $\Delta\eta$ deviation values is due to the increased alkyl chain of the cation.

5.2.4. Refractive index deviation (Δn_D)

The "Δn_D" values can be used to determine the electronic polarizability of a molecule and provide useful information about the intermolecular interactions between molecules. In this regard, the data of Δn_D of liquid mixtures are required as to better the understanding of the electronic polarizability of the molecule and intermolecular interactions between unlike molecules in mixture. However, an accurate Δn_D data for ILs with molecular solvents are still scarce. In the context, **Figure 4.8 (a, b, c and d)** show Δn_D for binary mixture of alkyl imidazolium-based ILs with acetophenone and indicates that both negative and positive values for Δn_D over a wide mole fraction range at T= (293.15 to 333.15) K under atmospheric pressure and these curves are asymmetric with both minimum and maximum values reaching near 0.4000-0.6000 and 0.9000 mole fraction of IL, respectively. The Δn_D values increased as the temperature increased. The positive values of Δn_D may be due to the stronger interactions of ions of ILs with acetophenone and negative values attributed to weaker interaction ions of ILs with acetophenone. The values for Δn_D are dependent mainly on the difference in intermolecular interactions occurring between the two components. It can be seen that positive or negative V^E_m values corresponded to negative or positive Δn_D values, and the minimum or maximum of both values exist at almost the same mole fraction of IL of corresponding systems. On the other hand, the followed the order is $[EMIM]^+[BF_4]^-$ > $[EMIM]^+[EtSO_4]^-$ > $[BMIM]^+[PF_6]^-$ > $[BMIM]^+[BF_4]^-$. The Δn_D values deceased as alkyl chain length increased and have higher values of the mixture of $[EMIM]^+[BF_4]^-$ than $[BMIM]^+[BF_4]^-$. These results reveal that Δn_D values also depend on the size of anion with the same cation. The opposite signs between V^E_m and Δn_D is mainly because there will be less free volume available (if V^E_m is negative) and more free volume available (if V^E_m is positive) than in an ideal solution and

photons will be more likely to interact with molecules or ions constituting the compound [150, 179-180].

5.3. Quantum chemical calculations analysis

The interaction energies and change in Gibb's free energies are given in Table 4.3. More negative ΔE_{int} is an indication of stronger interaction when comparing interactions between two or more systems [181-182]. As shown in the Table 4.3, ΔE_{int} of the ionic systems in the presence of acetophenone remarkably increased (less negative) as compared to when they were without the solvent. This is an indication of appreciable decrease in the cation-anion interaction in the presence of the solvent [183]. This can be attributed to the separate interactions of the cations and anions of the ionic liquids with the acetophenone molecules (i.e. ion-solvent interactions) rather than with each other (i.e cation-anion interactions) [160, 181]. The ionsolvent interaction reduces the cation-anion interaction by reducing the number of anion-cation pairs that are available for the cation-anion interaction [183-184]. Moreover, the acetophenone has the tendency to interact with the cation both by ion-dipole interaction and cation-pi interaction as shown in **Figure 4.9** which leads to dissociation of the ionic liquid system [184].

The Δ_{Eint} of the studied ionic liquid in solvent system, followed the order $[BMIM]^+[PF_6]^-$ > $[BMIM]^+[BF_4]^-$ > $[EMIM]^+[EtSO_4]^-$ > $[EMIM]^+[BF_4]^-$. This trend shows that the extent of the solvent-ion interactions in ionic liquids follows the same order because the lower the cation-anion interaction (i.e. less negative ΔE_{int}), the greater the ion-solvent interaction. The change in Gibb's free energy (ΔG) of the ionic systems also follows the similar trend as $\Delta Eint$, indicates a reduced spontaneity of the cation-anion interactions in the presence of the acetophenone in the order $[BMIM]^+[PF_6]^-$ > $[BMIM]^+[BF_4]^-$ > $[EMIM]^+[EtSO_4]^-$ > $[EMIM]^+[BF_4]^-$ because of energetically more favourable solvent-ion interaction. The $[BMIM]^+[PF_6]^-$ system has the highest ΔG (13.01 $kJmol^{-1}$) which means the cation-anion interaction is least favourable and

automatically the ion-solvent interaction is most favourable in this system relative to other systems of study.

The trends for the thermophysical properties and quantum chemical studies for the investigated systems are supporting each other. As stated before that the ΔE_{int} and ΔG follow the same trends due to the dominance of ion-solvent interactions occurring between the ILs and the solvents, a same trend is also observed for η because of the coulombic interactions which are strengthened upon adding acetophenone resulting in low mobility of ions therefore reducing the cation-anion interactions. A more similar trend is observed for, ρ, but for ΔE_{int} and ΔG the values increased with an increase in alkyl chain length whereas for the values increased with a decrease in alkyl chain length, especially for systems that possesses the same anion but different cation. The trends are observed for u and n_D are far more dissimilar to those observed for ΔE_{int}, because the values of u and n_D are depended on the size of the anion and the values increased with a decrease in alkyl in contrary to observed values of ΔE_{int}.

CHAPTER SIX

CONCLUSION

In order to gain some awareness into the new generation about novel class of green solvents, we have reported new data for densities (ρ), sound velocities (u), viscosities (η), and refractive indices (n_D) for binary mixtures of four alkyl imidazolium-based ionic liquids; $[BMIM]^+[BF_4]^-$, $[BMIM]^+[PF_6]^-$, $[EMIM]^+[BF_4]^-$ and $[EMIM]^+[EtSO_4]^-$, with acetophenone over the wide composition range at T= (293.15 to 333.15) K under atmospheric pressure. The study shows effects of temperature, concentration, alkyl chain as well as cation/anion of ILs on the molecular interaction behavior of alkyl imidazolium-based IL with acetophenone molecules. From the experimental data, excess and derived properties such as V^E_m, $\Delta\kappa_s$, $\Delta\eta$ and Δn_D were calculated and fitted to Redlich-Kister equation to check the accuracy of experimental results and were found to be in good agreement. Our results reveal that the values of, ρ, u and η increased as concentration of the IL increased whereas the opposite trend is observed for n_D and all the measured properties decreased with temperatures. Results obtained indicates that the ρ, u and n_D values decreased with an increase in the cation alkyl chain length, but an opposite trend was observed for η, in which the values of η increase when the number of carbon atoms in the alkyl chain length of cation of ILs increased. The excess and derived properties, V^E_m, $\Delta\kappa s$ and Δn_D are both negative and positive, while the $\Delta\eta$ values are negative over the entire composition range. This results shows that the cation and anion of ILs have a strong influence on the excess and deviation properties, especially on excess molar volume. Quantum chemical studies confirm the interactions of acetophenone with the ILs and also show that the solvent-ion interaction is highest in $[BMIM]^+[PF_6]^-$ system and lowest in $[EMIM]^+[BF_4]^-$ thereby confirming the experimental results.

REFERENCES

[1] P. Sun, D. W. Armstrong, Ionic liquids in analytical chemistry, *Anal. Chim. Acta* 661 (2010) 1–16.

[2] K. N. Marsh, J. A. Boxall, R. Lichtenthaler, Room temperature ionic liquids and their mixtures–a review, *Phys. Chem. Chem. Phys.* 219 (2004) 93–98.

[3] M. Freemantle, An introduction to ionic liquids, Cambridge: RSC, Chapter 1 (2010) 1–10.

[4] Z. Yang, W. Pan, Ionic liquids: Green solvents for nonaqueous biocatalysis, *Enzyme Microb. Technol.* 37 (2005) 19–28.

[5] S. Keskin, D. Kayrak-Talay, U. Akman, O. Hortac, A review of ionic liquids towards supercritical fluid applications, *J. Supercrit. Fluids* 43 (2007) 150–180.

[6] I. Krossing, J. M. Slattery, C. Daguenet, P. J. Dyson, A. Oleinikova, H. Weingaertner, Why are ionic liquids liquid? A simple explanation based on lattice and solvation energies, *J. Am. Chem. Soc.* 128 (2006) 13427–13434.

[7] G. Laus, G. Bentivoglio, H. Schottenberger, V. Kahlenberg, H. Kopacka, T. Röder, H. Sixta, Ionic liquids: current developments, potential and drawbacks for industrial applications, *Lenzinger Ber.* 84 (2005) 71–85.

[8] R. Renner, Ionic liquids: an industrial clean up solution, *Environ. Environ. Sci. Technol.* 35 (2001) 410A–413A.

[9] H. Li, G. Zhao, F. Liu, S. Zhang, Physicochemical characterization of MFm-based ammonium ionic liquids, *J. Chem. Eng. Data* 58 (2013) 1505−1515.

[10] D. Han, K. Ho Row, Recent applications of ionic liquids in separation technology, *Molecules* 15 (2010) 2405−2426.

[11] D. Shao, X. Lu, W. Fang, Y. Guo, L. Xu, Densities and viscosities for binary mixtures of the ionic liquid *N*-ethyl piperazinium propionate with *n*-alcohols at several temperatures, *J. Chem. Eng. Data* 57 (2012) 937–942.

[12] Q. Yang, D. D Dionysios, Photolytic degradation of chlorinated phenols in room temperature ionic liquids, *J. Photochem. Photobiol. A* 165 (2004) 229–240.

[13] H. Yao, S. Zhang, J. Wang, Q. Zhou, H. Dong, X. Zhang, Densities and viscosities of the binary mixtures of 1-ethyl-3-methylimidazolium bis(trifluoromethylsulfonyl)imide with *N*-methyl-2-pyrrolidone or ethanol at $T = 293.15$ to 323.15 K, *J. Chem. Eng. Data* 57 (2012) 875–881.

[14] T. Welton, Room-temperature ionic liquids. Solvents for synthesis and catalysis, *Chem. Rev.* 99 (1999) 2071–2084.

[15] A. Kumar, S. Pawar, Converting exo-selective Diels-Alder reaction to endo-selective in chloroloaluminate ionic liquids, *J. Org. Chem.* 69 (2004) 1419–1420.

[16] M. Freemantle, Designer solvents: ionic liquids may boost clean technology development, *Chem. Eng. News* 76 (1998) 32–37.

[17] K. Fletcher, S. Pandey, Surfactant aggregation within room temperature ionic liquid 1ethyl-3-methylimidazolium bis [(trifluoromethylsulfonyl)] imide, *Langmuir* 20 (2004) 33–36.

[18] D. Zhao, M. Wu, Y. Kou, E. Min, Ionic liquids: applications in catalysis. *Catal. Today* 74 (2002) 157–189.

[19] J. F. Brennecke, E. J. Maginn, Ionic liquids: Innovative fluids for chemical processing *AIChE J.* 47 (2001) 2384–2389.

[20] P. Wasserscheid, W. Keim, Ionic liquids—New "solutions" for transition metal *Catalysis Angew. Chem. Int. Ed.* 39 (2000) 3773–3789.

[21] J. S. Wilkes, Properties of ionic liquid solvents for catalysis, *J. Mol. Catal. A* 214 (2004) 11–17.

[22] V. R. Koch, L. A. Dominey, C. Nanjundiah, The intrinsic anodic stability of several anions comprising solvent_free ionic liquids, *J. Electrochem. Soc.* 143 (1996) 798–803.

[23] H. Every, A. G. Bishop, M. Forsyth, D. R. MacFarlane, Ion diffusion in molten salt mixtures, *Electrochim. Acta* 45 (2000) 1279–1284.

[24] M. Doyle, S. K. Choi, G. Proulx, High_temperature proton conducting membranes based on perfluorinated ionomer membrane_ionic liquid composites, *J. Electrochem. Soc.* 147 (2000) 34–37.

[25] V. V. Singh, K. Nigam, A. Batra, M. Boopathi, B. Singh, R. Vijayaraghavan, Applications of ionic liquids in electrochemical sensors and biosensors, *Int. J. Electrochem.* 2012 (2012) 1–19.

[26] F. Endres, S. Zein, E. L. Abedin, Air and water stable ionic liquids in physical chemistry, *Phys. Chem. Chem. Phys*. 8 (2006) 2101–2116.

[27] J. D. Hlbrey, R. D. Rogers, Ionic liquids in synthesis, Wiley-VCH, Weinheim, 2003, 41–55.

[28] S. Park, R. Kazlauskas, Biocatalysis in ionic liquids—advantages beyond green technology, *Curr. Opin. Biotechnol*. 14 (2003) 432– 437.

[29] P. Bonhôte, A. Dias, N. Papageorgiou, K. Kalyanasundaram, M. Grätzel, Hydrophobic, highly conductive ambient-temperature molten salts, *Inorg. Chem*. 35 (1996) 1168–1178.

[30] P. J. Carvalho, T. Regueira, L. M. N. B. F. Santos,| J. Fernandez, J. A. P. Coutinho, Effect of water on the viscosities and densities of 1-butyl-3-methylimidazolium dicyanamide and 1-butyl-3-methylimidazolium tricyanomethane at atmospheric pressure, J. Chem. Eng. Data 55 (2010) 645–652.

[31] U. Doma´nska, A. Pobudkowska, A. Wi´sniewska, Solubility and excess molar properties of 1,3-dimethylimidazolium methylsulfate, or 1-butyl-3-methylimidazolium methylsulfate, or 1-butyl-3-methylimidazolium octylsulfate ionic liquids with n-Alkanes and alcohols: Analysis in terms of the PFP and FBT models, J. Sol. Chem. 35 (2006).

[32] U. Domìnguez, M. Królikowska, Effect of temperature and composition on the surface tension and thermodynamic properties of binary mixtures of 1-butyl-3-methylimidazolium thiocyanate with alcohols, J. Col. Int. Sci. 348 (2010) 661–667.

[33] J. M. Prausnitz, Thermodynamics and the other chemical engineering sciences: old models for new chemical products and processes, *Fluid Phase Equilib.* 95 (1999) 158–160.

[34] P. B Mandal, K. Madhusree, S. S. Bandyopadhyay, Density and viscosity of aqueous solutions of *N*-methyldiethanolamine + monoethanolamine, *N*-methyldiethanolamine + diethanolamine, 2-amino-2-methyl-1-propanol + monoethanolamine, and 2-amino-2methyl-1-propanol + diethanolamine, *J. Chem. Eng. Data* 48 (2003) 703–707.

[35] M. J. Dávila, S. Aparicio, R. Alcalde, Thermophysical properties of binary and ternary mixtures containing lactams and methanol, *Ind. Eng. Chem. Res.* 48 (2009) 10065–10076.

[36] Y. Maham, L. Lebrette, A. E. Mather, Viscosities and excess properties of aqueous solutions of mono- and diethylethanolamines at temperatures between 298.15 and 353.15 K, *J. Chem. Eng. Data* 47 (2002) 550–553.

[37] P. Abrman, I. Malijevská, Solid–liquid equilibria in the acetic acid–propanoic acid and propanoic acid–trifluoroacetic acid systems, *Fluid Phase Equilib.* 166 (1999) 47–52.

[38] Z. Zhou, Y. Shi, X. Zhou, Theoretical studies on the hydrogen bonding interaction of complexes of formic acid with water, *J. Phys. Chem. A* 108 (2004) 813–822.

[39] W. Dongqing, J. F. Truchon, S. Sirois, D. Salahub, Solvation of formic acid and proton transfer in hydrated clusters, *J. Chem. Phys.* 116 (2002) 6028–6038.

[40] G. F. Velardez, J. C. Ferrero, J. A. Beswick, J. P. Daudey, Ab initio study of the structures and π^* n electronic transition in formic acid – (water) n (n = 3, 4, and 5) hydrogen bonded complexes, *J. Phys. Chem. A* 105 (2001) 8769–8774.

[41] S. Zhang, N. Sun, X. He, X. Lu, X. Zhang, Physical properties of ionic liquids: database and evaluation, *J. Phys. Chem Ref. Data* 35 (2006) 1475–1517.

[42] B. González, N. Calvar, E. González, A. Domínguez, Density and viscosity experimental data of the ternary mixtures 1-propanol or 2-propanol+ water+1-ethyl-3-methylimidazolium ethylsulfate, correlation and prediction of physical properties of the ternary systems, *J. Chem. Eng. Data* 53 (2008) 881–887.

[43] A. B. Pereiro, J. L Legido, A. Rodríguez, Physical properties of ionic liquids based on 1-Alkyl-3-methylimidazolium cation and hexafluorophosphate as anion and temperature dependence, *J. Chem. Thermodyn.* 39 (2007) 1168–1175.

[44] G. Annat, M. Forsyth, D. R. MacFarlane, Ionic liquid mixtures variations in physical properties and their origins in molecular structure, *J. Phys. Chem. B* 116 (2012) 8251–8258.

[45] M. Deetlefs, K. R. Seddon, M. Shara, Predicting physical properties of ionic liquids, *Phys. Chem. Chem. Phys.* 8 (2006) 642–649.

[46] S. P. Verevkin, V. N. Emel'yanenko, I. Krossing, R. Kalb, Thermochemistry of ammonium based ionic liquids: Tetra-alkyl ammonium nitrates – experiments and computations, *J. Chem. Thermodyn.* 51 (2012) 107–113.

[47] V. Govinda, P. Attri, P. Venkatesu, P. Venkateswarlu, Thermophysical properties of dimethylsulfoxide with ionic liquids at various temperatures, *Fluid Phase Equilib.* 304 (2010) 35–43.

[48] B. Mokhtarani, A. Sharifi, H. R. Mortaheb, M. Mirzaei, M. Mafi, F. J. Sadeghian, Density and viscosity of pyridinium-based ionic liquids and their binary mixtures with water at several temperatures, *J. Chem. Thermodyn.* 41 (2009) 323–329.

[49] M. Wagner, O. Stanga, W. Schröer, Corresponding states analysis of the critical points in binary solutions of room temperature ionic liquids, *Phys. Chem. Chem. Phys.* 5 (2003) 3943–3950.

[50] J. Ortega, R. Vreekamp, E. Marrero, E. Penco, Thermodynamic properties of 1-butyl-3-methylpyridinium tetrafluoroborate and its mixtures with water and alkanols, *J. Chem. Eng. Data* 52 (2007) 52, 2269–2276.

[51] S. M. Walas, Phase equilibria in chemical engineering, Butterworths, Stoneham, MA 1985.

[52] T. M. Letcher, The excess volumes of some mixtures of saturated and unsaturated C6 hydrocarbons, *J. Chem. Thermodyn.* 7 (1975) 205–209.

[53] R. Battino, Volume changes on mixing for binary mixtures of liquids, *Chem. Rev.* 71 (1971) 5–45.

[54] Y. P. Handa, G. C. Benson, Volume changes on mixing two liquids: A review of the experimental techniques and the literature data, *Fluid Phase Equilib.* 3 (1979) 185–249.

[55] L. A. Beath, S. P. O`. Neill, A. G. Williamson, Thermodynamics of ether solutions II. Volumes of mixing of ethers with carbon tetrachloride and with chloroform at 250 C, *J. Chem. Thermodyn.* 1 (1969) 293–300.

[56] H. D. Pflug, G. C. Benson, Molar excess volumes of binary n-alcohol systems at 25 °C, *Can. J. Chem.* 46 (1968)287–294.

[57] R. H. Stokes, K. N. Marsh, Solutions of nonelectrolytes, *J. Chem. Thermodyn.* 23 (1972) 65–92.

[58] K. N. Marsh, Thermodynamics of liquid mixtures, *Annu. Rep. Prog. Chem. Sect. C: Phys. Chem.* Chapter 4. 77 (1980) 101–120.

[59] K. N. Marsh, Thermodynamics of liquid mixtures, *Annu. Rep. Prog. Chem. Sect. C: Phys. Chem.* Chapter 7. 81 (1984) 209–245.

[60] M. K. Kumaran, M. L. McGlashan, An improved dilution dialometer for measurements of excess volumes, *J. Chem. Thermodyn.* 9 (1977) 259–267.

[61] S. E. Wood, J. P. Brusie, The volume of mixing and the thermodynamic functions of benzene-carbon tetrachloride mixture, *J. Am. Chem. Soc.* 65 (1943) 1891–1895.

[62] F. Franks, H. T. Smith, Apparent molal volumes and expansibilities of electrolytes in dilute aqueous solution, *Trans. Faraday Soc.* 63 (1967) 2586–2598.

[63] J. A. Nevines, Thermodynamics of nonelectrolytes liquid mixtures, PhD thesis, UKZN, Durban (1997) 78–80.

[64] G. G. Redhi, Thermodynamics of liquid mixtures containing carboxylic acids, PhD thesis, UKZN, Durban (2003) 6–16.

[65] D. B Keyes, J. H. Hildebrand, A study of the system aniline-hexane, *J. Am. Chem. Soc.* 39 (1917) 2126–2137.

[66] G. A. Bottomly, R. L. Scott, A grease – free continuous dilution dilatometer; excess volumes for benzene + carbon tetrachloride, *J. Chem. Thermodyn.* 6 (1974) 973–981.

[67] R. Azevedo, J. Szydlowski, P. F. Pires, J. M. S. S. Esperança, H. J. R. Guedes, L. N. P. Rebelo, Novel nonintrusive microcell for sound-speed measurements in liquids. Speed of sound and thermodynamic properties of 2-propanone at pressures up to 160 MPa, *J. Chem. Thermodyn.* 36 (2004) 211–222.

[68] Y. A. Urzhumov, Sub-wavelength electromagnetic phenomena in plasmonic and polaritonic nanostructures: from optical magnetism to super-resolution", PhD thesis, The University of Texas at Austin (2007).

[69] M. A. Iglesias-Otero, J. Troncoso, E. Carballo, L. Romanı´, Density and refractive index in mixtures of ionic liquids and organic solvents: Correlations and predictions, *J. Chem. Thermodyn.* 40 (2008) 949–956.

[70] G.E. Leblanc, R.A. Secco, M. Kostic, Viscosity measurement, CRC Press LLC (1999).

[71] F. Gui, T. F. Irvine Jr, Theoretical and experimental study of the falling cylinder viscometer, *Int. J. Heat and Mass Transfer* 37 (1994) 41-50.

[72] A. Kovács, R. J. M. Konings, J. K. Gibson, I. Infante, L. Gagliardi, Quantum chemical calculations and experimental investigations of molecular actinide oxides, *Chem. Rev.* 115 (2015) 1725−1759.

[73] A. Jardy, A. L. Lasalle-Molin, M. Keddam, H. Takenouti, Copper dissolution in acidic sulphate media studied by QCM and rrde under ac signal, *Electrochim. Acta* 37 (1993) 2195−2201.

[74] D. Tromans, Aqueous Potential_pH Equilibria in Copper_Benzotriazole Systems, *J. Electrochem. Soc.* 145 (1998) L42−L45.

[75] R. Walter, Benzotriazole as a Corrosion Inhibitor for Immersed Copper, *Corrosion* 29 (1973) 290−298.

[76] V. Brusic, M. A. Frisch, B. N. Eldridge, F. P. Novak, F. B. Kaufman, B. M. Rush, G. S. Frankel, Copper Corrosion With and Without Inhibitors, *J. Electrochem. Soc.* 138 (1991) 2253– 2259.

[77] S. L. F. da Costa, S. M. L. Agostinho, K. Nobe, Rotating Ring_Disk Electrode Studies of Cu_Zn Alloy Electrodissolution in 1M HCl Effect of Benzotriazole, *J. Electrochem. Soc.* 140 (1993) 3483–3488.

[78] D. Tromans, R. Sun, Anodic polarization behavior of copper in aqueous chloride/benzotriazole solutions, *J. Electrochem. Soc.* 138 (1991) 3235–3244.

[79] K. F. Khaled, Molecular simulation, quantum chemical calculations and electrochemical studies for inhibition of mild steel by triazoles, *Electrochim. Acta* 53 (2008) 3484–3492.

[80] T. E. Shubina, M. T. M. Koper, Quantum-chemical calculations of CO and OH interacting with bimetallic surfaces, *Electrochim. Acta* 47 (2002) 3621–3628.

[81] N. Lopez, F. Illas, Ab initio modeling of the metal−support interface: The interaction of Ni, Pd, and Pt on MgO(100), *J. Phys. Chem. B* 102 (1998) 1430–1436.

[82] J. Andrés, J. Beltran, Química Teóricay Computacional, Universitat Jaume I, Castellón de la Plana, Espãna, 2000.

[83] S. Biing-Ming, S. Zhang, Z. C. Zhang, Structural elucidation of thiophene interaction with ionic liquids by multinuclear NMR spectroscopy, *J. Phys. Chem.* 108 (2004) 19510–19517.

[84] B. O. Roos, K. P. Lawley, Advances in chemical physics; Ab initio methods in quantum chemistry II England: Wiley-Chichester, Inc. (1987).

[85] S. Zhang, X. Lu, Y. Zhang, Q. Zhou, J. Sun, L. Han, G. Yue, X. Liu, X. Cheng, S. Li, Ionic liquids and relative process design, Springer-Verlag, 2008; DOI: 10.1007/430.

[86] I. G Cruz, D. Valencia, T. Klimova, R. O. Roa, J. M. Magadan, R. D. Balderas, F. Illas, Proton affinity of S-containing aromatic compounds: Implications for crude oil hydrodesulfurization, *J. Mol. Catal. A: Chem.* 281 (2008) 79–84.

[87] N. Deenadayalu, I. Bahadur, T. Hofman, Ternary excess molar volumes of {methyltrioctylammonium bis(trifluoromethylsulfonyl)imide + ethanol + methyl acetate, or ethyl acetate} systems at T = (298.15, 303.15, and 313.15) K, *J. Chem. Thermodyn.* 42 (2010) 726–733.

[88] N. Deenadayalu, I. Bahadur, T. Hofman, Ternary excess molar volumes of {methyltrioctylammonium bis[(trifluoromethyl)sulfonyl]imide + methanol + methyl

acetate or ethyl acetate} systems at (298.15, 303.15, and 313.15) K, *J. Chem. Eng. Data* 55 (2010) 2636–2642.

[89] N. Deenadayalu, I. Bahadur, T. Hofman, Volumetric properties for (ionic liquid + methanol or ethanol or 1-propanol + nitromethane) at 298.15 K and atmospheric pressure, *J. Chem. Eng. Data* 56 (2011) 1682–1686.

[90] I. Bahadur, N. Deenadayalu, Apparent molar volume and isentropic compressibility for the binary systems {methyltrioctylammonium bis(trifluoromethylsulfonyl)imide + methyl acetate or methanol} and (methanol + methyl acetate) at T = 298.15, 303.15, 308.15 and 313.15 K and atmospheric pressure, *J. Solution Chem.* 40 (2011) 1528–1543.

[91] I. Bahadur, N. Deenadayalu, Z. Tywabi, S. Sen, T. Hofman, Volumetric properties of ternary (IL + 2-propanol or 1-butanol or 2-butanol + ethyl acetate) systems and binary (IL + 2-propanol or 1-butanol or 2-butanol) and (1-butanol or 2-butanol + ethyl acetate) systems, *J. Chem. Thermodyn.* 49 (2012) 24–38.

[92] I. Bahadur, N. Deenadayalu, Apparent molar volume and apparent molar isentropic compressibility for the binary systems {methyltrioctylammoniumbis(trifluoromethylsulfonyl)imide + ethyl acetate orethanol} at different temperatures under atmospheric pressure, *Thermochim. Acta* 566 (2013) 77–83.

[93] I. Bahadur, N. Deenadayalu, Densities and excess molar volume for the ternary systems (1-butyl-3-methylimidazolium methyl sulphate + nitromethane + methanol or ethanol or 1-propanol) at T = (303.15 and 313.15) K, *S. Afr. J. Chem.* 66 (2013) 200–206.

[94] V. Govinda, P. M. Reddy, I. Bahadur, P. Attri, P. Venkatesu, P. Venkateswarlu, Effect of anion variation on the thermophysical properties of triethylammonium based protic ionic liquids with polar solvent, *Thermochim. Acta* 566 (2013) 75–88.

[95] I. Bahadur, T. M. Letcher, S. Singh, G. G. Redhi, P. Venkatesu, D. Ramjugernath, Excess molar volumes of binary mixtures (an ionic liquid + water): A review, *J. Chem. Thermodyn.* 82 (2015) 34–46.

[96] S. Singh, I. Bahadur, G. G. Redhi, D. Ramjugernath, E. E. Ebenso, Density and speed of sound measurements of imidazolium-based ionic liquids with acetonitrile at various temperatures, *J. Mol. Liq.* 200 (2014) 160–167.

[97] S. Singh, I. Bahadur, G. G. Redhi, E. E. Ebenso, D. Ramjugernath, Influence of the alkyl group on thermophysical properties of carboxylic acids in 1-butyl-3methylimidazolium thiocyanate ionic liquid at various temperature, *J. Chem. Thermodyn.* 89 (2015) 104–111.

[98] S. Singh, I. Bahadur, G. G. Redhi, E. E. Ebenso, D. Ramjugernath, S. Singh, I. Bahadur, G. G. Redhi, E. E. Ebenso, D. Ramjugernath, Density and speed of sound of 1-ethyl-3-methylimidazolium ethyl sulphate with acetic or propionic acid at different temperatures, *J. Mol. Liq.* 199 (2014) 518–523.

[99] F. M. Maia, N. Calvar, E. J. González, A. P. Carneiro, O. Rodriguez, E. A. Macedo, Modeling of ionic liquid systems: Phase equilibria and physical properties - New aspects for the future, InTech, DOI: 10.5772/51812.

[100] S. Govardhana Rao, T. Madhu Mohan, T. Vijaya Krishna, B. Subba Rao, Volumetric properties of 1-butyl-3-methylimidazolium tetrafluoroborate and 2-pyrrolidone from T = (298.15 to 323.15) K at atmospheric pressure, *J. Chem. Thermodyn.* 94 (2016) 127–137.

[101] A. Pal, M. Saini, B. Kumar, Volumetric, ultrasonic and spectroscopic (FT-IR) studies for the binary mixtures of imidazolium based ILs with 1, 2-propanediol, *Fluid Phase Equilib.* 411 (2016) 66-73.

[102] M. Srinivasa Reddy, Sk.Md Nayeem, C. Souminic, K. T. S. S. Raju, B. Hari Babu, Study of molecular interactions in binary liquid mixtures of [EMIM][BF_4] with 2methoxyethanol using thermo acoustic, volumetric and optical properties, *Thermochim. Acta* 630 (2016) 37–49.

[103] M. Srinivasa Reddy, Sk.Md Nayeem, S. S. Raju, V. Srinivasa Rao, B. Hari Babu, The study of solute–solvent interactions in 1-ethyl-3-methylimidazoliumethylsulfate + 2ethoxyethanol from density, speed of sound and refractive index measurements, *J. Mol. Liq.* 218 (2016) 83–94.

[104] T. Srinivasa Krishna, K. T. S. S. Raju, M. Gowrisankar, A.K. Nain, B. Munibhadrayya, Volumetric, ultrasonic and spectroscopic studies of molecular interactions in binary mixtures of 1-butyl-3-methylimidazolium hexafluorophosphate with 2-propoxyethanol at temperatures from 298.15 to 323.15 K, *J. Mol. Liq.* 216 (2016) 484–495.

[105] X-H Fan, Y-P Chen, C-S Su, Density and viscosity measurements for binary mixtures of 1-ethyl-3-methylimidazolium tetrafluoroborate ($[EMIM]^+[BF_4]^-$) with dimethylacetamide, dimethylformamide, and dimethyl sulfoxide, *J. Chem. Eng. Data 61* (2016) 920–927.

[106] T. Krishna, M. Sankar, K. Raju, S. Rao, B. Munibhadrayya, Acoustic, volumetric, and optic study of binary mixtures of 1-butyl-3- methylimidazolium tetrafluoroborate with propylene glycols at T = 298.15 to 323.15 K, *J. Mol. Liq.* 206 (2015) 350–358.

[107] S. Govardhana Rao, T. Madhu Mohan, T. Vijaya Krishna, K. T. S. S. Raju, B. Subba Rao, Excess thermodynamic properties of ionic liquid 1-butyl-3-methylimidazolium tetrafluoroborate and *N*-octyl-2-pyrrolidone from T = (298.15 to 323.15) K at atmospheric pressure, *J. Chem. Thermodyn.* 89 (2015) 286–295.

[108] S. Govardhana Rao, T. Madhu Mohan, T. Vijaya Krishna, T. Srinivasa Krishna, B. Subba Rao, Density, refractive index, and speed of sound of the binary mixture of

1-butyl-3-methylimidazolium tetrafluoroborate + *N*-Vinyl-2- pyrrolidinone from T = (298.15 to 323.15) K at atmospheric pressure, *J. Chem. Eng. Data* 60 (2015) 886–894.

[109] S. Govardhana Rao, T. Madhu Mohan, T. Vijaya Krishna, K. Narendra, B. Subba Rao, Thermophysical properties of 1-butyl-3-methylimidazolium tetrafluoroborate and *N*-methyl-2-pyrrolidinone as a function of temperature, *J. Mol. Liq.* 211 (2015) 1009–1017.

[110] J-Y Wu, Y-P. Chen, C-S. Su, Density and viscosity of ionic liquid binary mixtures of 1-butyl-3-methylimidazolium tetrafluoroborate with acetonitrile, *N,N*-dimethylacetamide, methanol, and *N*-methyl-2-pyrrolidone, *J. Solution Chem.* 44 (2015) 395–412.

[111] E. Vercher, F. J. Llopis, V. Gonzalez-Alfaro, P. J. Miguel, V. Orchilles, A. Martinez-Andreu, Volumetric properties, viscosities and refractive indices of binary liquid mixtures of tetrafluoroborate-based ionic liquids with methanol at several temperatures, *J. Chem. Thermodyn.* 90 (2015) 174–184.

[112] H. R. Rafiee, F. Frouzesh, Volumetric properties for binary and ternary mixtures of allyl alcohol, 1, 3-dichloro-2-propanol and 1-ethyl-3-methyl imidazolium ethyl sulfate [EMIM][EtSO4] from T = 298.15 to 318.15 K at ambient pressure, *Thermochim. Acta* 611 (2015) 36–46.

[113] Z. Vaid, U. More, S. P. Ijardar, N. I. Malek, Investigation on thermophysical and excess properties of binary mixtures of imidazolium based ionic liquids at temperatures (293.15 to 323.15) K: III [CnMIM][PF_6] (n = 4, 6, 8) + THF, *J. Chem. Thermodyn.* 86 (2015) 143–153.

[114] Z. Vaid, U. U. More, R. L. Gardas, N. I. Malek, S. P. Ijardar, Composition and temperature dependence of excess properties of binary mixtures of imidazolium based

ionic liquids: II ([C_nMIM][PF_6]) + propylamine, *J Solution Chem.* 44 (2015) 4718–4741.

[115] J. Y. Wua, Y. P. Chen , C. S. Su, The densities and viscosities of a binary liquid mixture of 1-butyl-3-methylimidazolium tetrafluoroborate, $[BMIM]^+[BF_4]^-$ with acetone, methyl ethyl ketone and *N,N*-dimethylformamide, at 303.15 to 333.15 K, *J. Taiwan Inst. Chem. Eng.* 45 (2014) 2205–2211.

[116] S. Singh, I. Bahadur, G. G. Redhi , E. E. Ebenso, D. Ramjugernath, Density and speed of sound of 1-ethyl-3-methylimidazolium ethyl sulphate with acetic or propionic acid at different temperatures, *J. Mol. Liq.* 199 (2014) 518–523.

[117] S. Singh, I. Bahadur, G. G. Redhi, D. Ramjugernath, E. E. Ebenso, Density and speed of sound measurements of imidazolium-based ionic liquids with acetonitrile at various temperatures, *J. Mol. Liq.* 200 (2014) 160–167.

[118] G. R. Chaudhary, S. Bansal, S. K. Mehta , A S. Ahluwalia, Thermophysical and spectroscopic studies of pure 1-butyl-3-methylimidazolium tetrafluoroborate and its aqueous mixtures, *J. Solution Chem.* 43 (2014) 340–359.

[119] O. Ciocirlan, O. Croitoru, O. Iulian, Density and refractive index of binary mixtures of two 1-alkyl-3-methylimidazolium ionic liquids with 1,4-dioxane and ethylene glycol, *J. Chem. Eng. Data* 59 (2014) 1165−1174.

[120] S. Bhagour, S. Solanki, N. Hooda, D. Sharma, V. K. Sharma, Thermodynamic properties of binary mixtures of the ionic liquid $[EMIM]^+[BF_4]^-$ with acetone and dimethylsulphoxide, *J. Chem. Thermodyn.* 60 (2013) 76–86.

[121] O. Iulian, O. Ciocirlan, Volumetric properties of binary mixtures of two 1-alkyl-3-methylimidazolium tetrafluoroborate ionic liquids with molecular solvents, *J. Chem. Eng. Data* 57 (2012) 2640−2646.

[122] E. Rilo , L. M. Varela, O. Cabeza, Density and derived thermodynamic properties of 1- ethyl-3 methylimidazolium alkyl sulphate ionic liquid binary mixture with water and with ethanol from 288K to 318 K, *J. Chem. Eng. Data* 57 (2012) 2136–2142.

[123] A. Pal, B. Kumar, Volumetric and acoustic properties of binary mixtures of the ionic liquid 1-butyl-3-methylimidazolium tetrafluoroborate $[BMIM]^+[BF_4]^-$ with alkoxyalkanols at different temperatures, *J. Chem. Eng. Data* 57 (2012) 688–695.

[124] M. M. Taib, T. Murugesan, Density, refractive index, and excess properties of 1-butyl 3-methylimidazolium tetrafluoroborate with water and monoethanolamine, *J. Chem. Eng. Data* 57 (2012) 120–126.

[125] A. Bhattacharjee, C. Varanda, M. G. Freire, S. Matted, L. M. N. B. F. Santos, I. M. Marrucho, J. A. P. Coutinho, Density and viscosity data for binary mixtures, of 1-alkyl-3-methylimidazolium alkylsulfates + water, *J. Chem. Eng. Data* 57 (2012) 3473–3482.

[126] G. R. Chaudhary , S. Bansal, S. K. Mehta, A. S. Ahluwalia, Thermophysical and spectroscopic studies of room temperature ionic liquid, 1- butyl-3-methylimidazolium hexafluorophosphate in tritons, *J. Chem. Thermodyn.* 50 (2012) 63–70.

[127] O. Ciocirlan, O. Croitoru, O. Iulian, Densities and viscosities for binary mixtures of 1butyl-3- methylimidazolium tetrafluoroborate ionic liquid with molecular solvents, *J. Chem. Eng. Data* 56 (2011) 1526–1534.

[128] J. Lehmann, H. Rausch, A. Leipertz, A. Fröba, Densities and excess molar volumes for binary mixtures of ionic liquid 1-ethyl-3-methylimidazolium ethylsulfate with solvents, *J. Chem. Eng. Data* 55 (2010) 4068–4074.

[129] Y. Li, H. Ye, P. Zeng, F. Qi, Volumetric properties of binary mixtures of the ionic liquid 1-butyl-3-methylimidazolium tetrafluoroborate with aniline, *J. Solution Chem.* 39 (2010) 219–230.

[130] T. Singh, A. Kumar, Volumetric behaviour of 1-butyl-3-methylimidazolium hexafluorophosphate with ethylene glycol derivatives: Application of Prigogine-FloryPatterson theory, *J. Mol. Liq.* 153 (2010) 117–123.

[131] A. Pal, R. Gaba, T. Singh, A. Kumar, Excess thermodynamic properties of binary mixtures of ionic liquid(1-butyl-3-methylimidazolium hexafluorophosphate) with alkoxyalkanols at several temperatures, *J. Mol. Liq.* 154 (2010) 41–46.

[132] C. Han, S. Xia, P. Ma, F. Zeng, Densities of ionic liquid [BMIM][BF_4] + ethanol, + benzene, and + acetonitrile at different temperature and pressure, *J. Chem. Eng. Data* 54 (2009) 2971–2977.

[133] W. Fan, Q. Zhou, J. Sun, S. Zhang, Density, excess molar volume, and viscosity for the methyl methacrylate +1-butyl-3-methylimidazolium hexafluorophosphate ionic liquid binary system at atmospheric pressure, *J. Chem. Eng. Data* 54 (2009) 2307–2311.

[134] H. Gao, F. Qi, H. Wang, Densities and volumetric properties of binary mixtures of the ionic liquid 1-butyl-3-methylimidazolium tetrafluoroborate with benzaldehyde at T = (298.15 to 313.15) K, *J. Chem. Thermodyn.* 41 (2009) 888–892.

[135] Y. Tian, X. Wang, J. Wang, Densities and viscosities of 1-butyl-3-methylimidazolium tetrafluoroborate + molecular solvent binary mixtures, *J. Chem. Eng. Data* 53 (2008) 2056–2059.

[136] I. B. Malham, M. Turmine, Viscosities and refractive indices of binary mixtures of 1-butyl-3-methylimidazolium tetrafluoroborate and 1-butyl-2, 3-dimethylimidazolium tetrafluoroborate with water at 298 K, *J. Chem. Thermodyn.* 40 (2008) 718–723.

[137] U. Domínguez, M. Laskowska, Phase equilibria and volumetric properties of 1-ethyl-3-methylimidazolium ethylsulfate + alcohol or water binary systems, *J. Solution Chem.* 37 (2008) 1271–1287.

[138] E. J. González, B. González, N. Calvar, A Domínguez, Physical properties of binary mixtures of the ionic liquid 1-ethyl-3-methylimidazolium ethyl sulphate with several alcohols at T = 298.15, 313.15, and 328.15 K and atmospheric pressure, *J. Chem. Eng. Data* 52 (2007) 1641–1648.

[139] Y. Huo, S. Xia, P. Ma, Densities of ionic liquids, 1-butyl-3-methylimidazolium hexafluorophosphate and 1-butyl-3-methylimidazolium tetrafluoroborate, with benzene, acetonitrile, and 1-propanol at T = (293.15 to 343.15) K, *J. Chem. Eng. Data* 52 (2007) 2077–2082.

[140] M. A. Iglesias-Otero, J. Troncoso, E. Carballo, L. Romaní, Density and refractive index for binary systems of the ionic liquid [BMIM][BF_4] with methanol, 1,3dichloropropane, and dimethyl carbonate, *J. Solution Chem.* 36 (2007) 1219–1230.

[141] M. T Zafarani-Moattar, R. Majdan-Cegincara, Viscosity, density, speed of sound, and refractive index of binary mixtures of organic solvent + ionic liquid, 1-butyl-3-methylimidazolium hexafluorophosphate at 298.15 K, *J. Chem. Eng. Data* 52 (2007) 2359–2364.

[142] Y. Zhong, H. Wang, K. Diao, Densities and excess volumes of binary mixtures of the ionic liquid1-butyl-3-methylimidazolium hexafluorophosphate with aromatic compound at T = (298.15 to 313.15) K, *J. Chem. Thermodyn.* 39 (2007) 291–296.

[143] A. E. Gómez, B. González, N. Calvar, E. Tojo, A. Domìnguez, Physical properties of pure 1-ethyl-3-methylimidazolium ethyl sulphate and its binary mixtures with ethanol and water at several temperatures, *J. Chem. Eng. Data* 51 (2006) 2096–2102.

[144] A. Arce, E. Rodil, A. Soto, Volumetric and viscosity study for the mixtures of 2-ethoxy-2-methylpropane, ethanol, and 1-ethyl-3-methylimidazolium ethyl sulphate ionic liquid, *J. Chem. Eng. Data* 51 (2006) 1453–1457.

[145] Q. Zhou, L. S. Wang, H. P. Chen, Densities and viscosities of 1-butyl-3methylimidazolium tetrafluoroborate + H_2O binary mixtures from (303.15 to 353.15) K, *J. Chem. Eng. Data* 51 (2006) 905–908.

[146] M. T Zafarani-Moattar, H. Shekaari, Volumetric and compressibility behaviour of ionic liquid, 1-butyl-3-methylimidazolium hexafluorophosphate and tetrabutylammonium hexafluorophosphate in organic solvents at T = 298.15 K, *J. Chem. Thermodyn.* 38 (2006) 624–633.

[147] M. T. Zafarani-Moattar, H. Shekaari, Application of Prigogine–Flory–Patterson theory to excess molar volume and speed of sound of 1-butyl-3-methylimidazolium hexafluorophosphate or 1-butyl-3-methylimidazolium tetrafluoroborate in methanol and acetonitrile, *J. Chem. Thermodyn.* 38 (2006) 1377–1384.

[148] M. T. Zafarani-Moattar, H. Shekaari, Volumetric and speed of sound of ionic liquid, 1butyl-3-methylimidazolium hexafluorophosphate with acetonitrile and methanol at T= (298.15 to 318.15) K, *J. Chem. Eng.* 50 (2005), 1694–1699.

[149] S. Zhang, X. Li, H. Chen, J. Wang, J. Zhang, M. Zhang, Determination of physical properties for the binary system of 1-ethyl-3-methylimidazolium tetrafluoroborate + H_2O, *J. Chem. Eng. Data* 49 (2004) 760–764.

[150] R. Gomes de Azevedo, J. M. S. S. Esperanca, V. Najdanovic-Visak, Thermophysical and thermodynamic properties of 1-butyl-3-methylimidazolium tetrafluoroborate and 1-butyl-3-methylimidazolium hexafluorophosphate over an extended pressure range, *J. Chem. Eng. Data* 50 (2005) 997–1008.

[151] M. T. Zafarani-Moattar, H. Shekaari, Volumetric and speed of sound of ionic liquid, 1-butyl-3-methylimidazolium hexafluorophosphate with acetonitrile and methanol at T = (298.15 to 318.15) K, *J. Chem. Eng. Data* 50 (2005) 1694–1699.

[152] Y. A. Sanmamed, D. González-Salgado, J. Troncoso, L. Romani, A. Baylaucq, C. Boned, Experimental methodology for precise determination of density of RTILs as a function of temperature and pressure using vibrating tube densimeters, *J. Chem. Thermodyn.* 42 (2010) 553−563.

[153] K. Saravanakumar, R. B. Askran, T. R. Kubendran, Density, viscosity, refractive indices, ultrasonic velocities and thermo acoustical parameters of acetophenone + isoamyl acetate at 303.15, 313.15 and 323.15 K, *Asian J. Chem.* 23 (2011) 2643–264

[154] G. Zuo, Z. Zhao, S. Yan, X. Zhang, Thermodynamic properties of a new working pair: 1-rthyl-3-methylimidazolium ethylsulfate and water, *Chem. Eng. J.* 156 (2010) 613–617.

[155] T. J. Fortin, A, Laesecke, M. Freund, S. Outcalt, Advanced calibration, adjustment, and operation of a density and sound speed analyser, *J. Chem. Thermodyn.* 57 (2013) 276–285.

[156] E. Cances, B. Mennucci, J. Tomasi, A new integral equation formalism for the polarizable continuum model: Theoretical background and applications to isotropic and anisotropic dielectrics, *J. Phys. Chem.* 107 (1997) 3032–3041.

[157] J. P. Perdew, Electronic structure of solids '91, Akademie Verlag Berlin (1991) 11– 20.

[158] K. Burke, J. P. Perdew, Y. Wang, Electronic density functional theory: Recent progress and new directions, New York (1998) 81–111.

[159] R. Ditchfield, W. J. Hehre, J. A. Pople. Self-consistent molecular_orbital methods. IX. An extended Gaussian_type basis for molecular_orbital studies of organic molecules, *J. Chem. Phys.* 542 (1971) 724–728.

[160] D. Singh, V. Singh, N. Islam, R. L. Gardas, Elucidation of molecular interactions between a DBU based protic ionic liquid and organic solvents: thermophysical and computational studies, *RSC Adv.* 6 (2016) 623– 631.

[161] V. H. Álvarez, D. Serrão, J. L. da Silva Jr, M. R. Barbosa, M. Aznar, Vapor–liquid and liquid–liquid equilibrium for binary systems ester+ a new protic ionic liquid, *Ionics* 19 (2013) 1263–1269.

[162] D. Keshapolla, R. L. Gardas, Apparent molar volumes and isentropic compressions of benzylalkylammonium ionic liquids in dimethylsulfoxide from 293.15 K to 328.15 K, *Fluid Phase Equilib.* 382 (2014) 32–42.

[163] B. A Marekha, M. Bria, M. Moreau, I. De Waele, F-A. Miannay, Y. Smortsova, T. Takamuku, O. N. Kalugin, M. Kiselev, I. Drissi, Intermolecular interactions in mixtures of 1-butyl-3-methylimidazolium acetate and water: Insights from IR, Raman, NMR spectroscopy and quantum chemistry calculations, *J. Mol. Liq.* 10 (2015) 227–237.

[164] M. J. Frisch, G. W. Trucks, H. B. Schlegel, G. E. Scuseria, M. A. Robb, J. R. Cheeseman, G. Scalmani, V. Barone, B. Mennucci, G. A. Petersson, H. Nakatsuji, M. Caricato, X. Li, H. P. Hratchian, A. F. Izmaylov, J. Bloino, G. Zheng, J. L. Sonnenberg, M. Hada, M. Ehara, K. Toyota, R. Fukuda, J. Hasegawa, M. Ishida, T. Nakajima, Y. Honda, O. Kitao, H. Nakai, T. Vreven, J. A. Montgomery, Jr., J. E. Peralta, F. Ogliaro, M. Bearpark, J. J. Heyd, E. Brothers, K. N. Kudin, V. N. Staroverov, T. Keith, R. Kobayashi, J. Normand, K. Raghavachari, A. Rendell, J. C. Burant, S. S. Iyengar, J. Tomasi, M. Cossi, N. Rega, J. M. Millam, M. Klene, J. E. Knox, J. B. Cross, V. Bakken, C. Adamo, J. Jaramillo, R. Gomperts, R. E. Stratmann, O. Yazyev, A. J. Austin, R. Cammi, C. Pomelli, J. W. Ochterski, R. L. Martin, K. Morokuma, V. G. Zakrzewski, G. A. Voth, P. Salvador, J. J. Dannenberg, S. Dapprich, A. D. Daniels, O. Farkas, J. B. Foresman, J. V. Ortiz, J. Cioslowski, D. J. Fox, G09a: GAUSSIAN 09, Revision B.01, Gaussian, Inc., Wallingford CT, 2010.

[165] O. Redlich, A. Kister, Algebraic representation of thermodynamic properties and the classification of solutions, *Ind. Eng. Chem.* 40 (1948) 345–348.

[166] I. M. Alecu, J. Zheng, Y. Zhao, D. G. Truhlar, Computational thermochemistry: Scale factor databases and scale factors for vibrational frequencies obtained from electronic model chemistries, *J. Chem. Theory Comput.* 6 (2010) 2872–2887.

[167] M. Freemantle, An introduction to ionic liquids, RSC Publishing, Cambridge, UK, 2010.

[168] J. A. Riddick, W. B. Bunger, T. K. Sakano, Organic solvents, 4th ed.; Wiley-Interscience: New York, 1986.

[169] S. Singh, I. Bahadur, G. G. Redhi, D. Ramjugernath, E. E. Ebenso, Influence of alkyl group on interactions between carboxylic acid and acetonitrile at different temperatures, *J. Chem. Thermodyn.* 98 (2016) 102–110.

[170] C. Kolbeck, J. K. Lehmann, R. J Lovelock, T. Cremer, N. Paape, P. Wasserscheid, A. P. Fröba, F. Maier, H.-P. Steinrück, Density and surface tension of ionic liquids, *J. Phys. Chem.* B 114 (2010) 17025−17036.

[171] Y. T. Wang, G. A. Voth, Unique spatial heterogeneity in ionic liquids, *J. Am. Chem. Soc.* 127 (2005) 12192−12193.

[172] J. N. A. C. Lopes, A. A. H. Pádua, Nanostructural organization in ionic liquids, *J. Phys. Chem.* B 110 (2006) 3330−3335.

[173] V. Govinda, P. Venkatesu, I. Bahadur, Molecular interactions between ammoniumbased ionic liquids and molecular solvents: current progress and challenges, *Phys. Chem. Chem. Phys.* 18 (2016) 8278–8326.

[174] S. B. Capelo, T. Méndez-Morales, J. Carrete, E. L. Lago, J. Vila, O. Cabeza, J. R. Rodríguez, M. Turmine, L. M. Varela, Effect of temperature and cationic chain length on the physical properties of ammonium nitrate-based protic ionic liquids, *J. Phys. Chem. B* 116 (2012) 11302–11312.

[175] V. Govinda, P. M. Reddy, P. Attri, P. Venkatesu, P. Venkateswarlu, Influence of anion on thermophysical properties of ionic liquids with polar solvent, *J. Chem. Thermodyn.* 58 (2013) 269–278.

[176] V. Govinda, P. Attri, P. Venkatesu, P. Venkateswarlu, Evaluation of thermophysical properties of ionic liquids with polar solvent: A comparable study of two families of ionic liquids with various ions, *Phys. Chem. B* 117 (2013) 12535–12548.

[177] T. Kavitha, P. Attri, P. Venkatesu, R. S. R. Devi, T. Hofman, Influence of alkyl chain length and temperature on thermophysical properties of ammonium-based ionic liquids with molecular solvent, *J. Phys. Chem. B* 116 (2012) 4561–4574.

[178] T. Kavitha, T. Vasantha, P. Venkatesu, R. S. R. Devi, T. Hofman, Thermophysical properties for the mixed solvents of *N*-methyl-2-pyrrolidone with some of the Imidazolium-based ionic liquids, *J. Mol. Liq.* 198 (2014) 11–20.

[179] L. Cammarata, S. G. Kazarian, P. A. Salterb, T. Welton, Molecular states of water in room temperature ionic liquids, *Phys. Chem. Chem. Phys.* 3 (2001) 5192–5200.

[180] M. Anouti, A. Vigeant, J. Jacquemin, C. Brigouleix, D. Lemordant, Volumetric properties, viscosity and refractive index of the protic ionic liquid, pyrrolidinium octanoate, in molecular solvents, *J. Chem. Thermodyn.* 42 (2010) 834–845.

[181] N. Cheng, P. Yu, T. Wang, X. Sheng, Y. Bi, Y. Gong, L. Yu, Self-aggregation of new alkylcarboxylate-based anionic surface active ionic liquids: Experimental and theoretical investigations, *J. Phys. Chem. B* 118 (2014) 2758–2768.

[182] W. Xu, T. Wang, N. Cheng, Q. Hu, Y. Bi, Y. Gong, L. Yu, Experimental and DFT studies on the aggregation behavior of imidazolium-based surface-active ionic liquids with aromatic counterions in aqueous solution, *Langmuir* 31 (2015) 1272–1282.

[183] Y. Zhao, J. Wang, H. Wang, Z. Li, X. Liu, S. Zhang, Is there any preferential interaction of ions of ionic liquids with DMSO and H_2O? A comparative study from MD simulation, J. Phys. Chem. B 119 (2015) 6686–6695.

[184] B-R. Marija, A. Stoppa, R. Buchner, Ion association of imidazolium ionic liquids in acetonitrile, *J. Phys. Chem. B* 118 (2014) 426–1435.

APPENDIX

List of publications

Influence of temperature on molecular interactions of imidazolium-based ionic liquids with acetophenone: thermophysical and quantum chemical studies [under review in RSC Advance (UK)].